

**MICHIGAN STATE UNIVERSITY  
CYCLOTRON PROJECT\***

**First Order Study  
of Some Beam Analyzing Systems  
for a Medium Energy Cyclotron**

*K. Kosaka*

September 1962

Department of Physics

East Lansing, Michigan

---

\*Research Supported in part by U.S. Atomic Energy Commission Contract AT(11-1)-872

## ABSTRACT

### FIRST ORDER STUDY OF SOME BEAM ANALYZING SYSTEMS FOR A MEDIUM ENERGY CYCLOTRON

by Kei Kosaka

In order to have a useful output some distance away from an accelerator, it is necessary to use magnetic systems which focus, bend, and resolve the beam. When such systems are compounded, it is cumbersome to try to hand calculate the beam properties. A computer program is presented here which calculates the first order optical properties of any combination of such systems and gives the combined effect of these systems on the beam properties. Results are presented for several typical systems of interest in handling cyclotron beams.

FIRST ORDER STUDY OF  
SOME BEAM ANALYZING SYSTEMS FOR  
A MEDIUM ENERGY CYCLOTRON

By

Kei Kosaka

A THESIS

Submitted to  
Michigan State University  
in partial fulfillment of the requirements  
for the degree of

MASTER OF SCIENCE

Department of Physics and Astronomy

1962

## ACKNOWLEDGMENTS

I would like to express my appreciation to Dr. H. G. Blosser and Dr. W. Johnson of this laboratory for their helpful suggestions.

I am grateful to the United States Atomic Energy Commission and the National Science Foundation for making this work financially possible.

Also, I would like to thank R. L. Dickenson for his work on the graphs.

## TABLE OF CONTENTS

	Page
INTRODUCTION . . . . .	1
I. EQUATIONS OF MOTIONS . . . . .	5
A. The Magnetic Quadrupole	6
B. Bending Magnets	13
C. Edge Effect for the Bending Magnet	21
D. Relative Orientation and Separation	28
E. Relation of Beam Properties to the Matrix Describing the Focusing Systems	30
II. THE COMPUTER PROGRAM FOR CALCULATING THE BEAM PROPERTIES . . . . .	34
III. RESULTS . . . . .	40
A. Single 90° Bending Magnets	40
B. Single Quadrupole Magnet	44
C. Bending Magnet Pairs	44
D. Quadrupole and Flat Bending Magnet Combinations	68
IV. APPENDIX . . . . .	77
A. Flow Chart for the Computer Code	78
B. Order Pairs for the Computer Code	79
REFERENCES . . . . .	107

## LIST OF FIGURES

Figure	Page
1. Magnetic quadrupole geometry. $d$ is the aperture and $L$ is the length of the quadrupole . . . .	6
2. Edge effect of the bending magnet. The central ray enters from the right and exits to the left, with angles $\beta_1$ and $\beta_2$ , respectively, away from the normals to the entrance and exit edges of the magnet . . . . .	22
3. Geometry of non-normal entry into a bending magnet . . . . .	26
4. Diagram showing the relative positions of the object plane, focal planes, principal planes, image planes, and the focusing region . . . . .	31
5. Radial resolution, radial image distance, and radial magnification of a single $n = 0$ , $\rho = 36$ in., $\alpha = 36$ in., $\alpha = 90^\circ$ and $\beta_1 = \beta_2 = 0^\circ$ bending magnet plotted against the object distance . . . . .	41
6. Radial resolution, radial and axial image distances, and radial and axial magnification of a single $n = 1/2$ , $\rho = 36$ in., $\alpha = 90^\circ$ and $\beta_1 = \beta_2 = 0^\circ$ bending magnet plotted against the object distance . . . . .	43
7. Radial and axial focal lengths and distances focal length away from the focal plane of a single magnetic quadrupole plotted against $K$ , where $K$ was defined to be $K^2 \equiv \frac{qG}{p_0}$ and has units of $\text{in}^{-1}$ . . . . .	45

8. Radial resolution of a system consisting of two  $n = 0$ ,  $\rho = 36$  in.,  $\alpha = 90^\circ$ , and  $\beta_1 = \beta_2 = 0^\circ$  bending magnets oriented so that  $\theta = 0^\circ$ . Plotted against the object distance in inches for the separation distances  $d = 10$  in., 60 in., 110 in., and 160 in. . . . . 47
9. Radial resolution for two  $n = 1/2$ ,  $\rho = 36$  in.,  $\alpha = 90^\circ$ , and  $\beta_1 = \beta_2 = 0^\circ$  bending magnets oriented so that  $\theta = 0^\circ$ . Plotted against the object distance for the separation distances  $d = 10$  in., 60 in., 110 in., and 160 in. . . . . 49
10. Radial and axial resolutions for two  $n = 0$ ,  $\rho = 36$  in.,  $\alpha = 90^\circ$ , and  $\beta_1 = \beta_2 = 0^\circ$  bending magnets oriented so that  $\theta = 45^\circ$ . The axial resolution is plotted with dashed lines. Plotted against the object distance for the separation distances  $d = 10$  in., 60 in., 110 in., and 160 in. . . . . 50
11. Radial and axial resolutions for two  $n = 1/2$ ,  $\rho = 36$  in.,  $\alpha = 90^\circ$ , and  $\beta_1 = \beta_2 = 0^\circ$  bending magnets oriented so that  $\theta = 45^\circ$ . Plotted against the object distance given in inches, for the separation distances  $d = 10$  in., 60 in., 110 in., and 160 in. Axial resolutions are plotted with dashed lines . . . . . 52
12. Radial and axial resolutions for two  $n = 0$ ,  $\rho = 36$  in.,  $\alpha = 90^\circ$ , and  $\beta_1 = \beta_2 = 0^\circ$  bending magnets oriented so that  $\theta = 90^\circ$ . The axial resolution is plotted with dashed lines. Plotted against the object distance for the separation distances  $d = 10$  in., 60 in., 110 in., and 160 in. . . . . 53
13. Radial and axial resolutions for two  $n = 1/2$ ,  $\rho = 36$  in.,  $\alpha = 90^\circ$ , and  $\beta_1 = \beta_2 = 0^\circ$  bending magnets oriented so that  $\theta = 90^\circ$ . Plotted against the object distance given in inches, for the separation distances  $d = 10$  in., 60 in., 110 in., and 164.16 in. Axial resolutions are plotted with dashed lines . . . 54

- 14. Radial and axial resolutions for two  $n = 0$ ,  $\rho = 36$  in.,  $\alpha = 90^\circ$ , and  $\beta_1 = \beta_2 = 0^\circ$  bending magnets oriented so that  $\theta = 135^\circ$ . The axial resolution is plotted with dashed lines. Plotted against the object distance for the separation distances  $d = 10$  in.,  $60$  in.,  $110$  in., and  $160$  in. . . . . 56
  
- 15. Radial and axial resolutions for two  $n = 1/2$ ,  $\rho = 36$  in.,  $\alpha = 90^\circ$ , and  $\beta_1 = \beta_2 = 0^\circ$  bending magnets oriented so that  $\theta = 135^\circ$ . Plotted against the object distance given in inches, for the separation distances  $d = 10$  in.,  $60$  in.,  $110$  in., and  $160$  in. Axial resolutions are plotted with dashed lines. . . . . 57
  
- 16. Radial resolution of a system consisting of two  $n = 0$ ,  $\rho = 36$  in.,  $\alpha = 90^\circ$ , and  $\beta_1 = \beta_2 = 0^\circ$  bending magnets oriented so that  $\theta = 180^\circ$ . Plotted against the object distance in inches for the separation distances  $d = 10$  in.,  $60$  in.,  $110$  in., and  $160$  in. . . . . 58
  
- 17. Radial resolution for two  $n = 1/2$ ,  $\rho = 36$  in.,  $\alpha = 90^\circ$ , and  $\beta_1 = \beta_2 = 0^\circ$  bending magnets oriented so that  $\theta = 180^\circ$ . Plotted against the object distance for the separation distances  $d = 10$  in.,  $60$  in.,  $110$  in., and  $160$  in. . . . . 59
  
- 18. Radial magnification for the two  $n = 0$ ,  $\rho = 36$  in.,  $\alpha = 90^\circ$ , and  $\beta_1 = \beta_2 = 0^\circ$  bending magnets oriented so that  $\theta = 0^\circ$  or  $180^\circ$ . Plotted against the object distance given in inches for the separation distances  $d = 10$  in.,  $60$  in.,  $110$  in., and  $160$  in. . . . . 60
  
- 19. Radial and axial magnifications for the two  $n = 0$ ,  $\rho = 36$  in.,  $\alpha = 90^\circ$ , and  $\beta_1 = \beta_2 = 0^\circ$  bending magnets oriented so that  $\theta = 45^\circ$  or  $135^\circ$ . Plotted against the object distance given in inches for the separation distances  $d = 10$  in.,  $60$  in.,  $110$  in., and  $160$  in. Axial magnifications are plotted with dashed lines . . . . . 61



20. Radial and axial magnifications for the two  $n = 0$ ,  $\rho = 36$  in.,  $\alpha = 90^\circ$ , and  $\beta_1 = \beta_2 = 0^\circ$  bending magnets oriented so that  $\theta = 90^\circ$ . Plotted against the object distance given in inches for the separation distances  $d = 10$  in.,  $60$  in.,  $110$  in., and  $160$  in. Axial magnifications are plotted with dashed lines . . . . . 62
21. Radial and axial magnifications of two  $n = 1/2$ ,  $\rho = 36$  in.,  $\alpha = 90^\circ$ , and  $\beta_1 = \beta_2 = 0^\circ$  bending magnets with any relative orientation plotted against the object distance given in inches for the separation distances  $d = 10$  in.,  $60$  in.,  $110$  in., and  $160$  in. . . . . 64
22. Radial image distance for the two  $n = 0$ ,  $\rho = 36$  in.,  $\alpha = 90^\circ$ , and  $\beta_1 = \beta_2 = 0^\circ$  bending magnets oriented so that  $\theta = 0^\circ$  or  $180^\circ$ . Plotted against the object distance given in inches for the separation distances  $d = 10$  in.,  $60$  in.,  $110$  in., and  $160$  in. . . . . 65
23. Radial and axial image distances for two  $n = 0$ ,  $\rho = 36$  in.,  $\alpha = 90^\circ$ , and  $\beta_1 = \beta_2 = 0^\circ$  bending magnets oriented so that  $\theta = 45^\circ$  or  $135^\circ$ . Plotted against the object distance given in inches for the separation distances  $d = 10$  in.,  $60$  in.,  $110$  in., and  $160$  in. Axial image distances are plotted with dashed lines . . . . . 66
24. Radial and axial image distances for two  $n = 0$ ,  $\rho = 36$  in.,  $\alpha = 90^\circ$ , and  $\beta_1 = \beta_2 = 0^\circ$  bending magnets oriented so that  $\theta = 90^\circ$ . Plotted against the object distance given in inches for the separation distances  $d = 10$  in.,  $60$  in.,  $110$  in., and  $160$  in. Axial image distances are plotted with dashed lines . . . . . 67
25. Radial and axial image distances for two  $n = 1/2$ ,  $\rho = 36$  in.,  $\alpha = 90^\circ$ , and  $\beta_1 = \beta_2 = 0^\circ$  bending magnets with any relative orientation, plotted against the object distance given in inches for the separation distances  $d = 10$  in.,  $60$  in.,  $110$  in., and  $160$  in. . . . . 69

26. Diagram showing the relative positions of the magnets in a system containing two  $n = 0$  bending magnets and one axially focusing magnetic quadrupole . . . . . 70
27. Radial and axial magnifications for the system with two  $n = 0$  bending magnets and an axially focusing quadrupole as shown in Figure 26. Plotted against the object distance given in inches for quadrupole fields specified by  $K = .04 \text{ in.}^{-1}$ ,  $.045 \text{ in.}^{-1}$ ,  $.05 \text{ in.}^{-1}$ , and  $.055 \text{ in.}^{-1}$ . The axial magnifications are plotted with dashed lines . . . . . 71
28. Radial and axial image distances for the system described in Figure 26, plotted against the field strength of the magnetic quadrupole. These are lines of unit magnification. The axial image distance is plotted with a dashed line . . . . . 72
29. Diagram of a system with two  $n = 0$  bending magnets and three magnetic quadrupoles; one of which is radially focusing and the other two axially focusing . . . . . 74
30. Radial and axial magnifications for the system as described in Figure 29, plotted against the object distance given in inches for the several field strengths of the radially focusing quadrupole as specified by  $K$ . The axial magnifications are plotted with dashed lines . . . . . 75
31. Radial and axial image distances for the system as described in Figure 29, plotted against the field strength of the radially focusing quadrupole. These are lines of unit magnification. The axial image distances are plotted with dashed lines . . . . . 76

## INTRODUCTION

The output beam from an accelerator consists of particles with momenta distributed over some range. In nuclear experiments, it is usually desirable to have a beam with small momentum spread, high intensity and small cross sectional area. Usually, the type of experiment and the quality of the beam from the accelerator make it expedient to sacrifice one or more of these beam properties to improve the third.

It is possible, by using bending magnets, to disperse particles of different momenta, and produce a spectrum at the image plane. If the image slit is to just include all of the particles with some selected momentum, it must have a width equal to the magnification times the source slit width.\* With such an image slit, and assuming the source slit is illuminated uniformly, the momentum distribution of the transmitted particles will be triangular with the peak

---

\*There is no advantage in making the slit narrower, since the transmitted intensity decreases while the width of the momentum distribution (measured at the usual half maximum intensity points) remains the same. If the slit is made wider, the width at half maximum, of course, increases.

located at the selected momentum.

The width of the triangular momentum distribution may be made smaller by either decreasing the magnification or increasing the momentum dispersion. Decreasing the magnification allows one to narrow the image slit and still pass through all of the particles with the selected momentum; increasing the momentum dispersion causes particles with momentum differing from the selected momentum, to be deflected through greater angles, so that some previously transmitted particles will now fail to pass through the image slit. Usually, for real systems, neither the magnification nor the momentum dispersion change independent of the other.

The momentum spread across an image slit sized to just admit all particles with a selected momentum, is a well known figure of merit--designated resolution--which combines the effect of both magnification and momentum dispersion. In the calculations that follow, the fractional half base width of the triangular momentum distribution at the image slit (equivalent to the fractional full width at half maximum of the distribution), is calculated. This quantity, calculated for a unit source slit width, is defined as the resolution.

For different systems, the resolution depends on the way in which the magnets are positioned, on the type of

bending magnets used, and/or on the number of various magnets which compose the complete system. The computer program presented here enables one to study this property for various simple and combined systems, as well as to study the more familiar optical properties, and to make useful comparisons between them.

Equations of motion for first order theory of the bending magnets were first developed in connection with magnetic spectrometers. Such a study of magnets giving general expressions for image distance, astigmatism, magnification, solid angle, dispersion, and resolution has been made by Judd.<sup>1\*</sup> The basic equations are, however, essentially the same as the betatron equations developed by Kerst and Serber.<sup>2</sup> The first order equations for the magnetic quadrupole developed here are much like those used by Enge.<sup>3</sup>

In such a first order treatment, the equations of trajectory are, of course, by definition linear in the initial displacement, angular spread, and momentum spread. This enables one to set up the problem in matrix form, which is convenient when several magnets are considered in series. The matrix method used here is based on the formalism developed by Penner.<sup>4</sup>

---

\*References are listed at the end.

The magnetic systems considered herein are the bending magnet and the magnetic quadrupole lens. Nonmagnetic systems such as the electrostatic quadrupole lens are not considered, since excessively high fields would be required in the energy range of interest ( $\cong 40$  Mev protons). It would not be difficult to handle the electrostatic quadrupole in the computer program, however, since the equations are exactly the same as the magnetic quadrupole except that the force constant has to be redefined.

In the examples calculated, comparisons are made between the performance of double focusing and flat field bending magnets. Combined systems focusing radially and axially have also been worked out using flat field bending magnets and magnetic quadrupoles. Such combined systems are attractive in that they combine double focusing with the usual advantages of flat field bending magnets, i.e., such magnets can easily be precisely stabilized by the use of a nuclear magnetic resonance probe.

## I. EQUATIONS <sup>OF</sup> IN MOTION

In setting up a sequence of quadrupole lenses and bending magnets to form an analyzing system, one, of course, designs with respect to some particular momentum value; all of the lenses and bending magnets are positioned and their strengths adjusted such that a particular ray of the specified momentum follows a central path through the system. This path is designated the "optic axis" of the system. An arbitrary trajectory is specified at any point along the optic axis by giving perpendicular displacements  $(x, y)$  from the optic axis in two independent directions (customarily at right angles to each other), the corresponding conjugate momentum  $(p_x, p_y)$ , and the momentum difference  $(\Delta p = |\vec{p}| - |\vec{p}_0|)$  between the trajectory in question and the optic axis. Following the procedures of Penner<sup>4</sup> and Livingood,<sup>5</sup> equations of motion accurate to first order in these displacement coordinates are derived in the following subsections for the magnetic quadrupoles and bending magnets. In each case the matrix formulation is specifically exhibited.

### A. The Magnetic Quadrupole

The geometry of the quadrupole is roughly shown in Figure 1, the z axis in the figure being the optic axis.

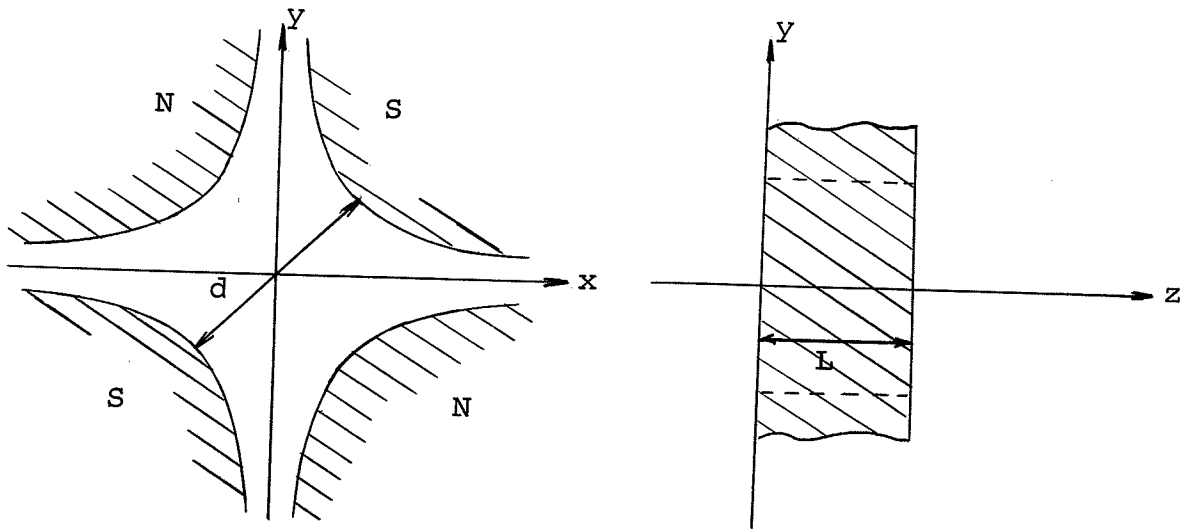


Figure 1. Magnetic quadrupole geometry.  $d$  is the aperture and  $L$  is the length of the quadrupole.

Hyperbolic equipotential lines, for field strengths less than saturation, are made possible by making the poles rectangular hyperbolic cylinders which are symmetrical about the  $x$  and  $y$  axes. If adjacent poles have opposite polarity, the gradients of the field components are constant and the force on the particle is proportional to the displacement from the  $z$  axis. The equipotential lines are hyperbolas expressed by the equation

$$V = Gxy \quad (1)$$

where  $G$  is a constant to be evaluated. There is no field component along the  $z$  axis within the quadrupole (at the edges, it exists only over a small range compared to the



length of normal quadrupoles), so that we need only to consider the other two components

$$B_x = \frac{dV}{dx} = Gy$$

$$B_y = \frac{dV}{dy} = Gx$$

The gradients of these components are

$$\frac{dB_x}{dy} = G \qquad \frac{dB_y}{dx} = G$$

These are equal and positive, since  $B_x$  is proportional to  $y$  and  $B_y$  is proportional to  $x$ .

The  $x$  and  $y$  components of the Lorentz force relation

$$\vec{F} = q \vec{v} \times \vec{B} \quad \text{are} \quad F_x = -q v_z B_y = -q v_z Gx \quad (2)$$

$$F_y = q v_z B_x = q v_z Gy \quad (3)$$

where the beam is moving parallel to the  $z$  axis. These equations show that with this choice of orientation of poles with respect to the  $x$  and  $y$  axes, the  $x$  component of the force drives the particle toward the  $z$  axis while the  $y$  component drives it away. It is not difficult to see that if the orientation were to be changed by a  $90^\circ$  rotation about the  $z$  axis, this situation would be reversed.

The equation of motion in the  $x$ - $z$  plane is from equation (2)

$$\frac{d}{dt} (m\dot{x}) = F_x = -q v_z Gx$$

since trajectories are considered only in magnetic fields, there is no energy change of the particles, and hence, no change in the velocity or mass of the individual particles. This makes it possible to take out the mass from the derivative in the above equation, i.e.,

$$m \frac{d^2 x}{dt^2} = -q v_z Gx$$

This can be rewritten by noting that

$$\frac{d^2 x}{dt^2} = \frac{d}{dt} \left( \frac{dz}{dt} \frac{dx}{dz} \right)$$

and

$$\frac{d}{dt} = \frac{dz}{dt} \frac{d}{dz} = v_z \frac{d}{dz}$$

as

$$mv_z \frac{d}{dz} \left( v_z \frac{dx}{dz} \right) = -q v_z Gx \quad (4)$$

Since

$$v_z = \sqrt{v^2 - v_x^2} = v \left[ 1 - \left( \frac{v_x}{v} \right)^2 + \dots \right]^{1/2}$$

equation (4) can be written to first order in  $x$  and  $v_x$  as:

$$v^2 \frac{d^2 x}{dz^2} = -\frac{qv}{m} Gx$$

Regrouping of the constants gives

$$\frac{d^2 x}{dz^2} + \frac{qG}{p} x = 0 \quad (5)$$

where  $p$  is the magnitude of the particle momentum.

In terms of the reference momentum,  $p_o$ , equation (5) can be written

$$\frac{d^2 x}{dz^2} + \frac{qG}{p_o + \Delta p} x = 0$$

and by defining  $K^2 \equiv \frac{qG}{p_o}$ , then

$$\frac{d^2 x}{dz^2} + K^2 \left(1 + \frac{\Delta p}{p_o}\right)^{-1} x = 0$$

which has a solution

$$x = A \cos K \left(1 + \frac{\Delta p}{p_o}\right)^{-1/2} z + B \sin K \left(1 + \frac{\Delta p}{p_o}\right)^{-1/2} z$$

Expanding the arguments of the trigonometric functions in a binomial series and keeping only terms of first order and lower,

$$x = A \cos K \left(1 - \frac{1}{2} \frac{\Delta p}{p_o}\right) z + B \sin K \left(1 - \frac{1}{2} \frac{\Delta p}{p_o}\right) z$$

Rewriting the trigonometric functions in terms of the sum of the angle relation

$$x = A (\cos K z \cos \frac{1}{2} \frac{\Delta p}{p_o} K z + \sin K z \sin \frac{1}{2} \frac{\Delta p}{p_o} K z) \\ + B (\sin K z \cos \frac{1}{2} \frac{\Delta p}{p_o} K z - \cos K z \sin \frac{1}{2} \frac{\Delta p}{p_o} K z)$$

Expanding the sine and cosine functions which have  $\frac{\Delta p}{p_o}$  in their arguments, and only keeping terms of first order and lower

$$x = A (\cos K z + \frac{1}{2} \frac{\Delta p}{p_o} K z \sin K z) + B (\sin K z - \frac{1}{2} \frac{\Delta p}{p_o} K z \cos K z)$$

whose derivative

$$x' = \frac{dx}{dz} = A (-K \sin K z + \frac{1}{2} \frac{\Delta p}{p_o} K \sin K z + \frac{1}{2} \frac{\Delta p}{p_o} K^2 z \cos K z) \\ + B (K \cos K z - \frac{1}{2} \frac{\Delta p}{p_o} K \cos K z + \frac{1}{2} \frac{\Delta p}{p_o} K^2 z \sin K z)$$

along with the initial conditions,  $x = x_0$ ,  $x' = x'_0$  when  $z = z_0 = 0$ , makes it possible to evaluate the constants.

These turn out to be  $A = x_0$  and  $B = \frac{x'_0}{K (1 - \frac{1}{2} \frac{\Delta p}{p_0})}$ . Expanding

$B$  in a binomial series and only keeping first order or lower terms,  $B = \frac{x'_0}{K} (1 + \frac{1}{2} \frac{\Delta p}{p_0})$ . Dropping all terms containing,

either of the products  $x_0 \frac{\Delta p}{p_0}$  or  $x'_0 \frac{\Delta p}{p_0}$ , in the equation for

$x$  and  $x'$ , and evaluating at  $Z = L$ , the terminating point of the quadrupole, gives, finally:

$$\begin{aligned} x &= x_0 \cos KL + x'_0 \frac{1}{K} \sin KL \\ x' &= -x_0 K \sin KL + x'_0 \cos KL \end{aligned} \quad (7)$$

Equation of motion in the  $y$ - $z$  plane is by equation (3)

$$\frac{d}{dt} m\dot{y} = q v Gy$$

In similar fashion to the previous calculation, all terms containing  $\Delta p$  can be shown to be of second order. The linear equation of motion, hence, reduces to

$$\frac{d^2 y}{dz^2} - K^2 y = 0 \quad (8)$$

where  $K$  is defined in the same way as before. This has a solution

$$y = C \cosh KZ + D \sinh KZ$$

whose derivative

$$y' = \frac{dy}{dz} = CK \sinh KZ + DK \cosh KZ$$

along with the initial conditions,  $y = y_0$  and  $y' = y'_0$  at  $z = z_0 = 0$ , yields  $C = y_0$  and  $D = \frac{y'_0}{K}$ , so that

$$\begin{aligned} y &= y_0 \cosh KL + y'_0 \frac{1}{K} \sinh KL \\ y' &= y_0 K \sinh KL + y'_0 \cosh KL \end{aligned} \tag{9}$$

where, once again,  $L$  is the effective length of the quadrupole.

It is possible to write both equations (7) and (9) in matrix form, since they are all linear equations. Equation (7), for example, becomes:

$$\begin{pmatrix} x \\ x' \end{pmatrix} = \begin{pmatrix} \cos KL & \frac{1}{K} \sin KL \\ -K \sin KL & \cos KL \end{pmatrix} \begin{pmatrix} x_0 \\ x'_0 \end{pmatrix} .$$

This arrangement has the attractive advantage that all information regarding the quadrupole is contained in the matrix entirely independent of any particular set of initial conditions. The effect of the quadrupole on any arbitrary trajectory is found simply by multiplying the phase space coordinate vector at entry by the matrix to obtain the phase space vector at exit. In similar fashion to (7), equation (9) can be written

$$\begin{pmatrix} y \\ y' \end{pmatrix} = \begin{pmatrix} \cosh KL & \frac{1}{K} \sinh KL \\ K \sinh KL & \cosh KL \end{pmatrix} \begin{pmatrix} y_0 \\ y'_0 \end{pmatrix}$$

It is convenient for calculations made in combination with the bending magnets, to combine these two matrices to make a single six by six matrix which includes the momentum spread as the third and sixth coordinates. It has been shown, above that the coefficient in front of the  $\frac{\Delta p}{p_0}$  term is to first order zero. Hence, the third and sixth columns of the transformation matrix can be set equal to zero, except for the unit transformation coefficient which accompanies each momentum coordinate. The combined matrix is

$$\begin{pmatrix} x \\ x' \\ \frac{\Delta p}{p_0} \\ y \\ y' \\ \frac{\Delta p}{p_0} \end{pmatrix} = \begin{pmatrix} \cos KL & \frac{1}{K} \sin KL & 0 & 0 & 0 & 0 \\ -K \sin KL & \cos KL & 0 & 0 & 0 & 0 \\ 0 & 0 & 1 & 0 & 0 & 0 \\ 0 & 0 & 0 & \cosh KL & \frac{1}{K} \sinh KL & 0 \\ 0 & 0 & 0 & K \sinh KL & \cosh KL & 0 \\ 0 & 0 & 0 & 0 & 0 & 1 \end{pmatrix} \begin{pmatrix} x_0 \\ x'_0 \\ \frac{\Delta p}{p_0} \\ y_0 \\ y'_0 \\ \frac{\Delta p}{p_0} \end{pmatrix} \quad (10)$$

Note that if the field direction is reversed or if the quadrupole is rotated by  $90^\circ$ , the same condition is achieved by

interchanging the two submatrices, i.e.,

$$\begin{pmatrix} x \\ x' \\ \frac{\Delta p}{p_0} \\ y \\ y' \\ \frac{\Delta p}{p_0} \end{pmatrix} = \begin{pmatrix} \cosh KL & \frac{1}{K} \sinh KL & 0 & 0 & 0 & 0 \\ K \sinh KL & \cosh KL & 0 & 0 & 0 & 0 \\ 0 & 0 & 1 & 0 & 0 & 0 \\ 0 & 0 & 0 & \cos KL & \frac{1}{K} \sin KL & 0 \\ 0 & 0 & 0 & -K \sin KL & \cos KL & 0 \\ 0 & 0 & 0 & 0 & 0 & 1 \end{pmatrix} \begin{pmatrix} x_0 \\ x'_0 \\ \frac{\Delta p}{p_0} \\ y_0 \\ y'_0 \\ \frac{\Delta p}{p_0} \end{pmatrix} \quad (11)$$

Equation (10) is converging in the x-z plane and diverging in the y-z plane. The reverse is true for equation (11).

### B. Bending Magnets

Consider, first, the axial motion. Use cylindrical coordinates with origin at the center of curvature of the optic axis of the magnet. Within the bending magnet  $B_\theta$  is zero, and edge phenomena will be treated separately later, so that the axial equation of motion is:

$$\frac{d}{dt} m\dot{z} = -q v_\theta B_r \quad (13)$$

We are interested in the first order terms in the variables expressing variation from the particle following the optic axis. These variables are taken to be the

displacement coordinates  $x = r - r_0$  and  $z$ , and their conjugate momenta  $p_x$  and  $p_z$  and the total momentum displacement  $\Delta p = |\vec{p}| - |\vec{p}_0|$ . First, expand  $B_r$  about  $z = 0$ , and  $v_\theta$  in terms of  $v_x$  and  $v_z$ .

$$\frac{d}{dt} m\dot{z} = -q v \left( 1 - \frac{1}{2} \frac{v_x^2 + v_z^2}{v^2} + \dots \right) \left( \left[ B_r(r, z) \right]_{z=0} + z \left[ \frac{dB_r}{dz} \right]_{z=0} + \frac{z^2}{2!} \left[ \frac{d^2 B_r}{dz^2} \right]_{z=0} + \dots \right)$$

Keeping only the linear terms in the variables mentioned above

$$\frac{d}{dt} m\dot{z} = -q v \left( \left[ B_r(r, z) \right]_{z=0} + z \left[ \frac{dB_r}{dz} \right]_{z=0} \right)$$

Since the field is symmetrical about  $z = 0$ ,  $\left[ B_r(r, z) \right]_{z=0} = 0$ .

Using the fact that the curl of  $B$  is zero for a source free region

$$\frac{d}{dt} m\dot{z} = -q v z \left[ \frac{dB_z}{dr} \right]_{z=0}$$

Expanding the field derivative about  $r = r_0$ , and since the mass is constant in a magnetic field

$$\ddot{z} = -\frac{q v^2}{p} z \left( \left[ \frac{dB_z}{dr} \right]_{\substack{r=r_0 \\ z=0}} + z \left[ \frac{d^2 B_z}{dr^2} \right]_{\substack{r=r_0 \\ z=0}} + \dots \right)$$

Expanding  $p$  in terms of  $\Delta p$  and  $v$  in terms of  $\Delta v$ , which is



related to  $\Delta p$ , and keeping only linear terms

$$\ddot{z} = - \frac{q v_o^2}{p_o} z \left[ \frac{dB_z(r, z)}{dr} \right]_{\substack{r=r_o \\ z=0}} \quad (14)$$

The momentum of central particle, i.e.,  $r = r_o$ ,  $z = 0$  and  $\Delta p = 0$  is given by

$$p_o = - q r_o \left[ B_z \right]_{\substack{r=r_o \\ z=0}}$$

which when substituted in equation (14) gives

$$\ddot{z} = \frac{v_o^2}{r_o} \frac{z}{\left[ B_z \right]_{\substack{r=r_o \\ z=0}}} \left[ \frac{dB_z(r, z)}{dr} \right]_{\substack{r=r_o \\ z=0}}$$

When  $\omega$  is defined as  $\omega \equiv \frac{v_o}{r_o}$

$$\ddot{z} = \omega^2 z \frac{r_o}{\left[ B_z \right]_{\substack{r=r_o \\ z=0}}} \left[ \frac{dB_z(r, z)}{dr} \right]_{\substack{r=r_o \\ z=0}}$$

Define a field index as

$$n(r) \equiv \frac{-r}{\left[ B_z(r, z) \right]_{z=0}} \left[ \frac{\partial B_z(r, z)}{\partial r} \right]_{z=0} \quad (15)$$

Using this and (to conform with the notation of the previous section) writing  $y$  in place of  $z$ , as the axial coordinate of the cylindrical system, the equation of motion simplifies to

$$\ddot{y} + \omega^2 n(r_0) y = 0 \quad (16)$$

This has a solution,

$$y = A \cos n^{1/2} \omega t + B \sin n^{1/2} \omega t$$

If  $\alpha$  is taken as the angle through which the magnetic field is effective,

$$y = A \cos n^{1/2} \alpha + B \sin n^{1/2} \alpha$$

Note that  $\alpha$  can also be written  $\frac{z}{\rho}$ , so that

$$y' = \frac{dy}{dz} = -\frac{An^{1/2}}{\rho} \sin n^{1/2} \alpha + \frac{Bn^{1/2}}{\rho} \cos n^{1/2} \alpha$$

With the initial conditions,  $y = y_0$  and  $y' = y'_0 = 0$ , the constants are  $A = y_0$  and  $B = \frac{y_0 \rho}{n^{1/2}}$ , and

$$y = y_0 \cos n^{1/2} \alpha + y'_0 \frac{\rho}{n^{1/2}} \sin n^{1/2} \alpha \quad (17)$$

$$y' = -y_0 \frac{n^{1/2}}{\rho} \sin n^{1/2} \alpha + y'_0 \cos n^{1/2} \alpha$$

Equation (17) can be rewritten in a single three by three matrix equation. As in the case for the magnetic quadrupole, the momentum terms appear only in second or higher order, so that zeros may be placed for the coefficients of the momentum term.

$$\begin{pmatrix} y \\ y' \\ \frac{\Delta p}{p_0} \end{pmatrix} = \begin{pmatrix} \cos n^{1/2} \alpha & \frac{\rho}{n^{1/2}} \sin n^{1/2} \alpha & 0 \\ -\frac{n^{1/2}}{\rho} \sin n^{1/2} \alpha & \cos n^{1/2} \alpha & 0 \\ 0 & 0 & 1 \end{pmatrix} \begin{pmatrix} y_0 \\ y'_0 \\ \frac{\Delta p}{p_0} \end{pmatrix} \quad (18)$$

Returning now to conventional custom, the axial coordinate of the cylindrical system is again written as  $Z$ , and the radial motion is considered.

Since  $B_\theta$  is zero, the radial component of the Lorentz force is

$$F_r = q v_\theta B_z.$$

Again the mass is independent of time and can be taken out of the time derivative of the momentum and the radial acceleration can, hence, be written as  $\ddot{r} - \frac{v_\theta^2}{r}$ . The equation of motion is then

$$\ddot{r} - \frac{v_\theta^2}{r} = \frac{q v_\theta B_z}{m} \quad (19)$$

Again, the equation is expanded in terms of the deviation from the optic axis and  $\Delta p$ . First, expanding  $v_\theta$ ,  $B_z$ , and  $r$ ,

$$\frac{d^2}{dt^2} (r_0 + x) - \frac{v^2}{r_0} \left( 1 - \frac{v_x^2 + v_z^2}{v^2} \right) \left( 1 - \frac{x}{r_0} + \dots \right) =$$

$$\frac{q}{m} v \left( 1 - \frac{1}{2} \frac{v_x^2 + v_z^2}{v^2} + \dots \right) \left( \left[ B_z \right]_{r=r_0} + x \left[ \frac{dB_z}{dr} \right]_{r=r_0} + \dots \right)$$

Keeping only the linear terms in the deviation from the optic axis,

$$\ddot{x} - \frac{v^2}{r_0} \left(1 - \frac{x}{r_0}\right) = \frac{q}{m} v \left( \left[ B_z \right]_{r=r_0} + x \left[ \frac{dB_z}{dr} \right]_{r=r_0} \right) \quad (20)$$

Expand  $p$ , in terms of  $\Delta p$  and  $v$  in terms of the corresponding  $\Delta v$ ,

$$\ddot{x} - \frac{(v_0 + \Delta v)^2}{r_0} \left(1 - \frac{x}{r_0}\right) = \frac{q}{p_0} (v_0 + \Delta v)^2 \left(1 - \frac{\Delta p}{p_0} + \dots\right) \left( \left[ B_z \right]_{r=r_0} + x \left[ \frac{dB_z}{dr} \right]_{r=r_0} \right)$$

If only the linear terms in the deviations from the central momentum and the optic axis is kept, this becomes

$$\ddot{x} - \frac{v_0^2}{r_0} + \frac{v_0^2}{r_0^2} x - \frac{2 v_0 \Delta v}{r_0} = \quad (21)$$

$$\frac{q}{p_0} v_0^2 \left[ B_z \right]_{r=r_0} + \frac{q}{p_0} v_0^2 x \left[ \frac{dB_z}{dr} \right]_{r=r_0} - \frac{q}{p_0} v_0^2 \frac{\Delta p}{p_0} \left[ B_z \right]_{r=r_0} + \frac{2q v_0 \Delta v}{p_0} \left[ B_z \right]_{r=r_0}$$

Using the relations  $p_0 = -q r_0 \left[ B_z \right]_{r=r_0}$  and  $\omega \equiv \frac{v_0}{r_0}$ ,

one can form the relations,

$$\frac{q v_o^2 \left[ B_z \right]_{r=r_o}}{p_o} = \frac{v_o^2}{r_o}; \quad \frac{q v_o^2}{p_o} = - \frac{r_o \omega^2}{\left[ B_z \right]_{r=r_o}}; \quad \text{and } \omega = - \frac{q v_o \left[ B_z \right]_{r=r_o}}{p_o}$$

Substituting these in equation (21) and combining terms,

$$\ddot{x} + \omega^2 x - r_o \omega^2 \frac{\Delta p}{p_o} + \omega^2 x \left[ \frac{B_z}{B_z} \right]_{r=r_o} \left[ \frac{dB_z}{dr} \right]_{r=r_o} = 0 \quad (22)$$

Making use of the field index defined by equation (15) and writing  $\rho$  in place of  $r_o$  yields

$$\ddot{x} + \omega^2 (1 - n) x = \rho \omega^2 \frac{\Delta p}{p_o} \quad (23)$$

The general solution to this equation is

$$\begin{aligned} x &= \frac{\rho}{1 - n} \frac{\Delta p}{p_o} + A \cos \omega (1 - n)^{1/2} t + B \sin \omega (1 - n)^{1/2} t \\ &= \frac{\rho}{1 - n} \frac{\Delta p}{p_o} + A \cos (1 - n)^{1/2} \alpha + B \sin (1 - n)^{1/2} \alpha \end{aligned}$$

where  $\alpha$  is the angle through which the magnetic field is effective.

Examine the solution to the equation  $\ddot{s} + \omega^2 (1 - n) s = 0$  which is the same as equation (23) except that the right side has been set equal to zero. A solution to this equation is

$$s = A \cos (1 - n)^{1/2} \alpha + B \sin (1 - n)^{1/2} \alpha$$

and the derivative is

$$s' = \frac{ds}{dz} = - \frac{(1-n)^{1/2}}{\rho} A \sin (1-n)^{1/2} \alpha + \frac{(1-n)^{1/2}}{\rho} B \cos (1-n)^{1/2} \alpha$$

The initial conditions,  $s = s_0$  and  $s' = s'_0$  at  $z = z_0 = 0$ , gives the constants,  $A = s_0$  and  $B = \frac{s'_0 \rho}{(1-n)^{1/2}}$ . Equations

for  $s$  and  $s'$  are

$$s = s_0 \cos (1-n)^{1/2} \alpha + \frac{\rho s'_0}{(1-n)^{1/2}} \sin (1-n)^{1/2} \alpha$$

$$s' = - \frac{(1-n)^{1/2}}{\rho} s_0 \sin (1-n)^{1/2} \alpha + s'_0 \cos (1-n)^{1/2} \alpha$$

which in matrix notation can be written

$$\begin{pmatrix} s \\ s' \end{pmatrix} = \begin{pmatrix} \cos (1-n)^{1/2} \alpha & \frac{\rho}{(1-n)^{1/2}} \sin (1-n)^{1/2} \alpha \\ - \frac{(1-n)^{1/2}}{\rho} \sin (1-n)^{1/2} \alpha & \cos (1-n)^{1/2} \alpha \end{pmatrix} \begin{pmatrix} s_0 \\ s'_0 \end{pmatrix}$$

Now change the variable,  $s$ , to  $x$ . Since  $s = x - \frac{\rho}{1-n} \frac{\Delta p}{p_0}$

and  $s' = x'$ ,

$$\begin{pmatrix} x - \frac{\rho}{1-n} \frac{\Delta p}{p_0} \\ x' \end{pmatrix} = \begin{pmatrix} \cos (1-n)^{1/2} \alpha & \frac{\rho}{(1-n)^{1/2}} \sin (1-n)^{1/2} \alpha \\ - \frac{(1-n)^{1/2}}{\rho} \sin (1-n)^{1/2} \alpha & \cos (1-n)^{1/2} \alpha \end{pmatrix} \begin{pmatrix} x_0 - \frac{\rho}{1-n} \frac{\Delta p}{p_0} \\ x'_0 \end{pmatrix}$$

Writing this out in terms of  $x$  and  $x'$ ,

$$x = x_0 \cos (1 - n)^{1/2} \alpha + x'_0 \frac{\rho}{(1 - n)^{1/2}} \sin (1 - n)^{1/2} \alpha +$$

$$\frac{\Delta p}{p_0} \frac{\rho}{1 - n} (1 - \cos (1 - n)^{1/2} \alpha)$$

$$x' = -x_0 \frac{(1 - n)^{1/2}}{\rho} \sin (1 - n)^{1/2} \alpha + x'_0 \cos (1 - n)^{1/2} \alpha +$$

$$\frac{\Delta p}{p_0} \frac{1}{(1 - n)^{1/2}} \sin (1 - n)^{1/2} \alpha$$

In matrix notation, this becomes

$$\begin{pmatrix} x \\ x' \\ \frac{\Delta p}{p_0} \end{pmatrix} = \begin{pmatrix} \cos (1 - n)^{1/2} \alpha & \frac{\rho}{(1 - n)^{1/2}} \sin (1 - n)^{1/2} \alpha & 0 \\ -\frac{(1 - n)^{1/2}}{\rho} \sin (1 - n)^{1/2} \alpha & \cos (1 - n)^{1/2} \alpha & 0 \\ 0 & 0 & 1 \end{pmatrix} \begin{pmatrix} x_0 \\ x'_0 \\ \frac{\Delta p}{p_0} \end{pmatrix} \quad (24)$$

$$\begin{pmatrix} \frac{\rho}{1 - n} [1 - \cos (1 - n)^{1/2} \alpha] \\ \frac{1}{(1 - n)^{1/2}} \sin (1 - n)^{1/2} \alpha \\ 1 \end{pmatrix} \begin{pmatrix} x_0 \\ x'_0 \\ \frac{\Delta p}{p_0} \end{pmatrix}$$

### C. Edge Effect for the Bending Magnet

Consider now the effect of the edges of the magnet. In the general case, these may be non-normal to the central ray (Figure 2).

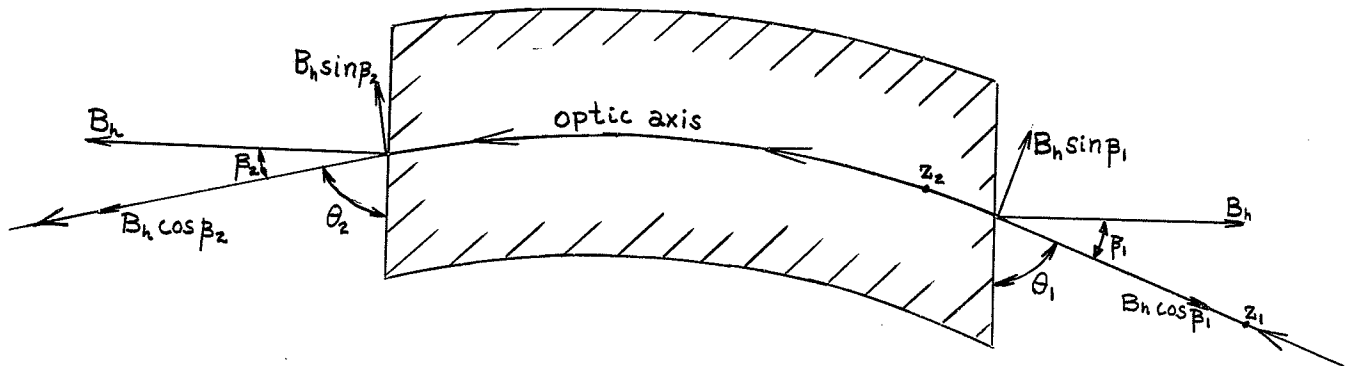


Figure 2. Edge effect of the bending magnet. The central ray enters from the right and exits to the left, with angles  $\beta_1$  and  $\beta_2$ , respectively, away from the normals to the entrance and exit edges of the magnet.

Consider, first the axial focusing effect of the edges. As long as  $\theta_1$  and  $\theta_2$ , as shown in the figure, are less than  $90^\circ$ , there is axial edge focusing. At any point displaced from the median plane, a component  $B_h$  of  $B$  exists due to the bulging field at the edge. Assume that this edge field exists over a very short range, and hence, assume that the force due to the field changes the direction of the particle but not its position. Using coordinates where the  $z$  - axis is along the optic axis, the axial equation of motion in the edge region is

$$\frac{d}{dt} m\dot{y} = q (v_x B_h \cos \beta_{1,2} - v_z B_h \sin \beta_{1,2}) \quad (25)$$

Take points,  $z_1$  and  $z_2$ , as in Figure 2, which are



outside the influence of the edge field  $B_h$ . Consider a rectangular path which lies in the  $y$ - $z$  plane between  $z_1$  and  $z_2$ . Let one side of the rectangle lie on the optic axis and the opposite side displaced by a distance,  $y$ , which is same as the axial coordinate of the particle as it passes through the edge region. Carrying a unit magnetic pole about this path, starting at  $z_1$  on the median plane, no work is done in carrying the pole away from the plane through a distance  $y$ , since no field exists at  $z_1$ . However, in going from  $z_1$  to  $z_2$  along the displaced path requires  $\int_{z_1}^{z_2} B_h \cos \beta_{1,2} dz$  of work. The work done in going back to the median plane at  $z_2$  is  $-yB$ , but the work done in going from  $z_2$  to  $z_1$  along the median plane is zero, since the field is perpendicular to the median plane at all points. Since there are no sources in the loop, the total work done in going around the loop has to be zero, so that

$$\int_{z_1}^{z_2} B_h \cos \beta_{1,2} dz = -yB \quad (26)$$

Since the edge field has been assumed to extend only over a very short distance, change in the coordinates in crossing the edge can be neglected. Hence, the contour of (26) corresponds to the particle trajectory.

Going back to equation (25), the first term on the right is second order, since  $B_h$  is proportional to  $y$  by equation (26). The mass is, again, independent of time and may be taken out of the time derivative.  $\frac{d}{dt} \dot{y}$  may be written as  $v_z \left( \frac{d}{dz} \frac{dy}{dt} \right)$ , so that

$$\frac{d}{dz} \dot{y} = - \frac{q}{m} B_h \sin \beta_{1,2}$$

Integrating this equation along the particle trajectory in the edge region,

$$\int_{z_1}^{z_2} d(\dot{y}) = \frac{q}{m} \sin \beta_{1,2} \int_{z_1}^{z_2} B_h dz = \frac{q}{m} \tan \beta_{1,2}$$

$$\int_{z_1}^{z_2} B_h \cos \beta_{1,2} dz$$

Using equation (26), this becomes

$$\dot{y} \Big|_{z_1}^{z_2} = \frac{q}{m} y B \tan \beta_{1,2}$$

but  $\dot{y} = \frac{dz}{dt} \frac{dy}{dz} = v_z y'$ , and as before,  $v_z = v$  to first order, so that

$$y' \Big|_{z_1}^{z_2} = \frac{q}{mv} y B \tan \beta_{1,2}$$

Consider a deviation from the central momentum, and

expand in terms of  $\Delta p$ ,

$$y' \begin{vmatrix} z_2 \\ z_1 \end{vmatrix} = \frac{q}{p_0} \left( 1 - \frac{\Delta p}{p_0} + \dots \right) y B \tan \beta_{1,2}$$

Keeping only first order terms in the small quantities, this becomes

$$y' \begin{vmatrix} z_2 \\ z_1 \end{vmatrix} = \frac{q}{p_0} y B \tan \beta_{1,2}$$

Using the relation,  $p_0 = -q r_0 B$

$$y' \begin{vmatrix} z_2 \\ z_1 \end{vmatrix} = -\frac{y}{\rho} \tan \beta_{1,2} \quad (27)$$

where  $r_0$  has been replaced by  $\rho$ .

Note that the equation holds for both entry and exit.

Radially, the rotation of the pole edge tends to defocus the beam when  $\theta_1$  and  $\theta_2$  are less than  $90^\circ$ . Consider the entry into the magnet in Figure 3. DG is the central ray entering the magnet at E and AC is another ray entering at B. Assume that AB and DE are very nearly parallel, so that  $BH \approx x$ , and  $\angle JBA = \angle HBE \approx \beta_1$ . Also assume that  $x$  is small enough so that  $EF \approx EH$ . When ray AC reaches B, ray DG from the same source has reached the point F. The angle  $\phi$

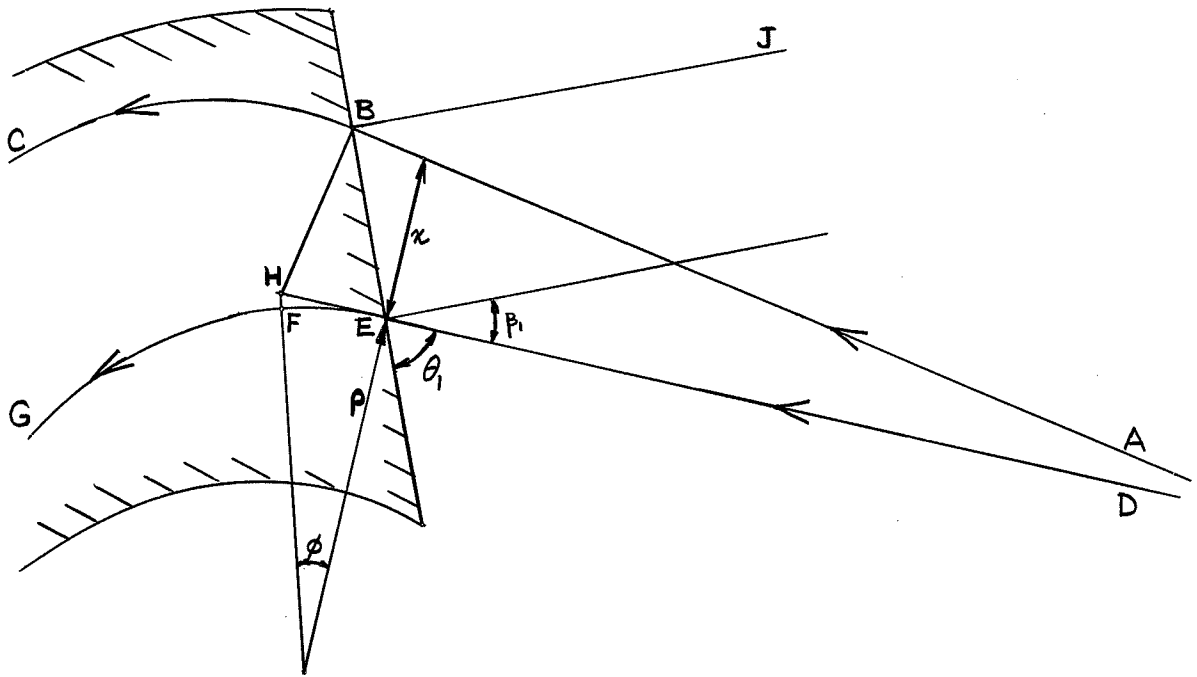


Figure 3. Geometry of non-normal entry into a bending magnet.

can be written

$$\phi = \frac{EF}{\rho} \approx \frac{HE}{\rho} = \frac{BE \sin \angle EBH}{\rho} \approx \frac{\frac{BH}{\cos \beta_1} \sin \beta_1}{\rho} \approx \frac{x \tan \beta_1}{\rho}$$

$$\text{Since } \phi = \frac{\Delta x}{\Delta z} \approx \frac{dx}{dz}, \quad x' = \frac{x \tan \beta_1}{\rho}$$

Similar argument will show that for  $\theta_2$  less than  $90^\circ$ ,  $x' = \frac{x \tan \beta_2}{\rho}$  at the exit. Writing these equations in matrix form, the radial motion can be written as

$$\begin{pmatrix} x \\ x' \end{pmatrix} = \begin{pmatrix} 1 & 0 \\ \frac{\tan \beta_1}{\rho} & 1 \end{pmatrix} \begin{pmatrix} x_i \\ x'_i \end{pmatrix}$$

and the axial motion

$$\begin{pmatrix} y \\ y' \end{pmatrix} = \begin{pmatrix} 1 & 0 \\ -\frac{\tan \beta_1}{\rho} & 1 \end{pmatrix} \begin{pmatrix} y_i \\ y'_i \end{pmatrix}$$

One can generalize the bending magnet equations by including these edge effects. For the radial matrix equation

$$M_x = \begin{pmatrix} 1 & 0 & 0 \\ \frac{\tan \beta_2}{\rho} & 1 & 0 \\ 0 & 0 & 1 \end{pmatrix} \begin{pmatrix} \text{3 X 3 matrix} \\ \text{given in (25)} \end{pmatrix} \begin{pmatrix} 1 & 0 & 0 \\ \frac{\tan \beta_1}{\rho} & 1 & 0 \\ 0 & 0 & 1 \end{pmatrix} \quad (28)$$

Similarly, for the axial matrix

$$M_Y = \begin{pmatrix} 1 & 0 & 0 \\ -\frac{\tan \beta_2}{\rho} & 1 & 0 \\ 0 & 0 & 1 \end{pmatrix} \begin{pmatrix} \text{3 X 3 matrix} \\ \text{given in (17)} \end{pmatrix} \begin{pmatrix} 1 & 0 & 0 \\ -\frac{\tan \beta_1}{\rho} & 1 & 0 \\ 0 & 0 & 1 \end{pmatrix} \quad (29)$$

In the same manner as in the case of the quadrupoles, these two matrices can be combined to form a single six by six matrix, i.e.,

$$M = \begin{pmatrix} M_X & (28) & 0 & 0 & 0 \\ & & 0 & 0 & 0 \\ & & 0 & 0 & 0 \\ 0 & 0 & 0 & & \\ 0 & 0 & 0 & & M_Y & (29) \\ 0 & 0 & 0 & & & \end{pmatrix} \quad (30)$$

#### D. Relative Orientation and Separation

It is desirable in many cases to have an angular orientation between two systems which is other than zero. To achieve this rotation, one can transform the quadrupole or bending magnet matrix by a rotation matrix. This is accomplished by making a conventional similarity transformation by an Euler transformation matrix. For a rotation about the z axis through an angle  $\theta$ ,

$$\begin{pmatrix} x \\ y \end{pmatrix} = \begin{pmatrix} \cos \theta & \sin \theta \\ -\sin \theta & \cos \theta \end{pmatrix} \begin{pmatrix} x_0 \\ y_0 \end{pmatrix}$$

A suitable transformation matrix is obtained by expanding this to a six by six matrix,

$$R = \begin{pmatrix} \cos \theta & 0 & 0 & \sin \theta & 0 & 0 \\ 0 & \cos \theta & 0 & 0 & \sin \theta & 0 \\ 0 & 0 & 1 & 0 & 0 & 0 \\ -\sin \theta & 0 & 0 & \cos \theta & 0 & 0 \\ 0 & -\sin \theta & 0 & 0 & \cos \theta & 0 \\ 0 & 0 & 0 & 0 & 0 & 1 \end{pmatrix} \quad (31)$$

To separate a magnetic system from another by empty space, a matrix is needed which will multiply the derivatives with respect to  $z$  by the separation distance, and add it on to the displacements. This matrix is simply,

$$D = \begin{pmatrix} 1 & d & 0 & 0 & 0 & 0 \\ 0 & 1 & 0 & 0 & 0 & 0 \\ 0 & 0 & 1 & 0 & 0 & 0 \\ 0 & 0 & \cancel{1} & \cancel{d} & d & 0 \\ 0 & 0 & 0 & 0 & 1 & 0 \\ 0 & 0 & 0 & 0 & 0 & 1 \end{pmatrix} \quad (32)$$

All the matrices necessary to form a final product which will describe the combined effect of placing several systems in series have been derived.

### E. Relation of Beam Properties to the Matrix Describing the Focusing Systems

The several properties of interest, derivable from the final combined matrix, are the focal lengths, magnifications, image distances, and the resolutions. We can find the correspondence between the matrix elements and the optical properties by considering the combined system to be a thick lens.

Consider just the two by two matrix equation

$$\begin{pmatrix} x \\ x' \end{pmatrix} = \begin{pmatrix} A_{11} & A_{12} \\ A_{21} & A_{22} \end{pmatrix} \begin{pmatrix} x_0 \\ x'_0 \end{pmatrix}$$

To find the distance,  $b$ , as given in Figure 4, which is the distance from the magnet boundary to the focal point, solve the following equation

$$\begin{pmatrix} 0 \\ x' \end{pmatrix} = \begin{pmatrix} 1 & b \\ 0 & 1 \end{pmatrix} \begin{pmatrix} A_{11} & A_{12} \\ A_{21} & A_{22} \end{pmatrix} \begin{pmatrix} x_0 \\ 0 \end{pmatrix} \quad (33)$$

which describes a parallel beam being bent by the lens and focusing at a point,  $b$ , beyond the magnet. When solved,

$b = \frac{-A_{11}}{A_{21}}$ . Similarly, by solving the following equation



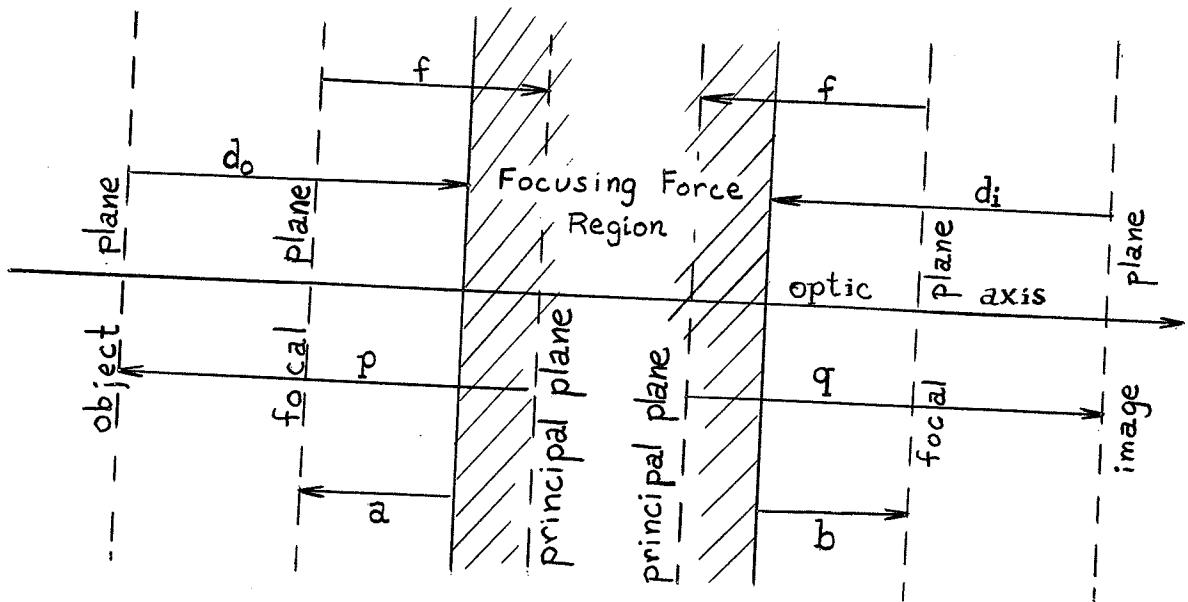


Figure 4. Diagram showing the relative positions of the object plane, focal planes, principal planes, image plane, and the focusing region.

$$\begin{pmatrix} x_o \\ o \end{pmatrix} = \begin{pmatrix} A_{11} & A_{12} \\ A_{21} & A_{22} \end{pmatrix} \begin{pmatrix} 1 & a \\ 0 & 1 \end{pmatrix} \begin{pmatrix} o \\ x' \end{pmatrix}, \quad (34)$$

$$a = -\frac{A_{22}}{A_{21}}.$$

The focal length,  $f$ , can be found by extending the equation (33) until the final displacement away from the  $z$  axis is same as the initial displacement, i.e.,

$$\begin{pmatrix} x \\ x' \end{pmatrix} = \begin{pmatrix} 1 & f \\ 0 & 1 \end{pmatrix} \begin{pmatrix} 1 & b \\ 0 & 1 \end{pmatrix} \begin{pmatrix} A_{11} & A_{12} \\ A_{21} & A_{22} \end{pmatrix} \begin{pmatrix} x \\ 0 \end{pmatrix} \quad (35)$$

This equation, when solved for  $f$ , gives  $f = -\frac{1}{A_{21}}$ .

The magnification is given by  $M = \frac{q}{p}$ . Use the

equation from optics,  $\frac{1}{p} + \frac{1}{q} = \frac{1}{f}$ , to rewrite  $M$  as  $M = \frac{f}{p - f}$ .

Looking at Figure 4,  $p - f = d_o - a$ , so that  $M = \frac{f}{d_o - a}$ .

$M$  can be also written as  $M = \frac{q - f}{f}$ . From the figure,

the image distance may be written as  $d_i = (q - f) + b$ ,

and making use of the magnification relation, this becomes

$$d_i = Mf + b.$$

The momentum resolution, as indicated previously, is defined as:

$$R = \frac{1}{s_o} \frac{\Delta p}{p}$$

where  $s_o$  is the full width of the object slit of the system, and  $\Delta p/p$  is the fractional full width at half maximum of the momentum distribution transmitted by an image slit just wide enough to completely transmit all particles of the reference momentum.

An expression for the resolution in terms of the matrix elements is obtained by calculating the transverse displacement at the image plane of a ray starting initially on the optic axis but with displaced momentum, i.e., we solve for  $x$  in the equation:

$$\begin{pmatrix} x \\ x' \\ \frac{\Delta p}{p} \end{pmatrix} = \begin{pmatrix} 1 & d_i & 0 \\ 0 & 1 & 0 \\ 0 & 0 & 1 \end{pmatrix} \begin{pmatrix} A_{11} & A_{12} & A_{13} \\ A_{21} & A_{22} & A_{23} \\ 0 & 0 & 1 \end{pmatrix} \begin{pmatrix} 0 \\ 0 \\ \frac{\Delta p}{p} \end{pmatrix}.$$

where  $d_i$  is the image distance and the middle matrix can represent a single magnet or a combination of magnets (forming a "thick lens"). Solving yields  $x = (A_{13} + d_i A_{23}) \Delta p/p$ .

If this displacement just equals the image width  $MS_o$  of a monochromatic object the  $\Delta p/p$  is easily shown to be that specified in the resolution definition. Hence we have:

$$R = \frac{1}{s_o} \frac{\Delta p}{p} = \frac{1}{s_o} \frac{MS_o}{A_{13} + d_i A_{23}} = \frac{M}{A_{13} + d_i A_{23}}.$$

In terms of the six by six matrix used in the computer program, these properties are summarized as follows:

$$f_x = -\frac{1}{A_{21}}; \quad a_x = -\frac{A_{22}}{A_{21}}; \quad b_x = -\frac{A_{11}}{A_{21}};$$

$$M_x = \frac{f_x}{d_{ox} - a_x}; \quad d_{ix} = f_x M_x + b_x; \quad \frac{1}{s_{ox}} \frac{\Delta p}{p} = \frac{M_x}{A_{13} + d_{ix} A_{23}}$$

$$f_y = \frac{1}{A_{54}}; \quad a_y = \frac{A_{55}}{A_{54}}; \quad b_y = -\frac{A_{44}}{A_{54}}$$

$$M_y = \frac{f_y}{d_{oy} - a_y}; \quad d_{iz} = f_y M_y + b_y; \quad \frac{1}{s_{oy}} \frac{\Delta p}{p} = \frac{M_y}{A_{43} + d_{iy} A_{53}}$$

## II. THE COMPUTER PROGRAM FOR CALCULATING THE BEAM PROPERTIES

A computer program was written for the MISTIC, a 4096 word memory computer, located at Michigan State University, to calculate the beam properties of combined magnetic systems.

In order to make calculations for a system composed of several magnetic elements, the parameters are written in the same order as the elements actually appear in the combined system. Parameters necessary for this code are listed below along with their scaling:

Location	Parameter	Scaling
30	$\beta_1$	radians (fraction $10^{-1}$ )
31	$\beta_2$	radians (fraction $10^{-1}$ )
32	n	(fraction $10^{-1}$ )
33	$\rho$	(fraction $10^{-3}$ )
34	$\alpha$	radians (fraction $10^{-1}$ )
35	K	(fraction $10^{-1}$ )
36	L	(fraction $10^{-2}$ )
37	a	integer, a=1 for radially diverging quadrupole. a=2 for radially converging quadrupole.

Location	Parameter	Scaling
38	$\theta$	radians (fraction $10^{-2}$ )
39	d	(fraction $10^{-4}$ )
40	b	integer, b=1 for bending magnet. b=2 for quadrupole.
41	c	integer, c=0 for any system other than last. c=1 for the last system.
42	N	integer, number of prints + 1
43	$d_{ox}$	(fraction $10^{-5}$ )
44	$d_{oy}$	(fraction $10^{-5}$ )
45	$\Delta d_{ox}$	(fraction $10^{-5}$ )
46	$\Delta d_{oy}$	(fraction $10^{-5}$ )

These parameters are input by the Special Input Routine. On the tape the address is followed by an equal sign, fractions terminated by a space and integers terminated by a period. The code will read the parameters for each element and its relative position and form the appropriate matrix as described in the previous sections. This is done separately for each element and the matrices are multiplied in the same order that the parameters are written. The character, N, punched after the parameters for each element, will transfer to the proper location in the code to calculate the matrix for that element. Parameters are not erased after each element so that it is not necessary to input parameters for an element which are

identical to those of the previous element. The code will continue to read the next parameter set for the succeeding magnetic element until the parameter, C, has been set equal to 1.

After the last element has been calculated and matrix multiplied with the previous elements, the code calculates the radial and axial focal lengths,  $a_x'$ ,  $a_y'$ ,  $b_x'$ ,  $b_y'$  magnifications, image distances, and the resolutions of the combined system as a function of the object distance. These properties may be calculated again for a different object distance by inputting an appropriate increment of the object distance and specifying the number of times this is to be repeated by the parameter N. The code will calculate these properties only after the matrix for the last element has been formed and multiplied.

The code tests these properties for singularities during the calculations, and if any quantity exceeds scaling limitations, the code will skip this calculation and output an appropriate number of spaces so that the output format is not affected.

The bending magnet parameter,  $n$ , is specially tested for singularities which may occur in the equations. Hyperbolic functions replace the trigonometric functions where  $n$  is greater than one, and cases where  $n = 0$ , and  $n = 1$  are treated

separately.

The code is written in fixed point and the limitations on the parameters are, roughly,  $-2 < n < 2$ ,  $\rho < 10^3$ ,  $\alpha < 3\pi$ ,  $\beta_{1,2} < \pi/4$ ,  $KL < 2$ , and  $d < 10^4$ .

The code outputs the relative orientation and separation parameters, along with the magnet parameters and the radial and axial matrices for the bending magnet or the parameters K and L for the magnetic quadrupole, in the same order as they appear in the combined system. This is followed by the final combined system matrix and the various beam properties of the final system.

The scaling of the output is as follows: the parameter output is scaled the same way as the input; the individual matrices for the bending magnets are scaled by  $10^{-3}$ ; the total combined matrix is scaled by  $10^{-4}$ ;  $f$ ,  $a$ ,  $b$ ,  $M$ ,  $d_o$ , and  $d_i$  are all scaled by  $10^{-5}$  and the resolutions are scaled by  $10^{-2}$ .

A sample calculation of a system where a quadrupole is placed after a bending magnet is given below. The necessary input parameters are:

```
30=0 0 05 036 15707964 005 05 1.0 0 1.0.N.
40=2.1.7.00005 00005 0001 0001 N
```

The output is as follows:

D: +0000000000 THETA: +0000000000

ALPHA: +1570796400  
RHO: +3600000000  
N: +0500000000  
BETA, 1: +0000000000  
BETA, 2: +0000000000

MX

+0004440158 +0456178379 +0400308628  
-0000175975 +0004440158 +0012671623  
+0000000000 +0000000000 +0010000000

MY

+0004440149 +0456175389 +0000000000  
-0000175995 +0004440149 +0000000000  
+0000000000 +0000000000 +0010000000

D: +0000000000 THETA: +0000000000

K: +0050000000 L: +0500000000 A=1

M

+000036897 +004929971 +004769408 +000000000 +000000000 +000000000  
-000001255 +000103500 +000181299 +000000000 +000000000 +000000000  
+000000000 +000000000 +000100008 +000000000 +000000000 +000000000  
+000000000 +000000000 +000000000 +000034288 +004639642 +000000000  
+000000000 +000000000 +000000000 -000002256 -000013370 +000000018  
+000000000 +000000000 +000000000 +000000000 +000000000 +000100008

FX AX BX  
+0007966125 +0008244977 +0002939271  
FY AY BY  
+0004432700 -0000592633 +0001519881

DOX MX DIX RES. RAD. DOY MY DIY  
0000500 -00001029 -00052543 00021624 0000500 +00004057 +00195029  
0001500 -00001181 -00064691 00016972 0001500 +00002118 +00109094  
0002500 -00001387 -00081067 00013967 0002500 +00001433 +00078733  
0003500 -00001679 -00104347 00011866 0003500 +00001083 +00063209  
0004500 -00002127 -00140059 00010314 0004500 +00000870 +00053782  
0005500 -00002902 -00201790 00009122 0005500 +00000728 +00047449  
0006500 -00004565 -00334275 00008176 0006500 +00000625 +00042902  
0007500 -00010693 -00822434 00007408 0007500 +00000548 +00039479



RES. AX.

...  
...  
...  
...  
...  
...  
...  
...  
...

Running instructions for the code are:

1. Bootstrap the program tape.
2. Black switch the parameters.

The DOI input may be used when overwrites are desired. This is accomplished by using the white switch instead of the black switch. The transfer at the end of an overwrite should go back to location 1253 where the black switch - white switch stop is located.

### III. RESULTS

The computer program described in the previous section, has been used to calculate properties of a number of analyzing and focusing systems.

#### A. Single $90^\circ$ Bending Magnets

Figure 5 shows the radial resolution, image distance, and magnification of an  $n = 0$  bending magnet with  $90^\circ$  bending angle, and the edges set for normal entry and exit ( $\beta_1 = \beta_2 = 0^\circ$ ). The field strength is such that the radius of curvature of the optic axis is 36 inches. The radial focal planes of this magnet are located exactly at the edges of the magnet and are 36 inches from their respective principal planes located in the field region. For unit magnification the object slit must be located a focal length, i.e., 36 inches, in front of the edge. The axial focal length is, of course, infinite for this magnet. The radial resolution is seen to improve as the object distance is increased, but there is a natural limit for this improvement, since the aperture of the magnet and the dimensions of the working area make it impractical to arbitrarily extend the object distance. The loss at the

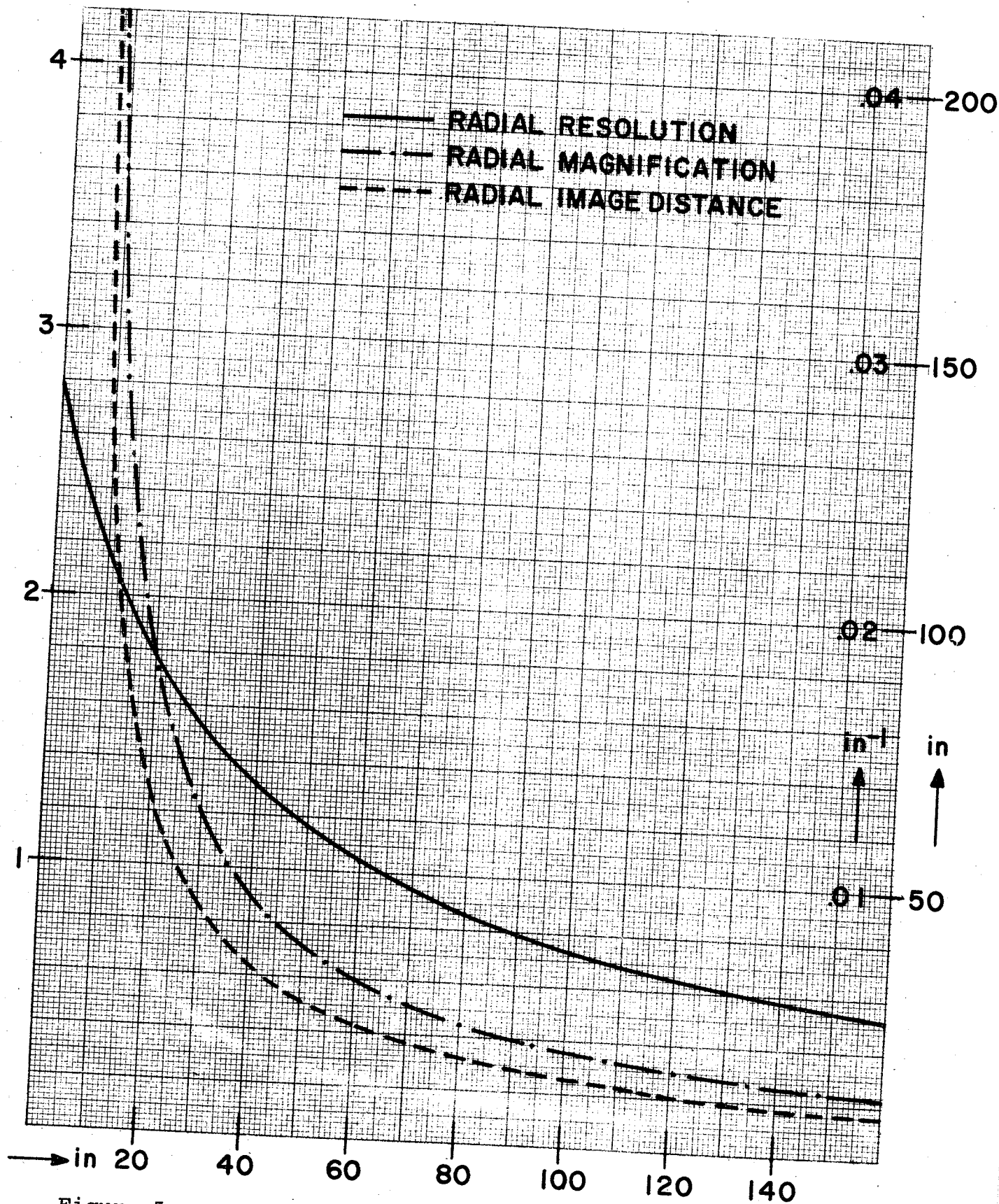


Figure 5. Radial resolution, radial image distance, and radial magnification of a single  $n = 0$ ,  $\rho = 36$  in.,  $\alpha = 90^\circ$  and  $\beta_1 = \beta_2 = 0^\circ$  bending magnet plotted against the object distance.

aperture occurs because the beam dimension becomes larger than the aperture, due to the increase in object distance. The fractional half maximum width of the momentum distribution transmitted by a matched image slit is obtained by multiplying the resolution by the source slit width. For example, in Figure 5, the resolution has a value  $.0116 \text{ in}^{-1}$  when the object distance is 50 inches. If the source slit width is  $.2$  inches, the fractional half maximum width of the transmitted momentum distribution will be  $.232\%$ .

Figure 6 shows the properties of an  $n = 1/2$  bending magnet with parameters otherwise the same as for  $n = 0$  magnet. This magnet is completely double focusing, i.e., radial and axial optical properties are identical to each other. The focal planes are located  $56.7$  inches from the principal planes and  $25.2$  inches away from the magnet edges. When the object slit is placed a focal length in front of the focal plane, we have unit magnification. The image distance is negative unless the object is placed, at least, beyond the focal plane. A parallel beam results, if the source slit is placed at the focal plane. Again the resolution improves with increasing object distance and is slightly better for a given object distance than that for an  $n = 0$  magnet. Although the magnification is infinite when the object distance is  $25.2$  inches, the resolution has a finite value,  $.014 \text{ in}^{-1}$ ,

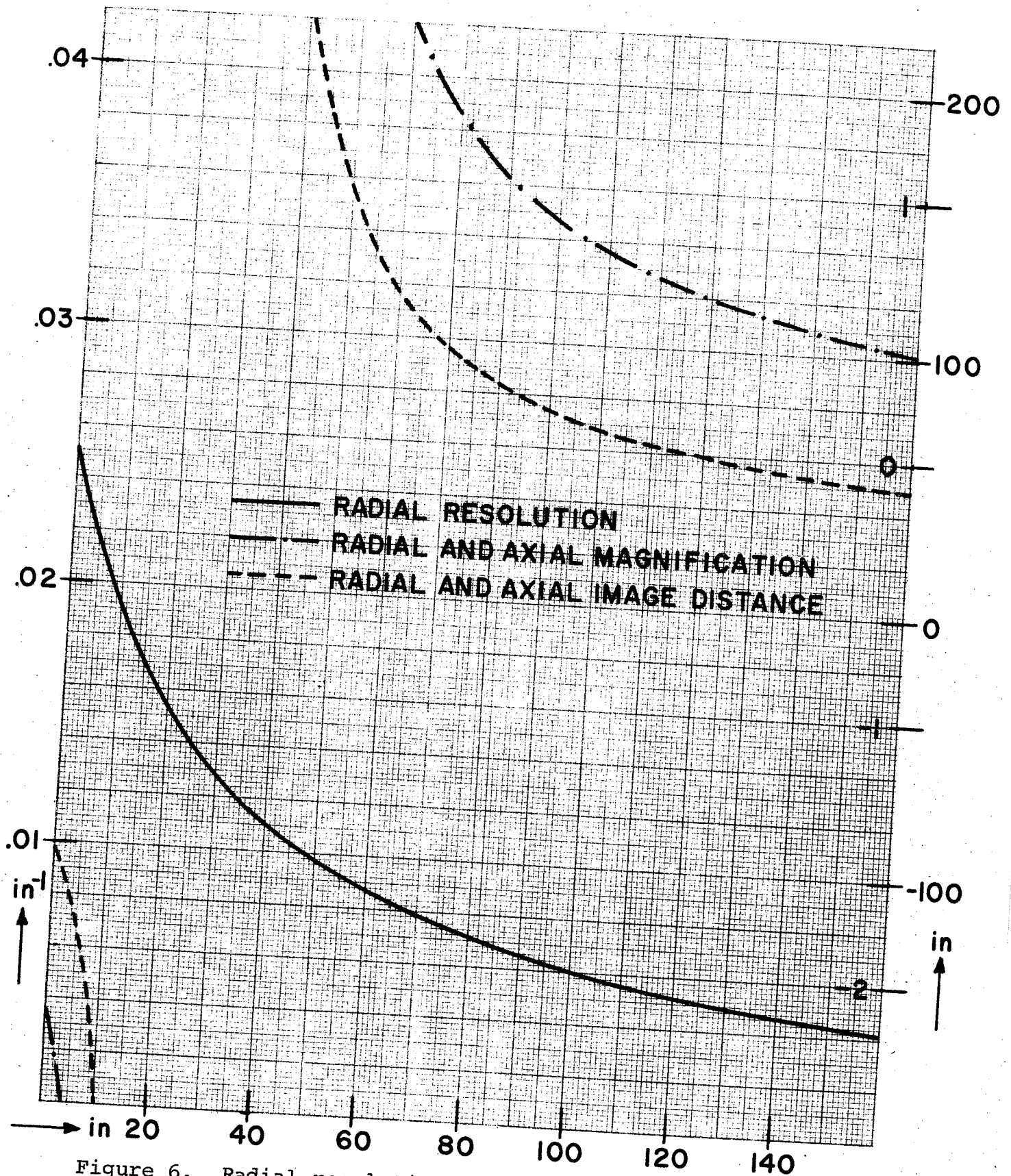


Figure 6. Radial resolution, radial and axial image distances, and radial and axial magnification of a single  $n = \frac{1}{2}$ ,  $\rho = 36$  in.,  $\alpha = 90^\circ$  and  $\beta_1 = \beta_2 = 0^\circ$  bending magnet plotted against the object distance.

since the image distance is also infinite at this point. The radial focusing of the  $n = 1/2$  magnet is seen to be weak as compared to the  $n = 0$  magnet. For example, unit magnification occurs at 81.9 inches for the  $n = 1/2$  magnet and at 36 inches for the  $n = 0$  magnet.

### B. Single Quadrupole Magnet

Figure 7 shows the properties of a single, five inch quadrupole as a function of field strength. Although not shown explicitly on the figure, when the object is placed a focal length before the focal plane, i.e., object distance equal to  $f + b$ , there is unit magnification as expected.

### C. Bending Magnet Pairs

Consider, now, systems consisting of two bending magnets. The bending planes for two bending magnets in a series need not be the same. It is possible to rotate the bending plane of the second magnet about the optic axis joining the two magnets so that it has some angular relation to the bending plane of the first magnet. The angle between the two bending planes, specified by  $\theta$ , is defined such that when  $\theta = 0^\circ$  the two magnets bend the beam in the same plane and to the same side of the optic axis entering each magnet. For example, if there are two  $90^\circ$  bending magnets which are

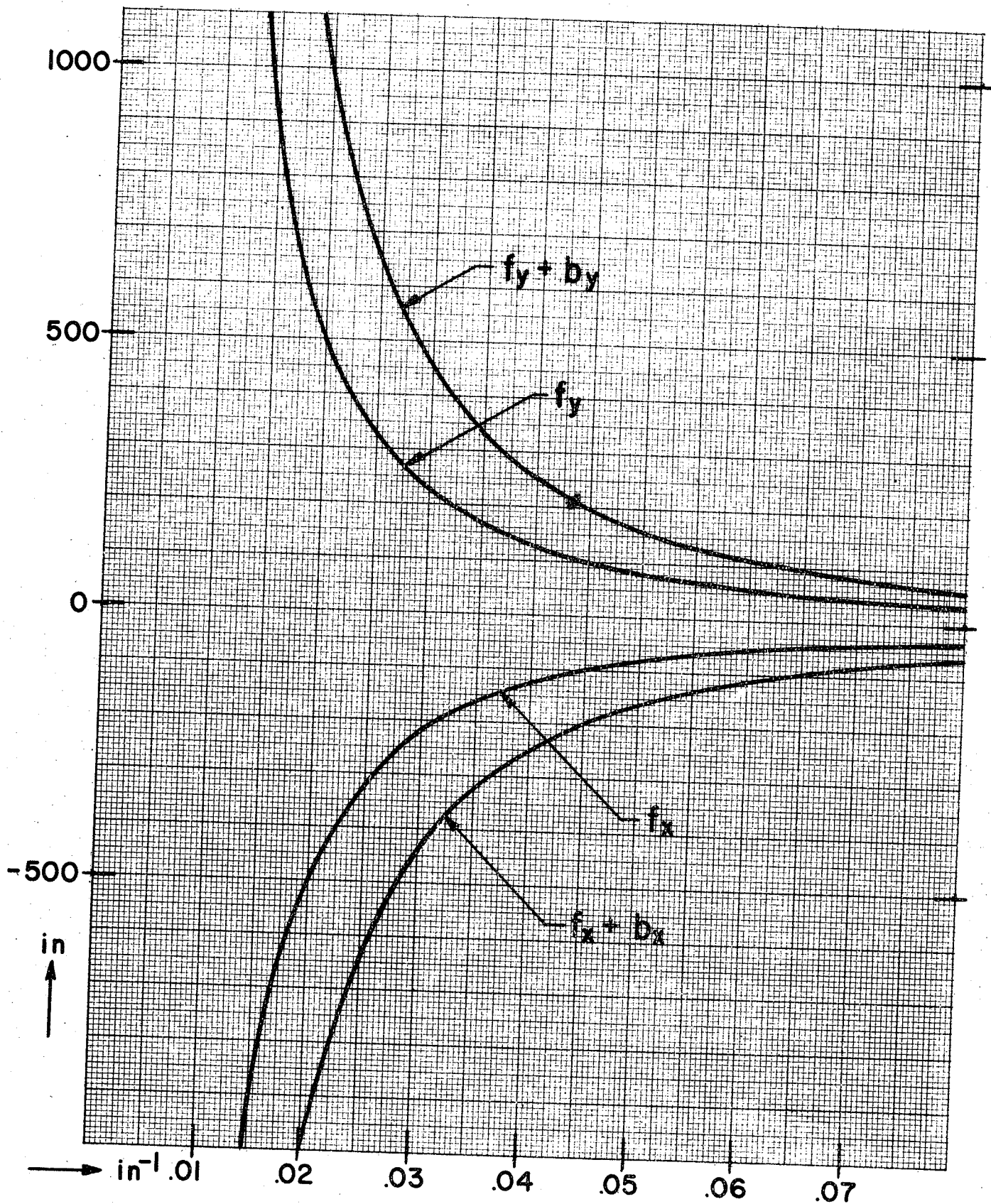


Figure 7. Radial and axial focal lengths and distances, focal length away from the focal plane of a single magnetic quadrupole, plotted against  $K$ , where  $K$  was defined to be  $K^2 = \frac{qG}{p_0}$  and has units of  $\text{in}^{-1}$ .

oriented such that  $\theta = 0^\circ$ , the outgoing beam from the system will be antiparallel to the incoming beam, and if these magnets are oriented such that  $\theta = 180^\circ$ , the outgoing beam will be parallel to the incoming beam.

Figures 8, 10, 12, 14, and 16 show the radial and axial resolutions of two  $n = 0$  bending magnets, which have the same field strength and bending angle as the single magnet described in A. Several relative angular orientations of the two magnets are considered, and for each orientation, several separation distances are taken. Figures 9, 11, 13, 15, and 17 show corresponding results for two  $n = 1/2$  magnets with the same field strengths and bending angles as the  $n = 0$  magnets.

In the several orientations taken for both the  $n = 0$  and  $n = 1/2$  magnet combinations, when the bending of the beam takes place in a single plane, there is first order resolution only in that plane. Figure 8 is a plot of the radial resolution for the  $n = 0$  bending magnets with  $\theta = 0^\circ$ . This plot shows three peaks in each of the three out of four curves plotted. From the way in which the  $d = 10$  inch curve corresponds to the other three, it can be seen that there exists a peak in this curve, also, for a greater object distance. These peaks correspond to maximum transmission and no resolution. For improved resolution the source slit has to be moved away from



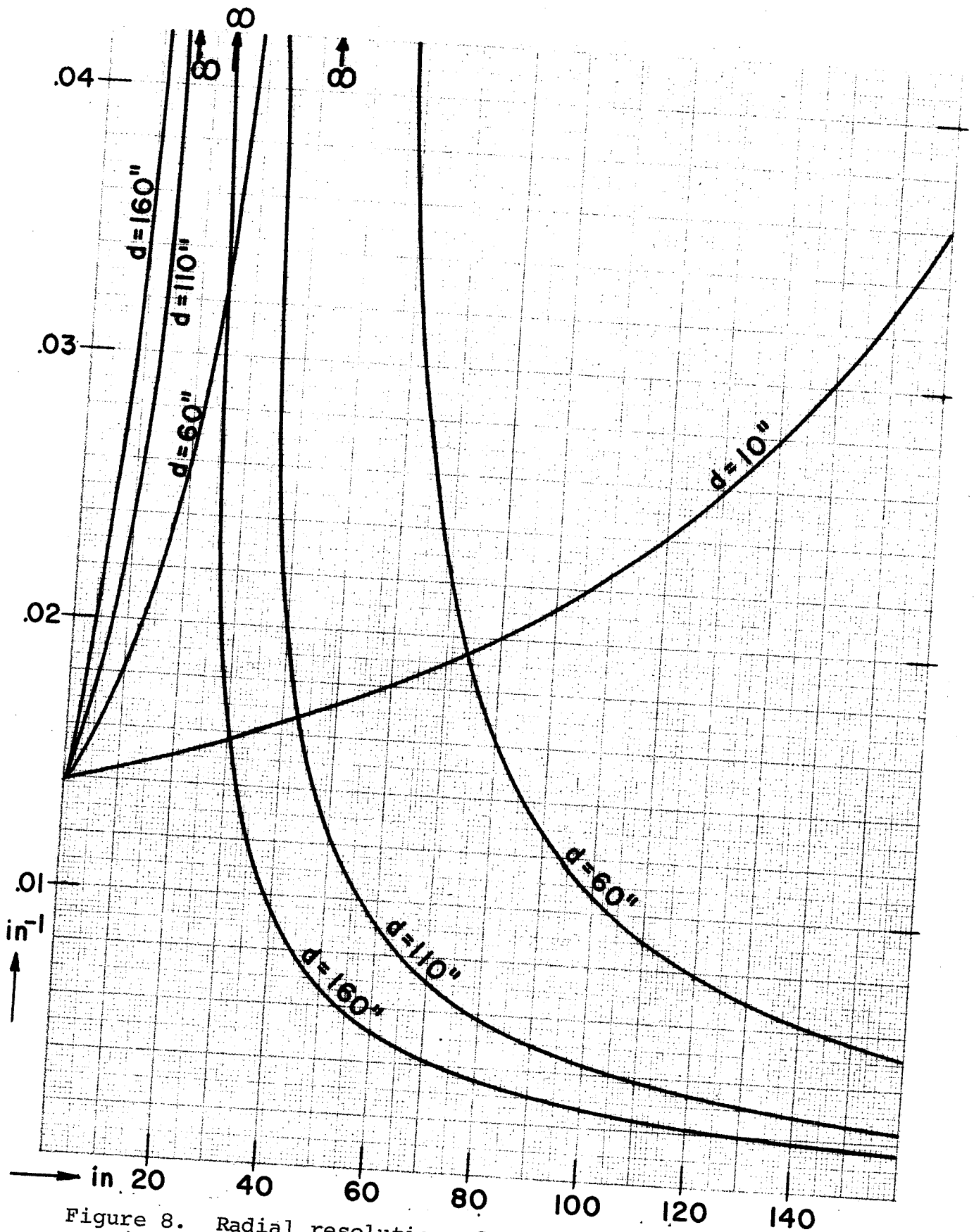


Figure 8. Radial resolution of a system consisting of two bending magnets oriented so that  $\beta_1 = \beta_2 = 0^\circ$ ,  $n = 0$ ,  $\rho = 36$  in.,  $\alpha = 90^\circ$ , and  $\theta = 0^\circ$ . Plotted against the object distance in inches for the separation distances  $d = 10$  in.,  $60$  in.,  $110$  in., and  $160$  in.

the positions where the peaks appear, and have to be placed either far away from the magnet or nearer the focal plane of the first magnet. The intensity is sacrificed with an increase in object distance, since the beam has a greater chance of having a larger dimension than the aperture of the magnet. Improved resolution without an increase in object distance is made possible by an increase in the separation distance, but when this is done, loss of the beam may occur at the entry to the second magnet.

Figure 9 is a resolution plot for the  $n = 1/2$  magnets which corresponds to the  $n = 0$  case given on Figure 8. The peaks follow the same pattern as the  $n = 0$  magnets but occur at greater object distances. The resolution, at a given distance away from a peak, however, is a little better than the  $n = 0$  magnets. With the object slit placed at the focal plane of the first magnet, for both cases, the resolution is about a factor of two better for the  $n = 1/2$  magnets.

Figure 10 shows the resolutions of a system of two  $n = 0$  bending magnets oriented so that each magnet bends the beam in different planes oriented  $45^\circ$  to each other. The first magnet resolves the beam in one plane, while the second magnet resolves the beam again in the other plane. In the axial direction of the first magnet, the resolution remains particularly good for reasonable separation between the two

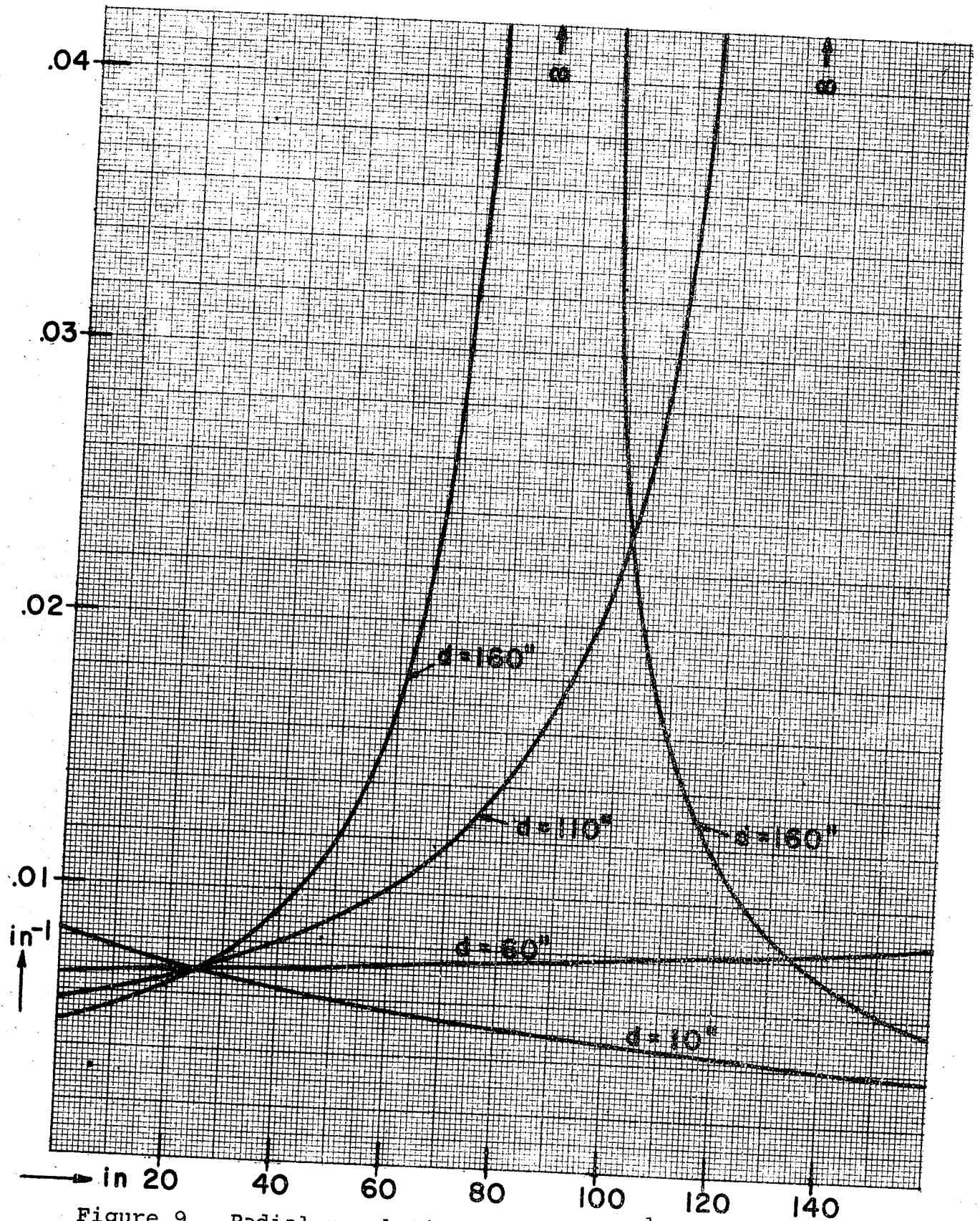


Figure 9. Radial resolution for two  $n = \frac{1}{2}$ ,  $\rho = 36$  in.,  $\alpha = 90^\circ$ , and  $\beta_1 = \beta_2 = 0^\circ$  bending magnets oriented so that  $\theta = 0^\circ$ . Plotted against the object distance for the separation distances  $d = 10$  in., 60 in., 110 in., and 160 in.

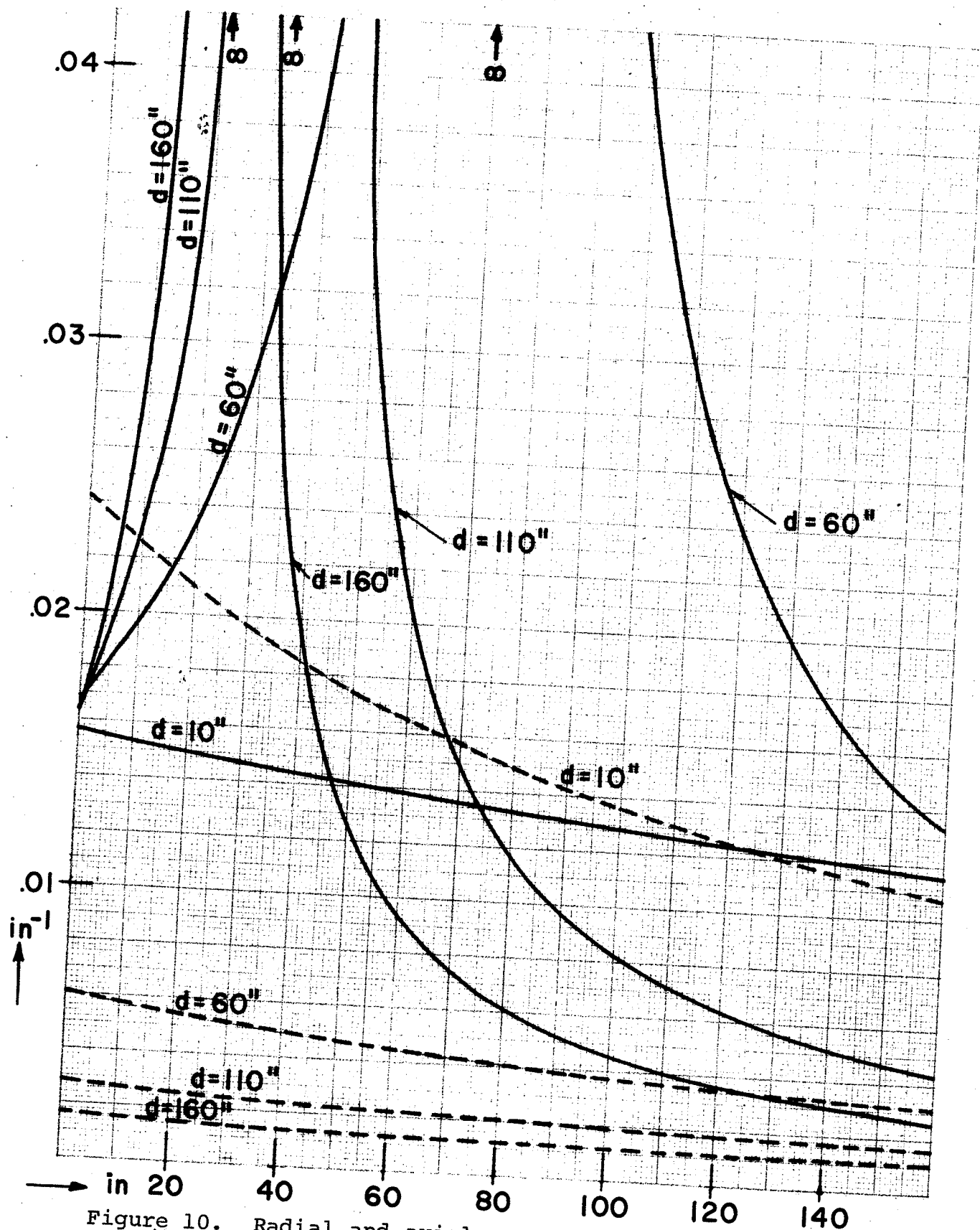


Figure 10. Radial and axial resolutions for two  $n = 0$ ,  $\rho = 36$  in.,  $\alpha = 90^\circ$ , and  $\beta_1 = \beta_2 = 0^\circ$  bending magnets oriented so that  $\theta = 45^\circ$ . The axial resolution is plotted with dashed lines. Plotted against the object distance for the separation distances  $d = 10$  in.,  $60$  in.,  $110$  in., and  $160$  in.

magnets for practically all object distances. The peaks in the curves for the resolution in the radial direction occur for object distances which are slightly longer than the  $\theta = 0^\circ$  case. The general character of the curves are, however, very much the same as those of Figure 8.

The resolution, in the axial direction, for the corresponding orientation for the  $n = 1/2$  magnets as plotted on Figure 11, is not very good for short separation distances. The radial resolution curves are very much like those for  $\theta = 0^\circ$  except for a slight shift in the object distances. It is not very easy to make a precise comparison between the  $n = 0$  and  $n = 1/2$  magnets for this orientation, since there is resolution in two planes for both cases.

Figure 12 is the resolution curve for the case where  $\theta = 90^\circ$  for the  $n = 0$  magnets, and Figure 13 is the corresponding plot for the  $n = 1/2$  magnets. The radial resolution, which is in the axial direction of the first magnet, is practically equal for both cases and is unchanged by a change in separation distance. The axial resolution for the  $n = 1/2$  magnets is peaked in practically the same way as the  $\theta = 45^\circ$  case, and reasonably good resolution is found when the object slit is placed at the focal plane, although it is about a factor of two inferior to the corresponding situation with  $\theta = 0^\circ$ . The resolutions for the  $n = 1/2$  magnets, at

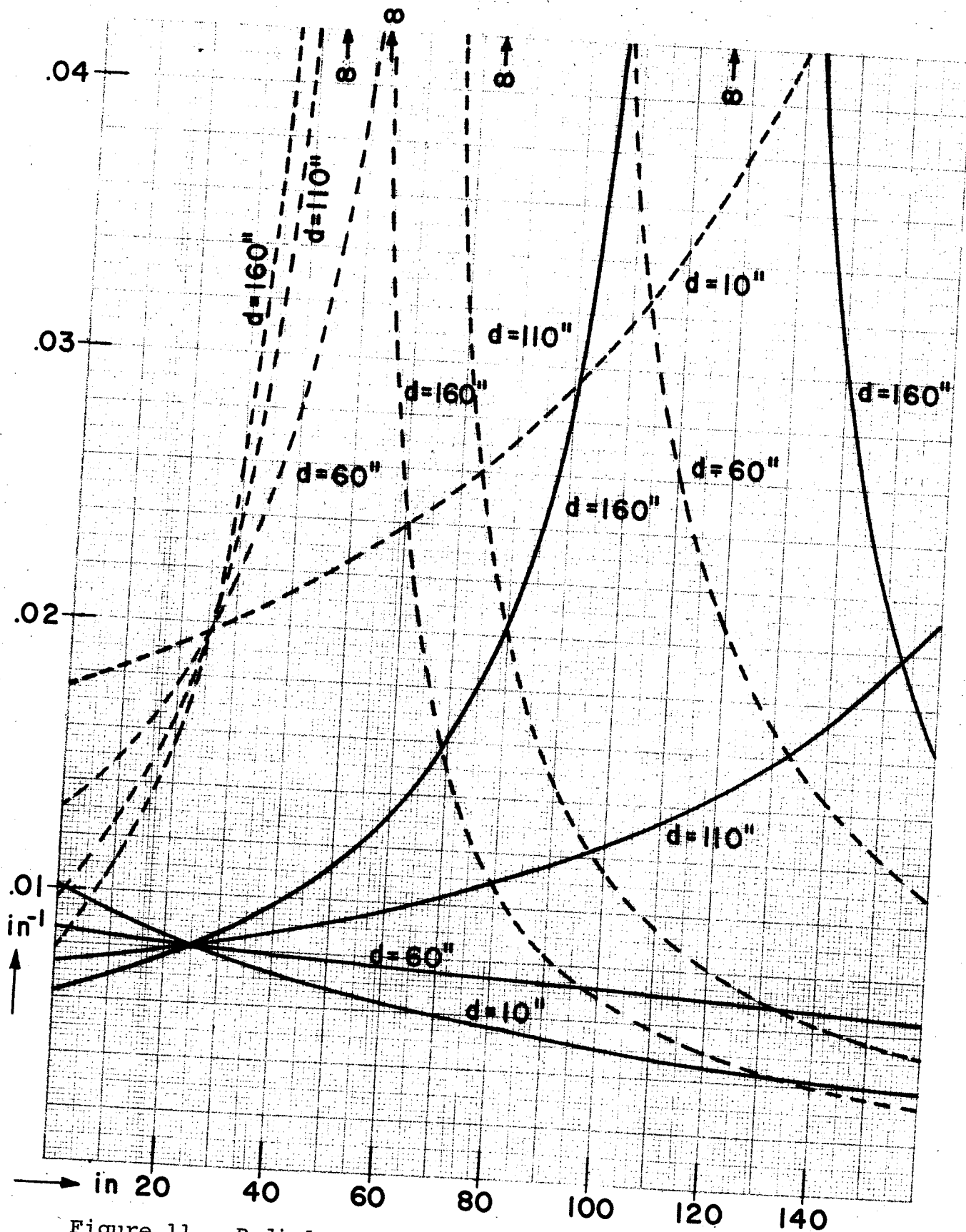


Figure 11. Radial and axial resolutions for two  $n = \frac{1}{2}$ ,  $\rho = 36$  in.,  $\alpha = 90^\circ$  and  $\beta_1 = \beta_2 = 0^\circ$  bending magnets oriented so that  $\theta = 45^\circ$ . Plotted against the object distance given in inches, for the separation distances  $d = 10$  in., 60 in., 110 in., and 160 in. Axial resolutions are plotted with dashed lines.

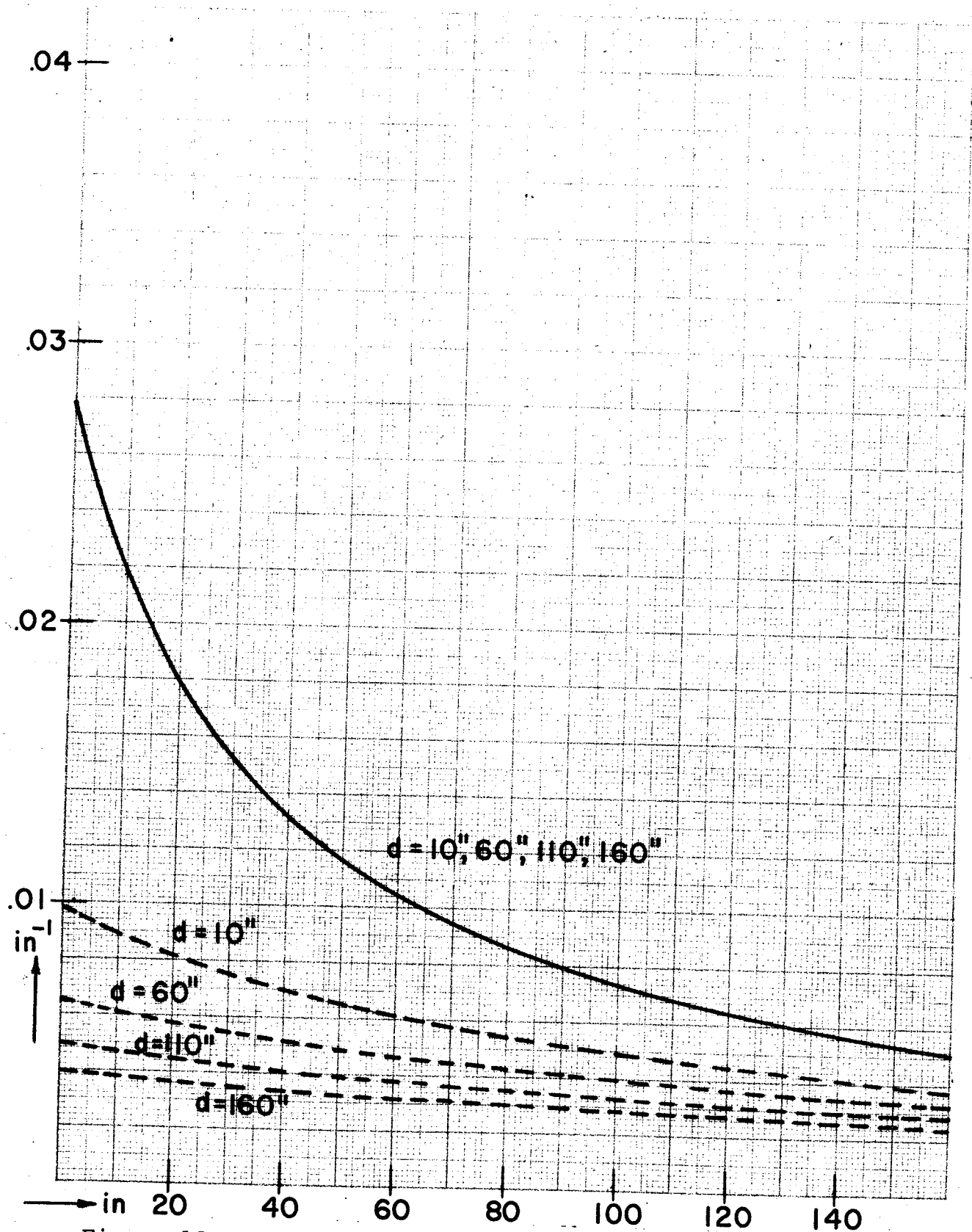


Figure 12. Radial and axial resolutions for two  $n = 0$ ,  $\rho = 36$  in.,  $\alpha = 90^\circ$ , and  $\beta_1 = \beta_2 = 0^\circ$  bending magnets oriented so that  $\theta = 90^\circ$ . The axial resolution is plotted with dashed lines. Plotted against the object distance for the separation distances  $d = 10$  in.,  $60$  in.,  $110$  in., and  $160$  in.

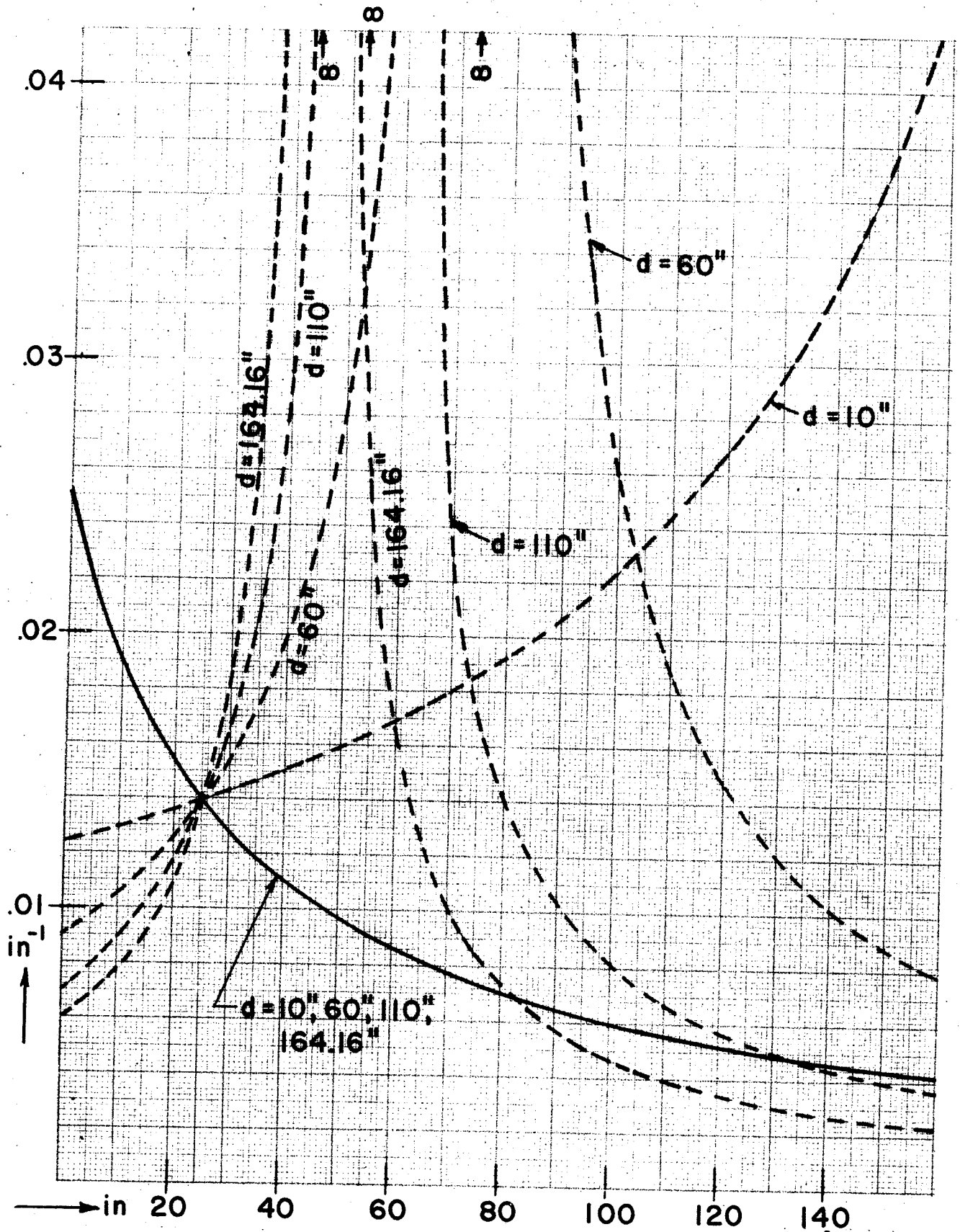


Figure 13. Radial and axial resolutions for two  $n = \frac{1}{2}$ ,  $\rho = 36$  in.,  $\alpha = 90^\circ$  and  $\beta_1 = \beta_2 = 0^\circ$  bending magnets oriented so that  $\theta = 90^\circ$ . Plotted against the object distance given in inches, for the separation distances  $d = 10$  in.,  $60$  in.,  $110$  in., and  $164.16$  in. Axial resolutions are plotted with dashed lines.



longer object distances and larger separations, are quite good, but there is a natural limit as discussed before. The  $n = 0$  curves, in Figure 12, show no peaks for the resolution in either of the planes, and the resolution remains good for all separation distances considered and a very wide range of object distances.

Figure 14 shows the resolution curves for the  $n = 0$  magnets for  $\theta = 135^\circ$ . The radial curves peak near the focal plane or the entry edge of the first magnet, and very little change is observed from one separation distance to another. The corresponding case for  $n = 1/2$  magnets, shown in Figure 15, has considerably poorer resolution, particularly in the axial direction of the first magnet.

Figures 16 and 17 are resolutions for  $n = 0$  and  $n = 1/2$  magnets, respectively, both with  $\theta = 180^\circ$ . The magnets in both cases are oriented in the same plane, and hence, they resolve the beam only in one plane. For both the  $n = 0$  and  $n = 1/2$  magnets, the resolution peaks when the object slit is placed at the focal planes of the first magnets, regardless of the separation distance. The way in which the curves tail off, as the object distance is increased, is approximately the same for the two cases.

Figure 18 through 20 show the magnification for the  $n = 0$  magnets for all the orientations discussed so far. In

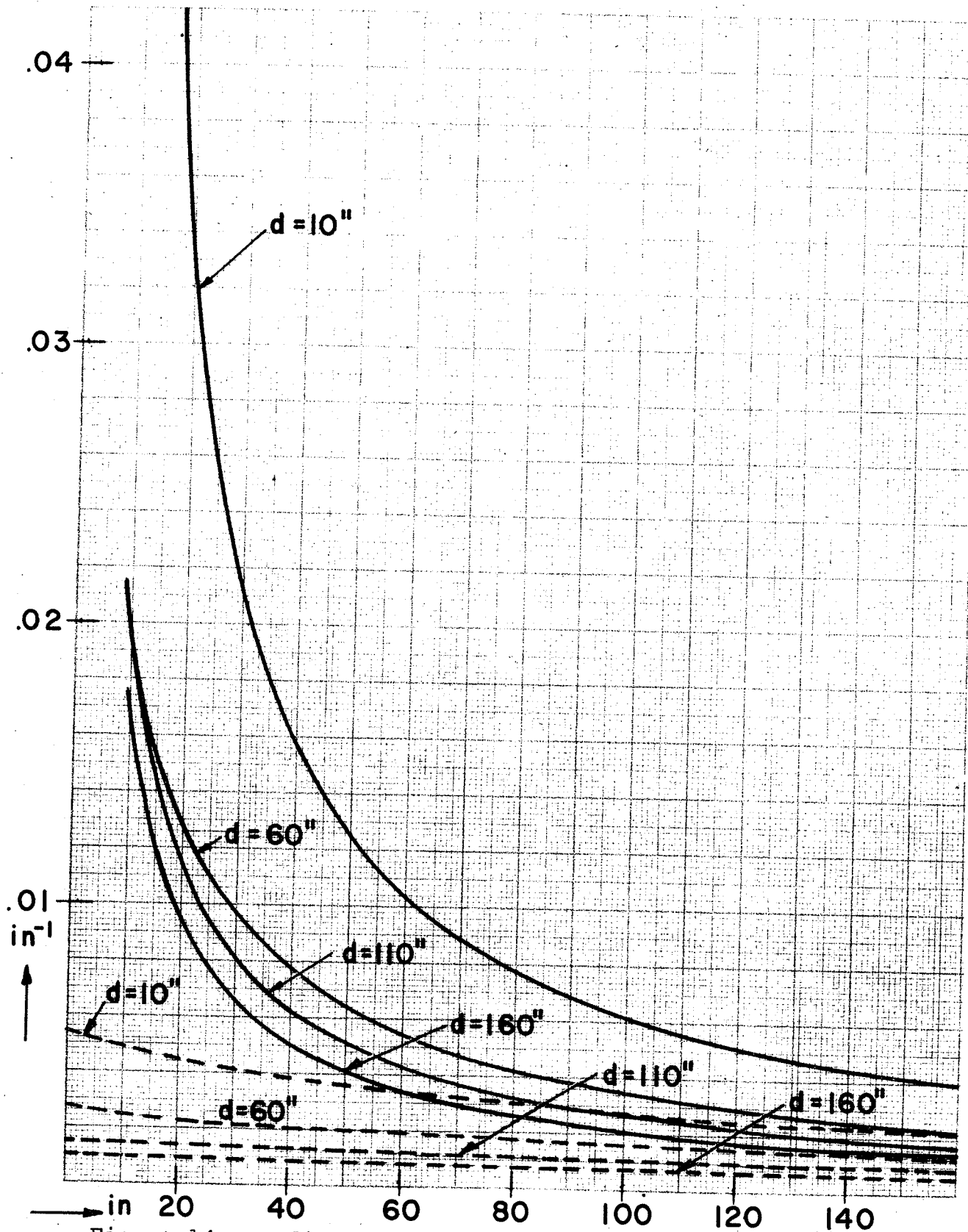


Figure 14. Radial and axial resolutions for two  $n = 0$ ,  $\rho = 36$  in.,  $\alpha = 90^\circ$ , and  $\beta_1 = \beta_2 = 0^\circ$  bending magnets oriented so that  $\theta = 135^\circ$ . The axial resolution is plotted with dashed lines. Plotted against the object distance for the separation distances  $d = 10$  in., 60 in., 110 in., and 160 in.

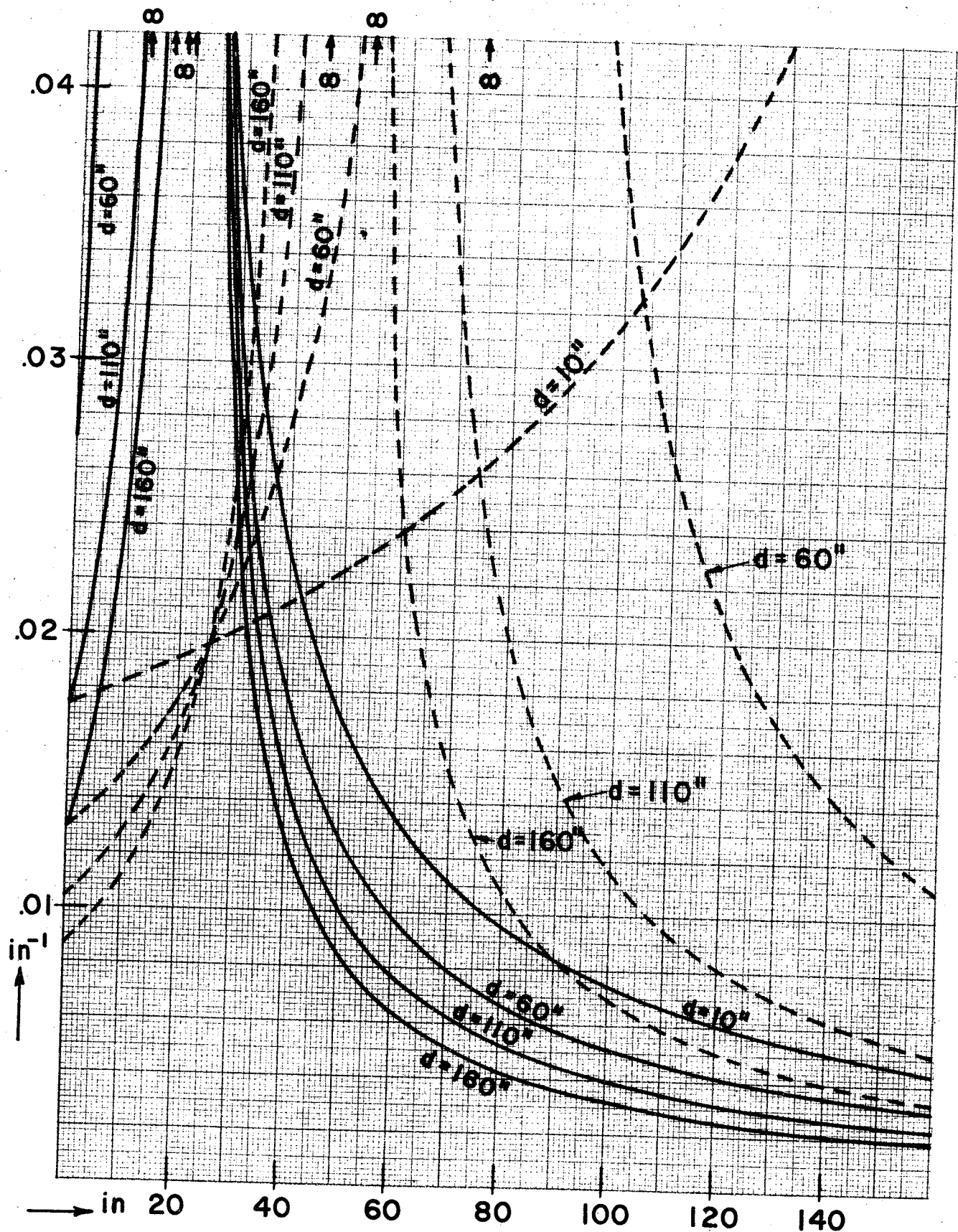


Figure 15. Radial and axial resolutions for two  $n = \frac{1}{2}$ ,  $\rho = 36$  in.,  $\alpha = 90^\circ$  and  $\beta_1 = \beta_2 = 0^\circ$  bending magnets oriented so that  $\theta = 135^\circ$ . Plotted against the object distance given in inches, for the separation distances  $d = 10$  in., 60 in., 110 in., and 160 in. Axial resolutions are plotted with dashed lines.

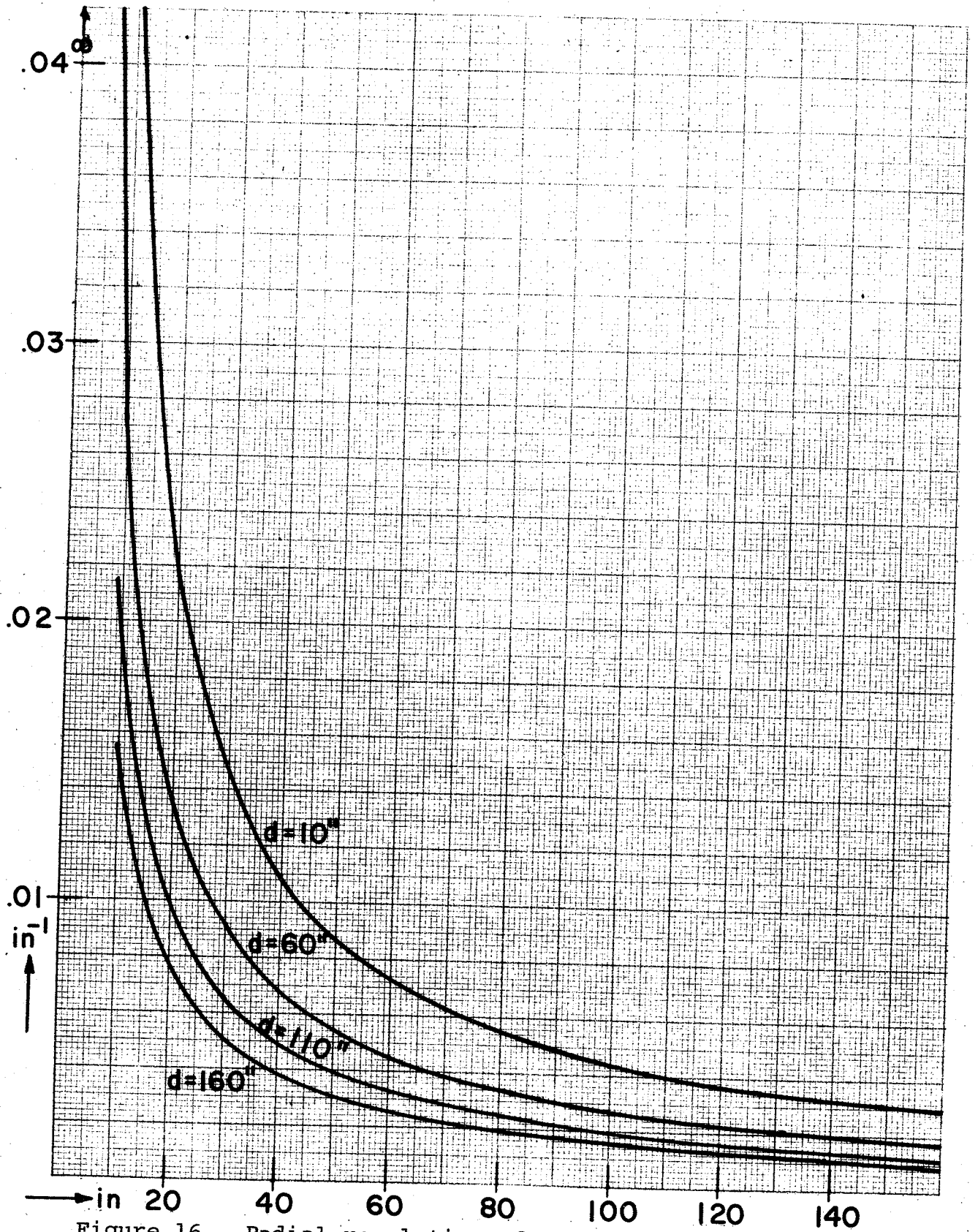


Figure 16. Radial resolution of a system consisting of two  $n = 0$ ,  $\rho = 36$  in.,  $\alpha = 90^\circ$ , and  $\beta_1 = \beta_2 = 0^\circ$  bending magnets oriented so that  $\theta = 180^\circ$ . Plotted against the object distance in inches for the separation distances  $d = 10$  in., 60 in., 110 in., and 160 in.

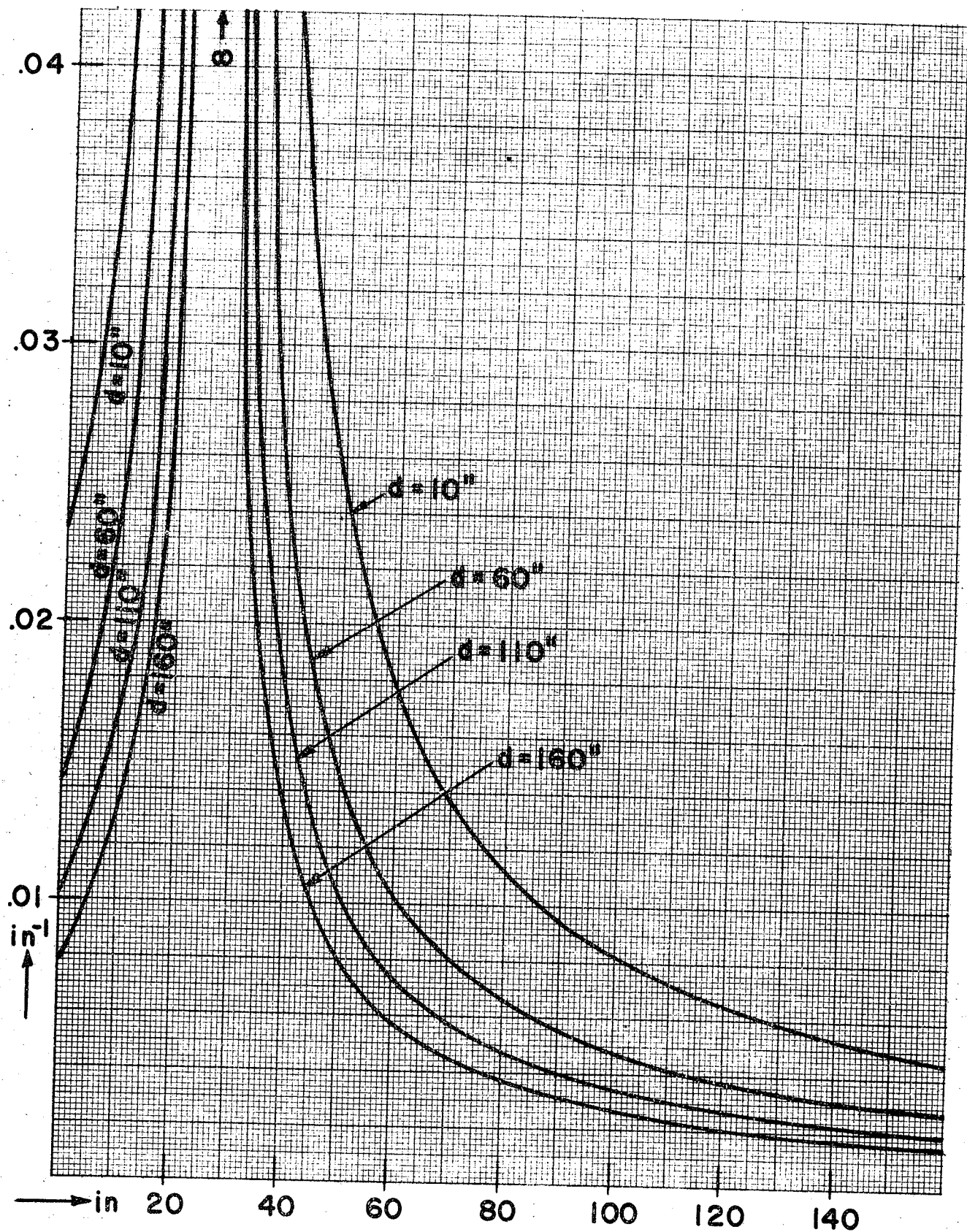


Figure 17. Radial resolution for two  $n = \frac{1}{2}$ ,  $\rho = 36$  in.,  $\alpha = 90^\circ$ , and  $\beta_1 = \beta_2 = 0^\circ$  bending magnets oriented so that  $\theta = 180^\circ$ . Plotted against the object distance for the separation distances  $d = 10$  in.,  $60$  in.,  $110$  in., and  $160$  in.

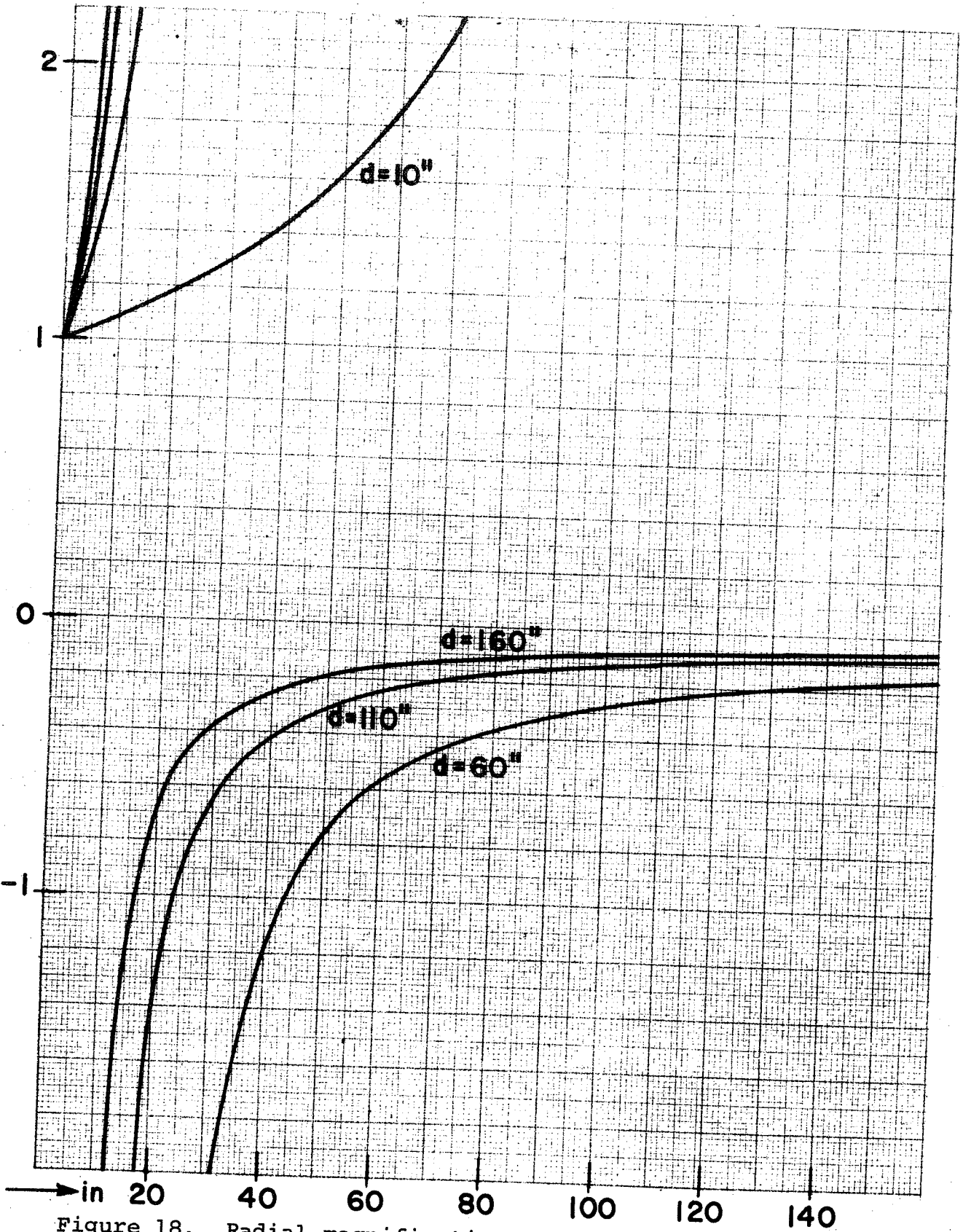


Figure 18. Radial magnification for the two  $n = 0$ ,  $\rho = 36$  in.,  $\alpha = 90^\circ$ , and  $\beta_1 = \beta_2 = 0^\circ$  bending magnets oriented so that  $\theta = 0^\circ$  or  $180^\circ$ . Plotted against the object distance given in inches for the separation distances  $d = 10$  in.,  $60$  in.,  $110$  in., and  $160$  in.



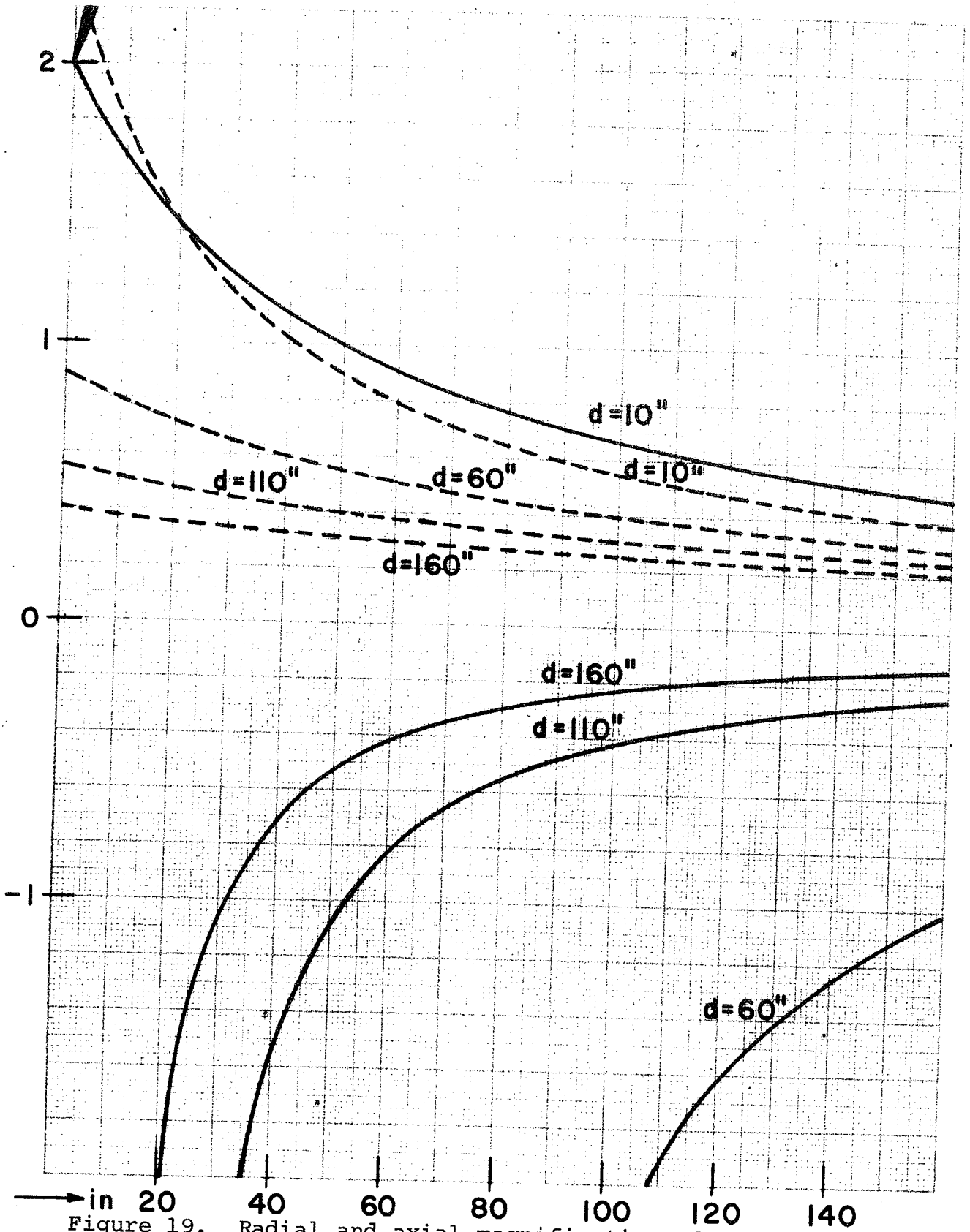


Figure 19. Radial and axial magnifications for the two  $n = 0$ ,  $\rho = 36$  in.,  $\alpha = 90^\circ$ , and  $\beta_1 = \beta_2 = 0^\circ$  bending magnets oriented so that  $\theta = 45^\circ$  or  $135^\circ$ . Plotted against the object distance given in inches for the separation distances  $d = 10$  in.,  $60$  in.,  $110$  in., and  $160$  in. Axial magnifications are plotted with dashed lines.

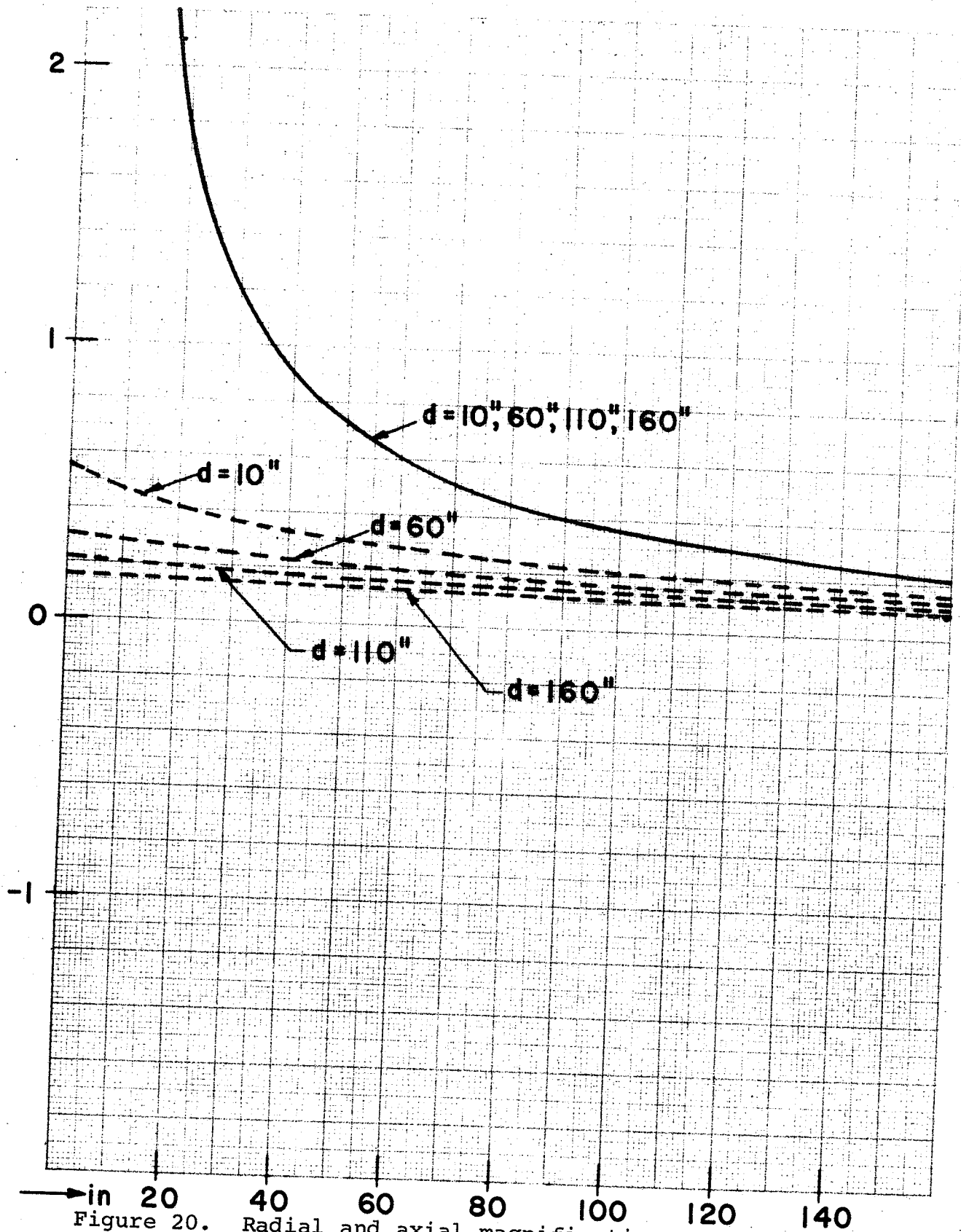


Figure 20. Radial and axial magnifications for the two  $n = 0$ ,  $\rho = 36$  in.,  $\alpha = 90^\circ$ , and  $\beta_1 = \beta_2 = 0^\circ$  bending magnets oriented so that  $\theta = 90^\circ$ .

Plotted against the object distance given in inches for the separation distances  $d = 10$  in.,  $60$  in.,  $110$  in., and  $160$  in. Axial magnifications are plotted with dashed lines.



general, the magnification blows up for small separations and small object distances. This makes it undesirable to consider placing the object slit at a distance which is left of the peaks in the resolution curves for most cases. There is no focusing in the axial direction when the magnets are oriented in the same plane.

Figure 21 is the magnifications for the  $n = 1/2$  magnets, and the curves are same for all orientations. Also, since this system is double focusing, the radial and axial focusing properties are the same. Except for very small separation distances, the magnification for object distances not very far from the focal plane blows up. When the object and separation distances are fairly large, the magnification is well behaved. There is unit magnification for all cases when the object slit is placed at the focal plane of the first magnet.

Figures 22 through 24 show the object distances for the  $n = 0$  magnets. In general, for the  $n = 0$  magnets, the image distances are in a more useful range for larger object and separation distances. In Figure 22, which describes the radial object distances for the  $n = 0$  magnets for the orientation angles  $\theta = 0^\circ$  and  $180^\circ$ , image distances less than 150 inches are available for separation distances greater than 110 inches. Figure 23 shows the object distances for the

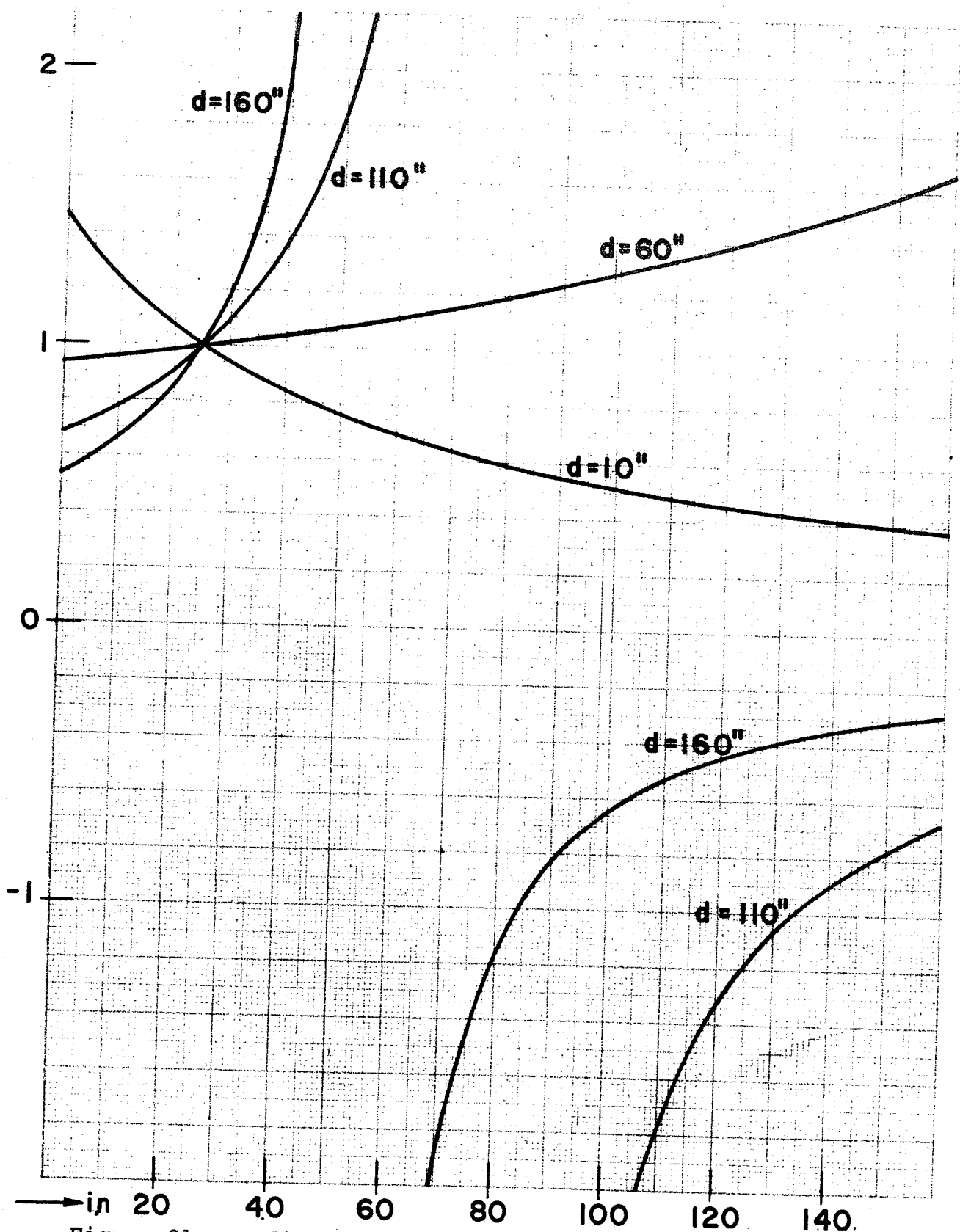


Figure 21. Radial and axial magnifications of two  $n = \frac{1}{2}$ ,  $\rho = 36$  in.,  $\alpha = 90^\circ$ , and  $\beta_1 = \beta_2 = 0^\circ$  bending magnets with any relative orientation plotted against the object distance given in inches for the separation distances  $d = 10$  in.,  $60$  in.,  $110$  in., and  $160$  in.

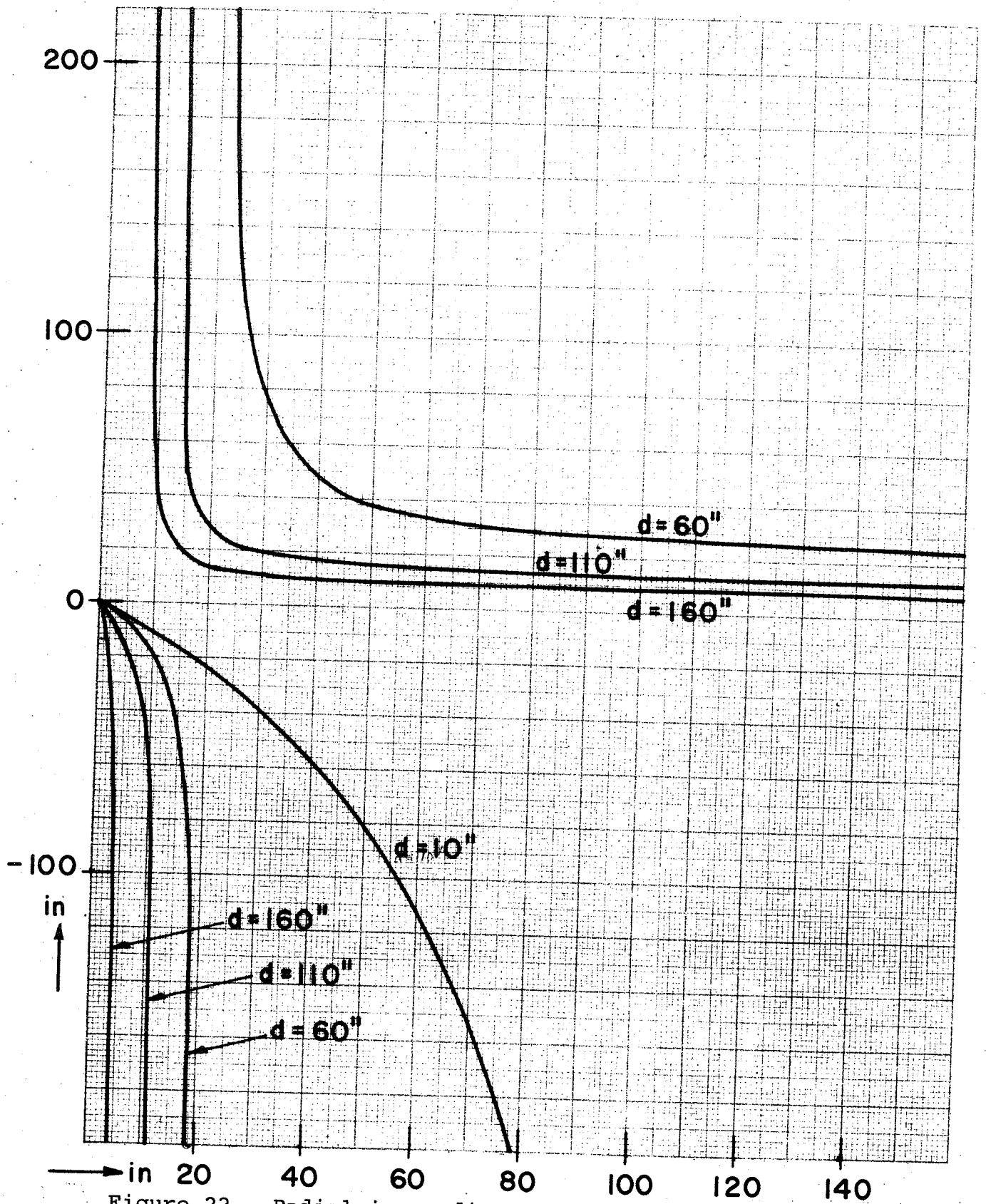


Figure 22. Radial image distance for the two  $n = 0$ ,  $\rho = 36$  in.,  $\alpha = 90^\circ$ , and  $\beta_1 = \beta_2 = 0^\circ$  bending magnets oriented so that  $\theta = 0^\circ$  or  $180^\circ$ . Plotted against the object distance given in inches for the separation distances  $d = 10$  in., 60 in., 110 in., and 160 in.

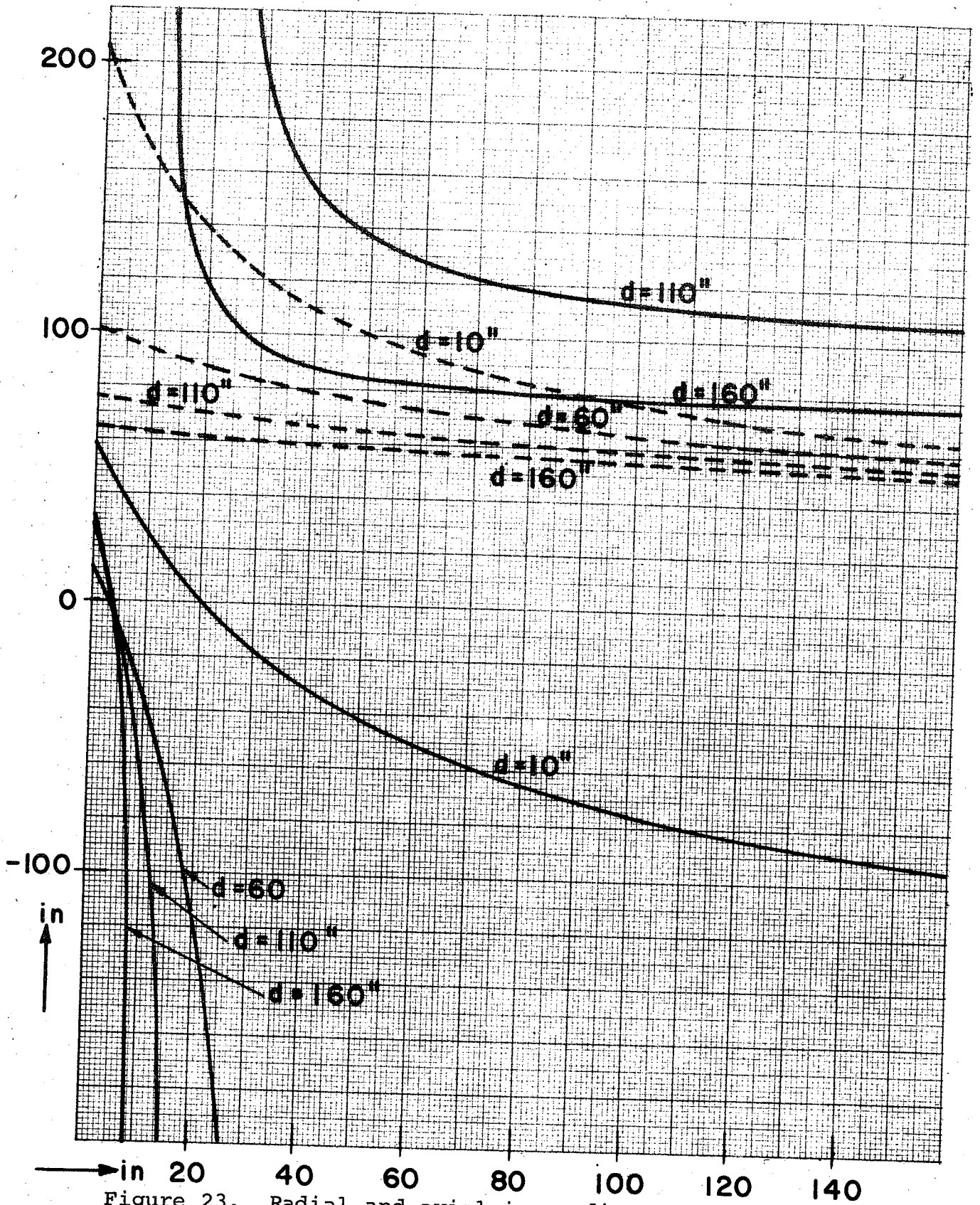


Figure 23. Radial and axial image distances for two  $n = 0$ ,  $\rho = 36$  in.,  $\alpha = 90^\circ$ , and  $\beta_1 = \beta_2 = 0^\circ$  bending magnets oriented so that  $\theta = 45^\circ$  or  $135^\circ$ . Plotted against the object distance given in inches for the separation distances  $d = 10$  in., 60 in., 110 in., and 160 in. Axial image distances are plotted with dashed lines.

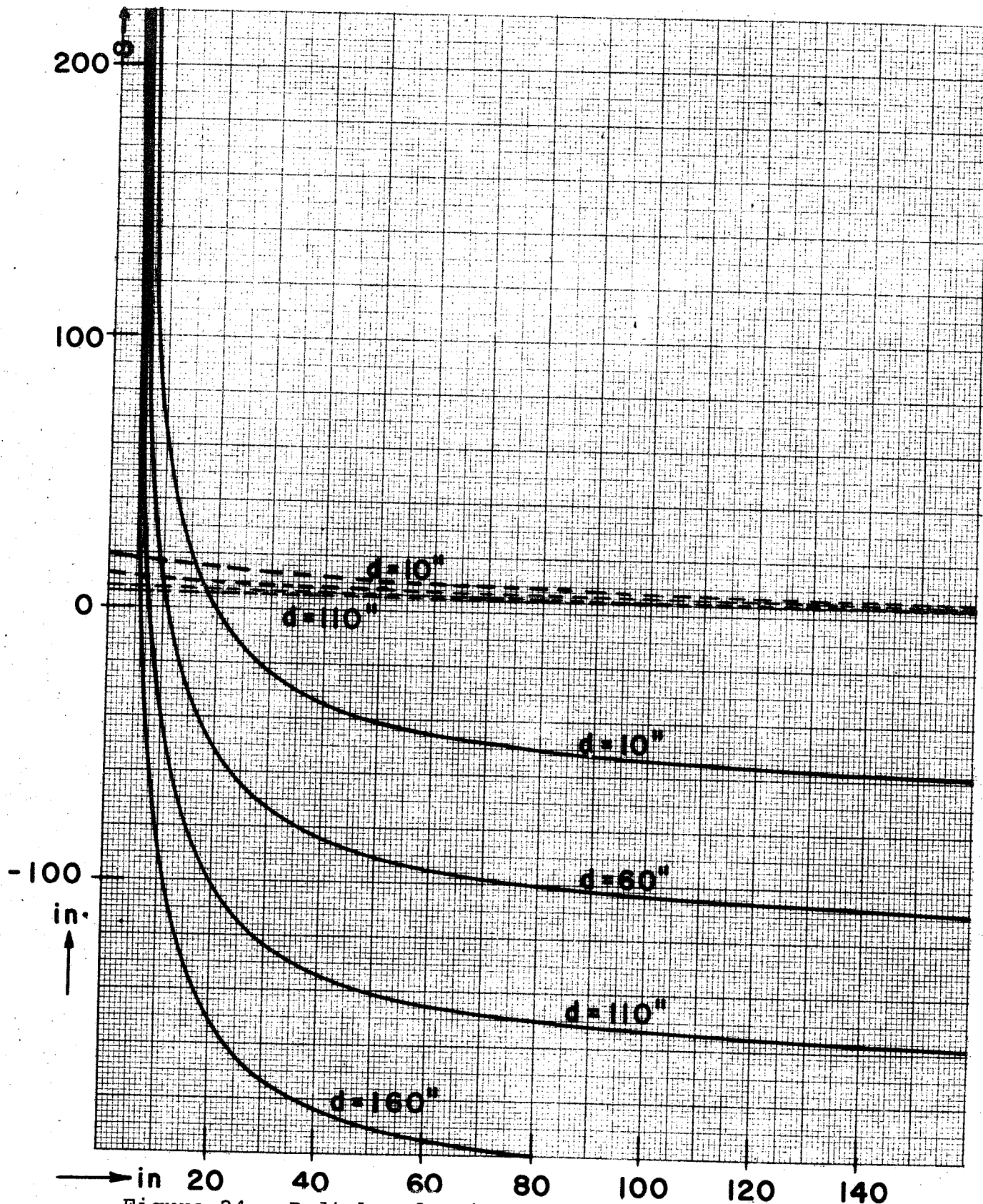


Figure 24. Radial and axial image distances for two  $n = 0$ ,  $\rho = 36$  in.,  $\alpha = 90^\circ$ , and  $\beta_1 = \beta_2 = 0^\circ$  bending magnets oriented so that  $\theta = 90^\circ$ . Plotted against the object distance given in inches for the separation distances  $d = 10$  in.,  $60$  in.,  $110$  in., and  $160$  in. Axial image distances are plotted with dashed lines.

$n = 0$  magnets at  $\theta = 45^\circ$  and  $135^\circ$ . The radial image distances are very much like the  $\theta = 0^\circ$  case, but there is axial focusing as well as radial focusing for these cases. Unless the separation distance is made very large, double focusing is not possible for this system. Figure 24 shows the image distances for  $\theta = 90^\circ$ . The positive image in the axial direction is located very close to the magnet edge for all object positions except when the object slit is placed very close to the magnet. The separation distance does not affect this axial image distance to any extent. Double focusing can be seen on the graph for the separation distances 10 inches and 60 inches at the intersection of the corresponding solid and dashed lines.

Figure 25 shows the object distances for the  $n = 1/2$  magnets at all orientations. A short range of small positive image distances are available for object distances near the focal plane of the first magnet. Longer image distances are available for large separations when correspondingly large object distances are used.

#### D. Quadrupole and Flat Field Bending Magnet Combinations

Next, consider the combination of quadrupoles and  $n = 0$  bending magnets. First case to be treated is a system

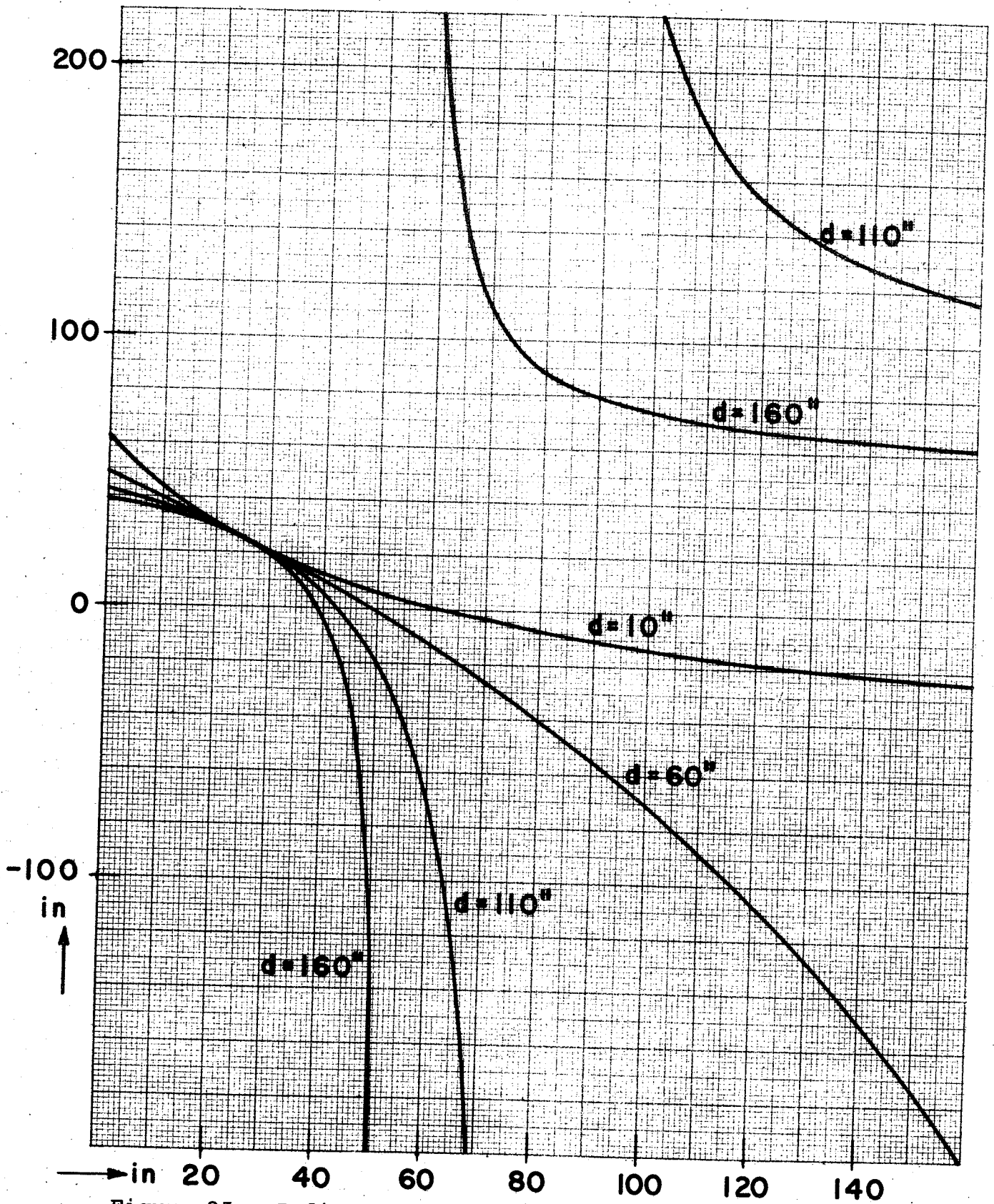


Figure 25. Radial and axial image distances for two  $n = \frac{1}{2}$ ,  $\rho = 36$  in.,  $\alpha = 90^\circ$ , and  $\beta_1 = \beta_2 = 0^\circ$  bending magnets with any relative orientation, plotted against the object distance given in inches for the separation distances  $d = 10$  in., 60 in., 110 in., and 160 in.

as diagramed in Figure 26. Figure 27 shows the magnifications for several quadrupole strengths as a function of object distance. For unit magnification, image distances are equal to object distance, and these can be plotted as a function of quadrupole strength, as can be seen on Figure 28. The intersection of these curves gives the condition for double focusing with unit magnification. At this point the radial resolution is found to be  $.01 \text{ in}^{-1}$ . The quadrupole strength for this condition is  $K = .053 \text{ in}^{-1}$  which is quite moderate.

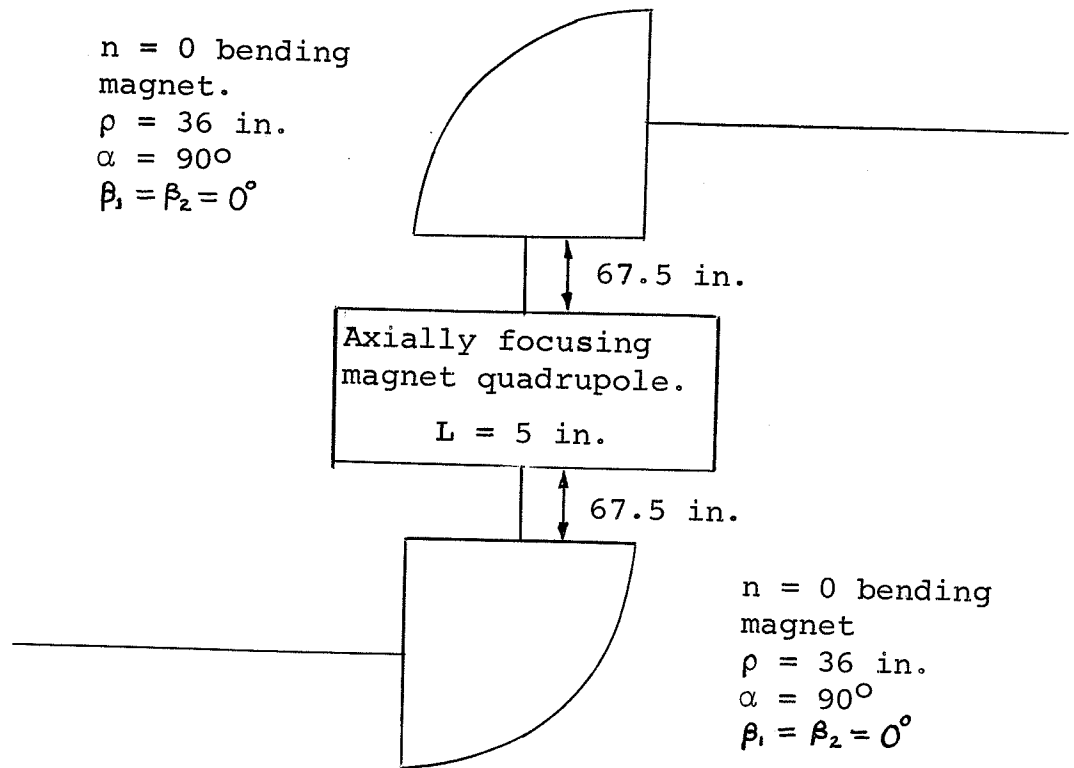


Figure 26. Diagram showing the relative positions of the magnets in a system containing two  $n = 0$  bending magnets and one axially focusing magnetic quadrupole.



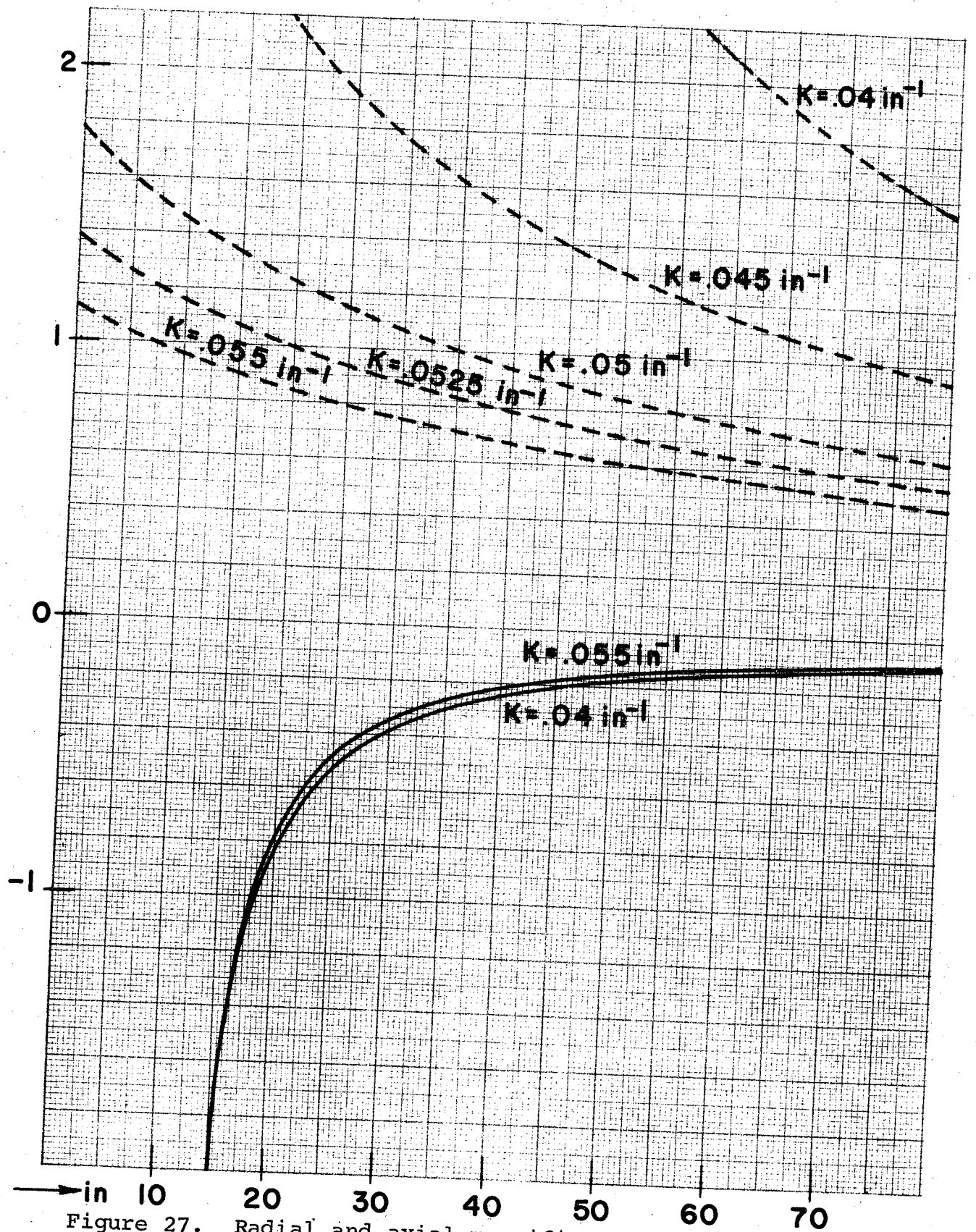


Figure 27. Radial and axial magnifications for the system with two  $n = 0$  bending magnets and an axially focusing quadrupole as shown in Figure 26. Plotted against the object distance given in inches for quadrupole fields specified by  $K = .04 \text{ in}^{-1}$ ,  $.045 \text{ in}^{-1}$ ,  $.05 \text{ in}^{-1}$ , and  $.055 \text{ in}^{-1}$ . The axial magnifications are plotted with dashed lines.

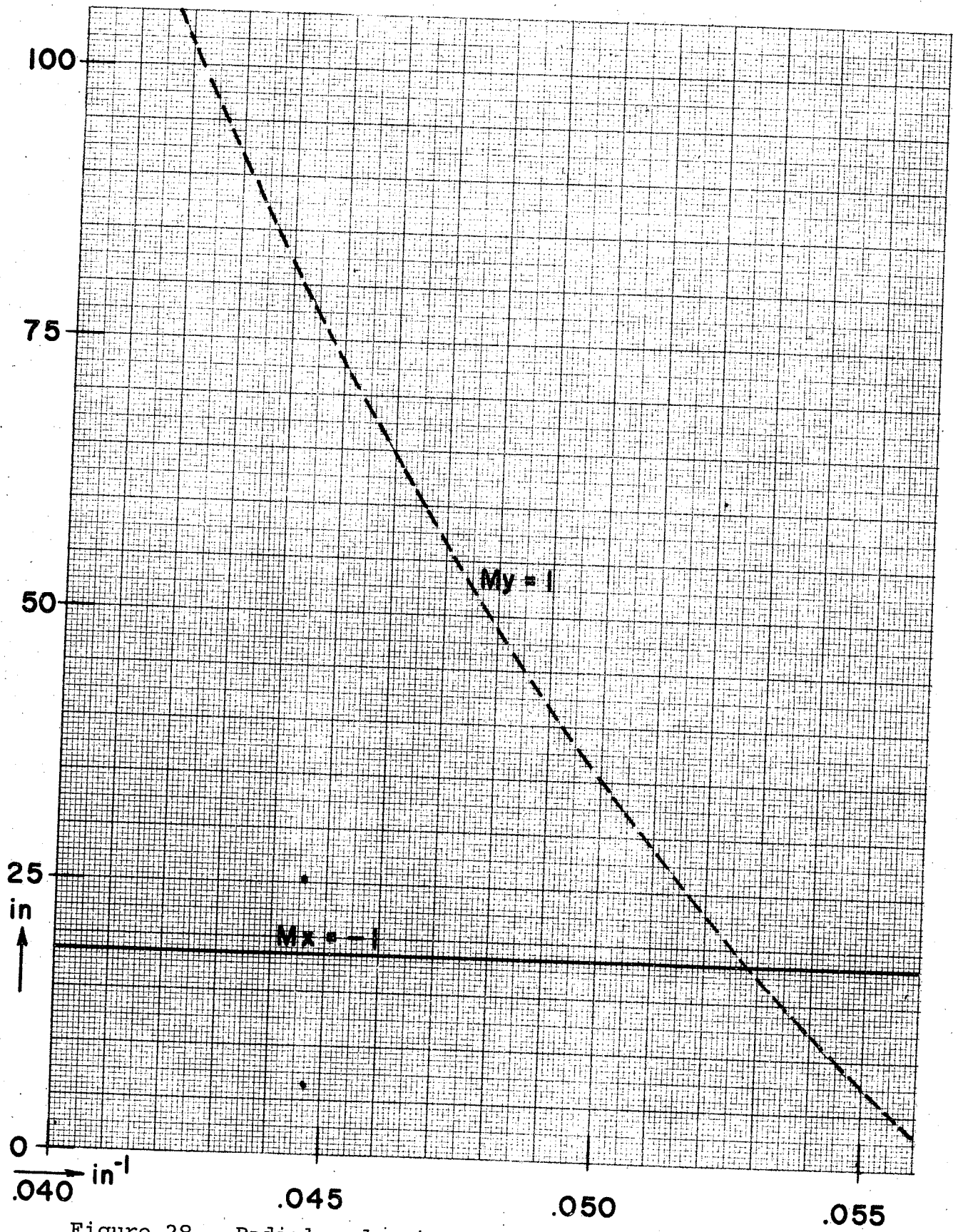


Figure 28. Radial and axial image distances for the system described in Figure 26, plotted against the field strength of the magnetic quadrupole. These are lines of unit magnification. The axial image distance is plotted with a dashed line.

This is a useful system, since the object, image distances are quite short for the double focusing condition, and the quadrupole strength is quite reasonable. This case can be compared with the two  $n = 1/2$  magnets where the object and image distances are 85 inches for unit magnification. The resolution is of the same order of magnitude for both cases, but the  $n = 1/2$  magnets give a slightly superior resolution around  $.004 \text{ in.}^{-1}$  as compared to  $.01 \text{ in.}^{-1}$  for this case.

Another combination was tried as shown in Figure 29. Figures 30 and 31 correspond to Figures 27 and 28 of the previous case, respectively. In this combination, the two outside quadrupoles are axially focusing and the one inside is radially focusing. The radially focusing magnetic quadrupole was made the variable magnet and the other two were set at a convenient field strength. Since we change the radially focusing quadrupole in this manner, the changes are mainly in the radial focusing properties, while the axial properties are practically unchanged. Unit magnification and double focusing occurs when  $K = .095 \text{ in.}^{-1}$  for the radially focusing magnetic quadrupole. The radial resolution is  $.07 \text{ in.}^{-1}$  for when the axial magnification is  $-1$ , while it is  $.12 \text{ in.}^{-1}$  for when the axial magnification is  $1$ . In both cases, however, the resolution is rapidly varying with object distance about

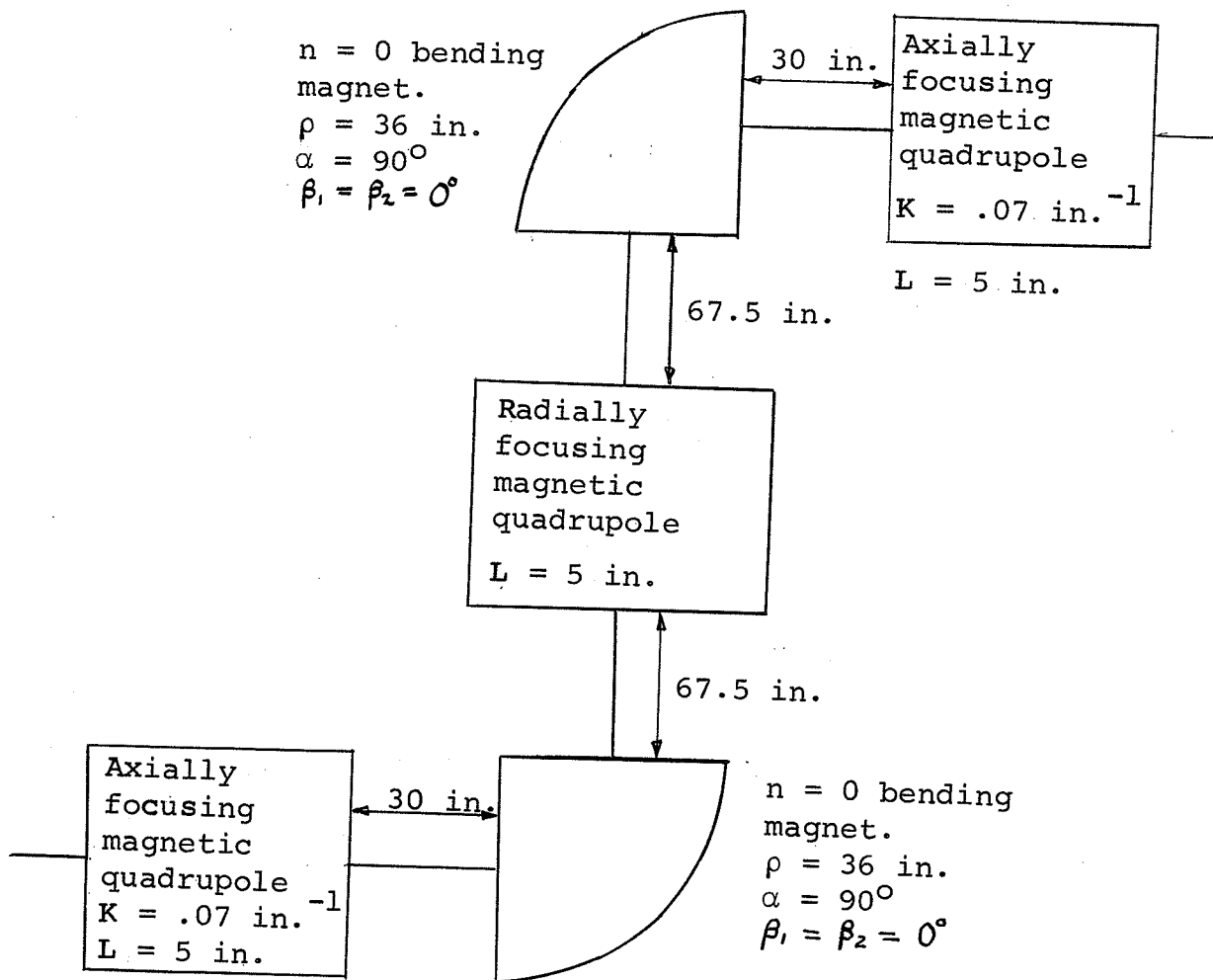


Figure 29. Diagram of a system with two  $n = 0$  bending magnets and three magnetic quadrupoles, one of which is radially focusing and the other two axially focusing.

these points. This can be compared to the two  $n = 1/2$  magnets where the object and image distances are 25.2 inches. Other than the fact that the quadrupoles and  $n = 0$  bending magnet system requires a little more physical dimension than the two  $n = 1/2$  magnets, there is very little difference in the properties of these two systems for this situation.

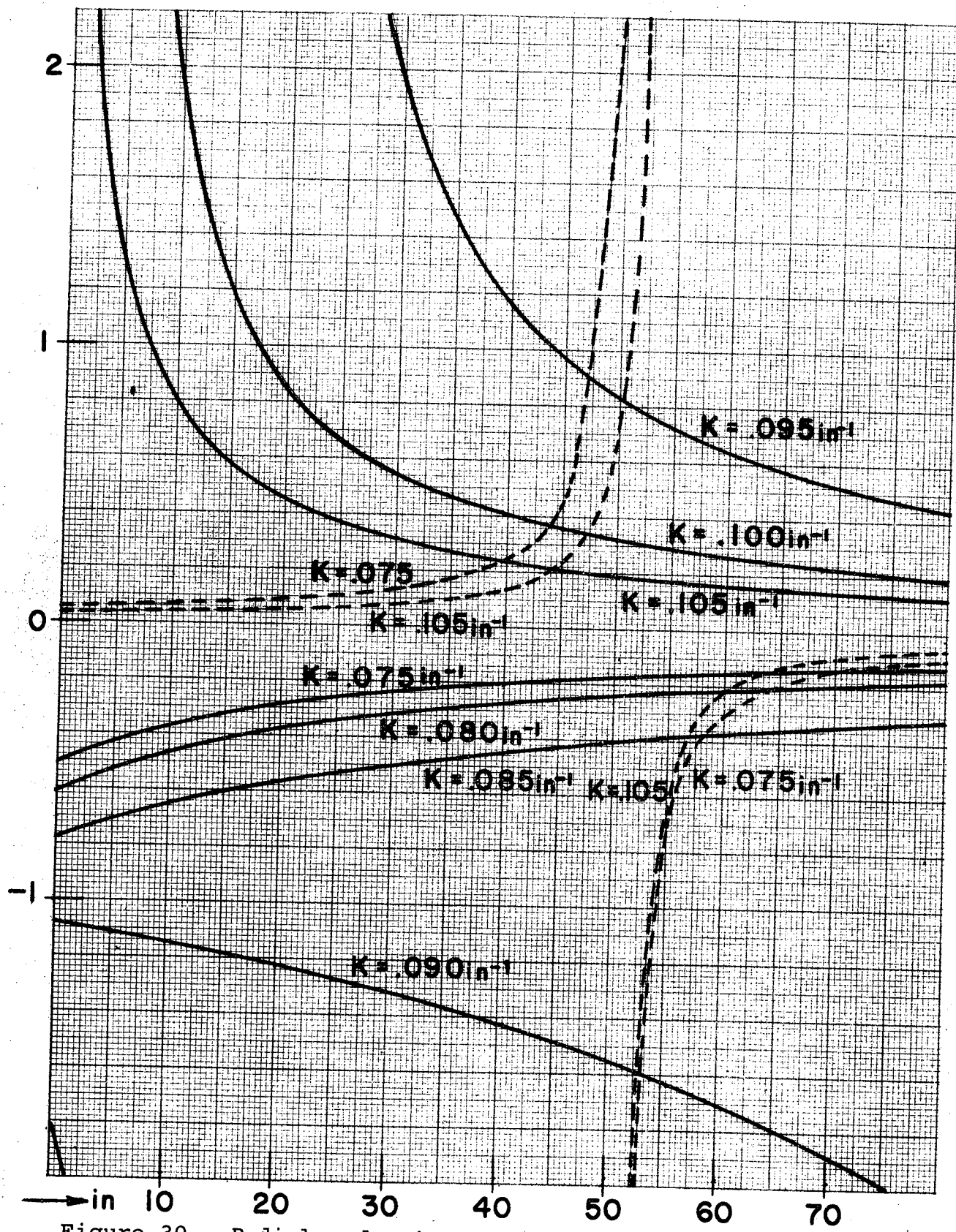


Figure 30. Radial and axial magnifications for the system as described in Figure 29, plotted against the object distance given in inches for the several field strengths of the radially focusing quadrupole as specified by K. The axial magnifications are plotted with dashed lines.

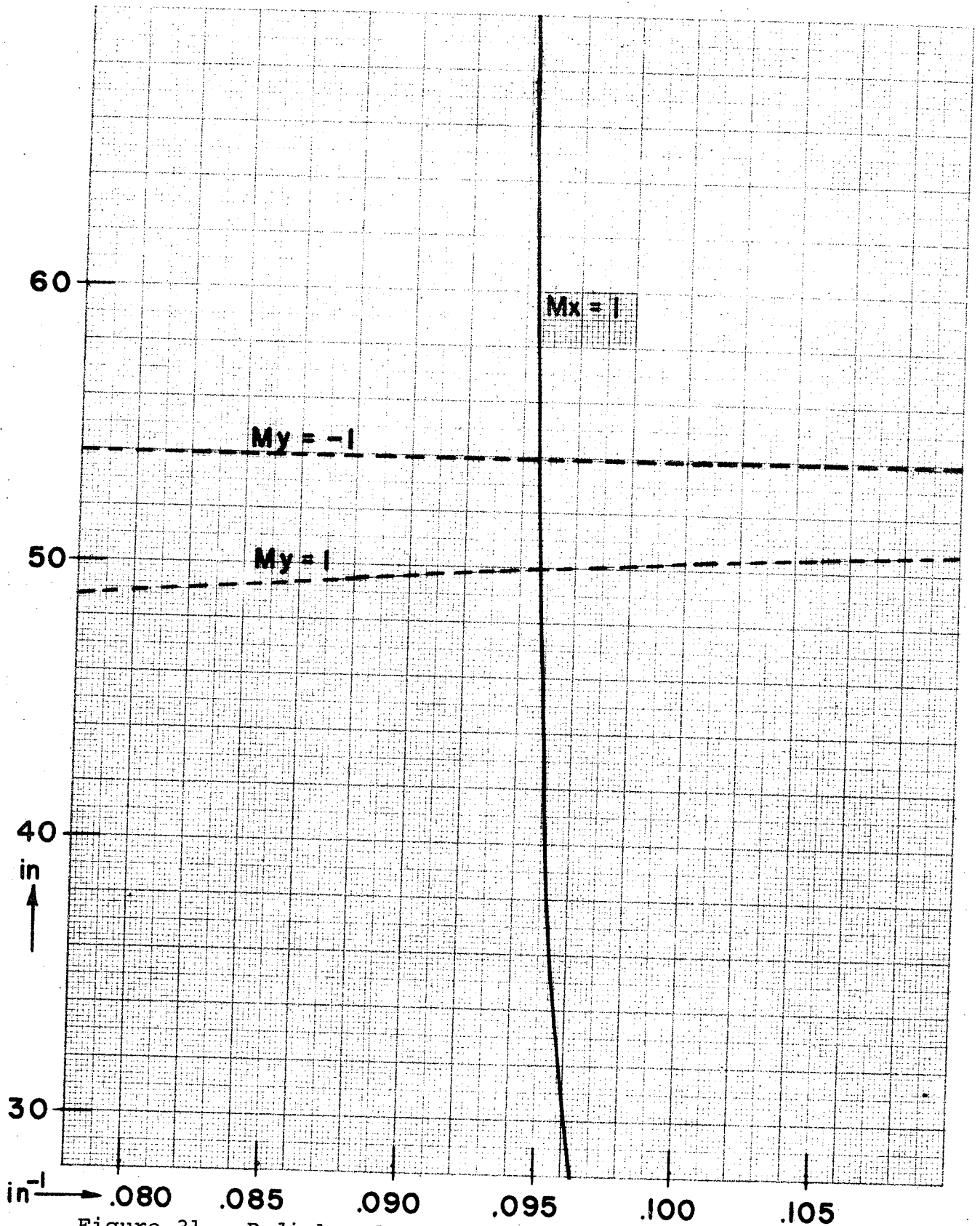
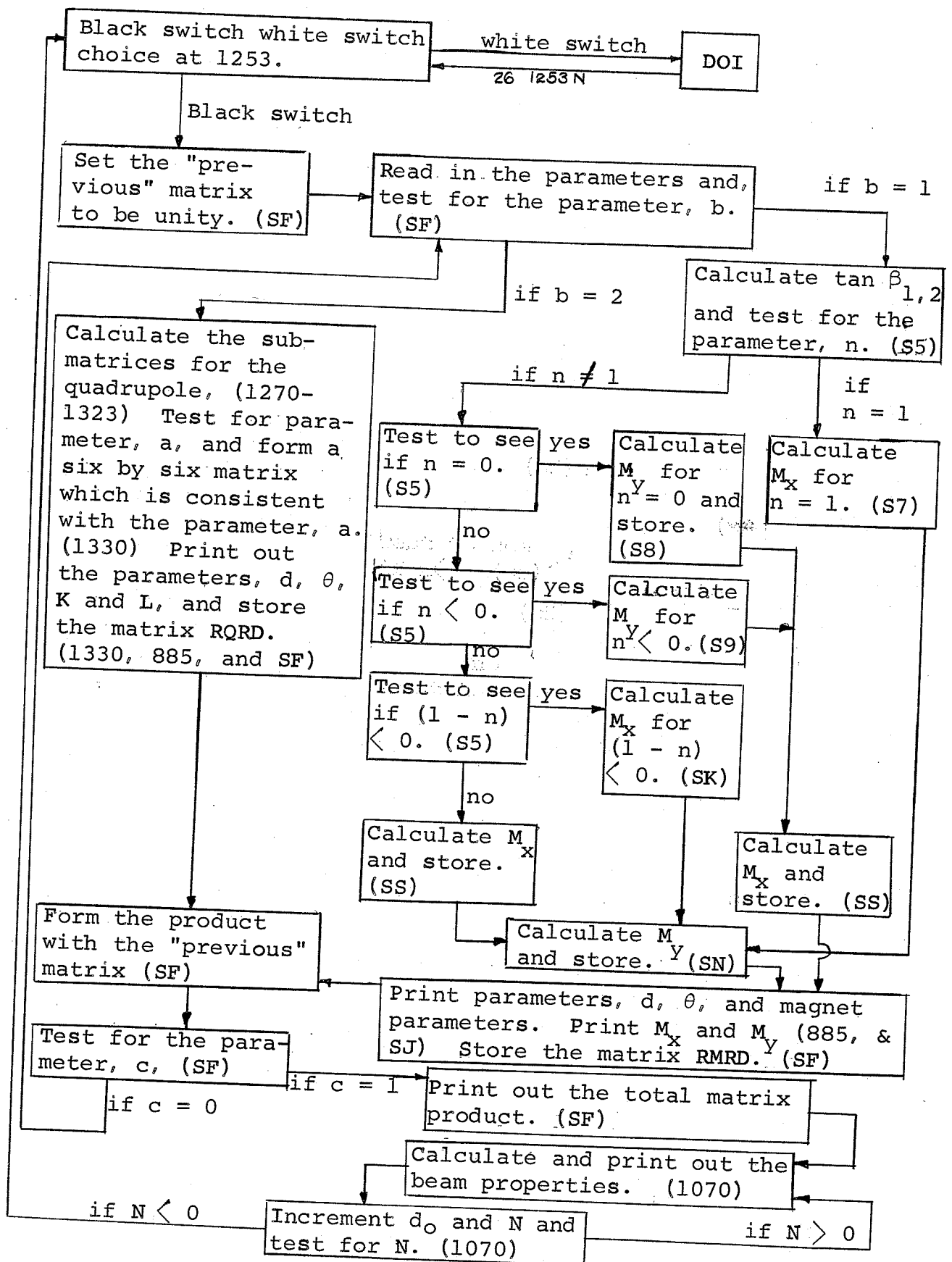


Figure 31. Radial and axial image distances for the system as described in Figure 29, plotted against the field strength of the radially focusing quadrupole. These are lines of unit magnification. The axial image distances are plotted with dashed lines.

#### IV. APPENDICES

## APPENDIX A. FLOW CHART FOR THE COMPUTER CODE





## B. ORDER PAIRS FOR THE COMPUTER CODE

## S - Box Settings

		00	3K			
S3	0	00	F	00	30F	Parameters
S4	1	00	F	00	60F	Constants
S5	2	00	F	00	100F	$\tan \beta$ . Test for n.
S6	3	00	F	00	1330F	Quadrupole matrix
S7	4	00	F	00	150F	Rad. Mag. Matrix. n = 1.
S8	5	00	F	00	182F	Axial Mag. Matrix n = 0.
S9	6	00	F	00	210F	Axial Mag. Matrix n < 0.
SK	7	00	F	00	600F	Rad. Mag. Matrix n > 1
SS	8	00	F	00	670F	Rad. Mag. Matrix 0 < n < 1
SN	9	00	F	00	730F	Axial Mag. Matrix 0 < n
SJ	10	00	F	00	780F	Print Mag. Matrix
SF	11	00	F	00	940F	Combined matrix
SL	12	00	F	00	3960F	Subroutines

## S4 Constants

Abs. Addr.	Addr.	Order Pairs				Comments
		00	60K			
60	0	00	F	00	314159265000J	$\pi/10$
61	1	00	F	00	1000000000J	1/1000
62	2	00	F	00	F	
63	3	00	F	00	F	
64	4	00	F	00	F	
65	5	00	F	00	100000001000J	
66	6	00	F	00	99999999000J	
67	7	00	F	00	1000J	
68	8	00	F	00	F	
69	9	00	F	00	100000000000J	1/10
70	10	00	F	00	100000000000J	1/100
71	11	00	F	00	9F	
72	12	00	F	00	2F	
73	13	00	F	00	3F	
74	14	00	F	00	5F	
75	15	00	F	00	143F	
76	16	40	3F	L5	300F	
77	17	NO	F	40	376F	
78	18	L5	8S4	40	376F	
79	19	L5	8S4	40	394F	
80	20	41	F	L5	309F	
81	21	NO	F	40	394F	
82	22	00	F	00	11F	

Abs. Addr.	Rel. Addr.	Order Pairs				Comments
83	23	00	F	00	6F	
84	24	00	F	00	340F	
85	25	00	F	00	412F	
86	26	00	F	00	484F	
87	27	00	F	00	376F	
88	28	00	F	00	520F	
89	29	00	F	00	448F	
90	30	26	SJ	NO	F	
91	31	00	F	00	556F	
92	32	00	F	00	71F	
93	33	00	F	00	2000F	
94	34	00	F	00	2036F	

An Appendage to S5

00 97K

97	0	L0	125F	40	100F	
98	1	L5	110F	L0	125F	
99	2	40	110F	26	126F	Reset addresses

S5 Tan  $\beta$ . Test for n.

00 100K

100	0	41	F	L5	S3	
101	1	10	4F	66	S4	
102	2	S5	F	00	4F	
103	3	NO	F	40	5F	
104	4	50	F	50	4L	
105	5	26	SL	40	6F	
106	6	LJ	5F	50	6L	
107	7	26	SL	40	7F	
108	8	50	6F	7J	1S4	
109	9	66	7F	S5	F	
110	10	NO	F	40	2S4	
111	11	F5	L	40	L	
112	12	F5	10L	40	10L	
113	13	L1	24L	36	16L	
114	14	L5	24L	L0	25L	
115	15	40	24L	26	L	
116	16	L1	24L	40	24L	
117	17	L5	10L	L0	25L	
118	18	42	19L	F5	19L	Calc. tan $\beta$ .

Abs. Addr.	Rel. Addr.	Order Pairs				Comments	
119	19	42	20L	50	F	tan $\beta_i$ tan $\beta_i + 1$	
120	20	NO	F	7J	F		
121	21	66	1S4	S5	F		
122	22	NO	F	40	4S4		
123	23	L5	L	26	97F		
124	24	00	F	00	1F		
125	25	00	F	00	2F		
126	26	L5	2S3	L0	5S4		
127	27	32	29L	L5	6S4		
128	28	L0	2S3	32	29L		if n = 1 $\longrightarrow$ S7
129	29	26	S7	L5	7S4		
130	30	L0	2S3	32	31L		if n = 0 $\longrightarrow$ S8 if n < 0 $\longrightarrow$ S9 if n > 1 $\longrightarrow$ SK
131	31	26	33L	L5	2S3		
132	32	L4	7S4	36	S8		
133	33	L1	2S3	36	S9		
134	34	L5	2S3	L0	6S4		
135	35	36	SK	26	SS		

## S7 Form Rad. Bend. Mag. Matrix for n = 1

		00	150K				
150	0	51	2S4	7J	4S3	$\frac{1}{10^3} (1 + \alpha \tan \beta_1)$	
151	1	66	9S4	S5	F		
152	2	L4	1S4	40	300F		
153	3	50	3S3	7J	4S3		
154	4	66	9S4	S5	F		$\frac{\rho\alpha}{10^3}$
155	5	40	301F	50	301F		$\frac{\rho\alpha^2}{2 \times 10^3}$
156	6	7J	4S3	10	1F		
157	7	66	9S4	S5	F		
158	8	40	302F	50	4S4		
159	9	7J	1S4	66	3S3		
160	10	7J	4S3	66	9S4	$\frac{\tan \beta_1 \tan \beta_2}{10^3 \rho} \alpha + \frac{\tan \beta_1}{10^3 \rho}$ $+ \frac{\tan \beta_2}{10^3 \rho}$	
161	11	S5	F	40	F		
162	12	50	2S4	7J	1S4		
163	13	66	3S3	S5	F		
164	14	40	1F	50	3S4		
165	15	7J	1S4	66	3S3		
166	16	S5	F	L4	F		
167	17	L4	1F	40	303F		
168	18	50	3S4	7J	4S3		
169	19	66	9S4	S5	F		
170	20	40	F	L4	1S4	$\frac{1}{10^3} (1 + \alpha \tan \beta_2)$	
171	21	40	304F	50	1S4		
172	22	7J	4S3	66	9S4		
173	23	S5	F	40	1F		

Abs. Addr.	Rel. Addr.	Order Pairs				Comments
174	24	50	F	7J	4S3	$\frac{1}{10^3} (\alpha + \frac{\alpha^2 \tan \beta_2}{2})$
175	25	10	1F	66	9S4	
176	26	S5	F	L4	1F	
177	27	40	305F	L5	8S4	
178	28	40	306F	40	307F	
179	29	L5	1S4	40	308F	
180	30	26	SN	NO	F	

## S8 Axial Bend. Mag. Matrix for n = 0

Abs. Addr.	Rel. Addr.	Order Pairs				Comments
		00	182K			
182	0	51	2S4	7J	4S3	$\frac{1}{10^3} (1 - \alpha \tan \beta_1)$
183	1	66	9S4	S5	F	
184	2	40	F	L5	1S4	
185	3	L0	F	40	309F	
186	4	50	3S3	7J	4S3	
187	5	66	9S4	S5	F	
188	6	40	310F	L5	8S4	
189	7	40	311F	50	4S4	$\frac{\rho\alpha}{10^3}$
190	8	7J	4S3	66	9S4	
191	9	7J	1S4	66	3S3	
192	10	S5	F	40	F	
193	11	50	2S4	7J	1S4	
194	12	66	3S3	S5	F	
195	13	40	1F	50	3S4	
196	14	7J	1S4	66	3S3	
197	15	S5	F	40	2F	
198	16	L5	F	L0	1F	
199	17	L0	2F	40	312F	$\frac{1}{10^3} (\alpha \tan \beta_1 \tan \beta_2 - \tan \beta_1 - \tan \beta_2)$
200	18	50	3S4	7J	4S3	
201	19	66	9S4	S5	F	
202	20	40	F	L5	1S4	
203	21	L0	F	40	313F	
204	22	L5	8S4	40	314F	
205	23	40	315F	40	316F	
206	24	L5	1S4	40	317F	
207	25	L5	30S4	40	58SS	
208	26	26	SS	NO	F	

S 9 Axial Bend. Mag. Matrix for  $n < 0$ 

Abs. Addr.	Rel. Addr.	Order Pairs				Comments
		00	210K			
210	0	L7	2S3	10	4F	
211	1	66	9S4	S5	F	
212	2	50	F	50	2L	
213	3	26	30SL	40	4F	
214	4	L5	4S3	10	4F	
215	5	66	9S4	S5	F	
216	6	40	1F	50	1F	
217	7	7J	4F	00	2F	
218	8	40	F	L1	F	
219	9	50	F	50	9L	
220	10	26	40SL	40	F	
221	11	50	F	7J	F	
222	12	40	F	50	F	
223	13	7J	F	40	F	
224	14	50	F	7J	F	
225	15	40	F	50	F	
226	16	7J	F	40	F	
227	17	50	1S4	7J	9S4	
228	18	66	F	S5	F	
229	19	40	1F	50	F	
230	20	7J	9S4	40	F	
231	21	50	F	7J	1S4	
343	22	40	F	L4	1F	
233	23	10	F	40	2F	
234	24	L5	1F	L0	F	
235	25	10	F	40	3F	
236	26	L5	2F	66	9S4	
237	27	S5	F	40	2F	
238	28	L5	3F	66	4F	
239	29	S5	F	10	2F	
240	30	66	9S4	S5	F	
241	31	40	5F	L5	2S4	
242	32	66	9S4	7J	5F	
243	33	66	10S4	S5	F	$\frac{1}{10^3} (\cos h \alpha  n ^{1/2} -$
244	34	40	F	L5	2F	$\frac{\sin h \alpha  n ^{1/2} \tan \beta_1}{ n ^{1/2}}$
245	35	L0	F	40	309F	$\frac{\sin h \alpha  n ^{1/2}  n ^{1/2}}{10^3  n ^{1/2}}$
246	36	50	5F	7J	3S3	
247	37	66	1S4	S5	F	
248	38	40	310F	L5	8S4	
249	39	40	311F	L7	2S3	
250	40	40	F	50	5F	
251	41	7J	F	40	F	

Abs. Addr.	Rel. Addr.	Order Pairs				Comments
252	42	50	F	7J	10S4	$\frac{1}{10^3 \rho} \left( \frac{\sinh \alpha  n ^{1/2} \tan \beta_1}{ n ^{1/2}} \right)$ $\frac{\tan \beta_2}{+ n ^{1/2} \sinh \alpha  n ^{1/2}}$ $- \cosh \alpha  n ^{1/2}$ $\tan \beta_1 - \cosh \alpha  n ^{1/2}$ $\tan \beta_2$
253	43	66	3S3	S5	F	
254	44	40	6F	50	4S4	
255	45	7J	5F	66	3S3	
256	46	S5	F	L4	6F	
257	47	40	6F	50	2F	
258	48	7J	2S4	66	3S3	
259	49	S5	F	40	7F	
260	50	50	2F	7J	3S4	
261	51	66	3S3	S5	F	
262	52	40	F	L5	6F	
263	53	L0	7F	L0	F	
264	54	40	312F	50	5F	
265	55	7J	3S4	66	1S4	
266	56	S5	F	40	F	
267	57	L5	2F	L0	F	
268	58	40	313F	L5	8S4	
269	59	40	314F	40	315F	
270	60	40	316F	L5	1S4	
271	61	40	317F	L5	30S4	
272	62	40	58SS	26	SS	

SK Radial Bend. Mag. Matrix for  $n > 1$ 

		00	600K		
600	0	L5	9S4	L0	2S3
601	1	40	F	L7	F
602	2	10	4F	66	9S4
603	3	S5	F	N0	F
604	4	50	F	50	4L
605	5	26	30SL	40	3F
606	6	L5	4S3	10	4F
607	7	66	9S4	S5	F
608	8	40	F	50	F
609	9	7J	3F	00	2F
610	10	40	2F	L1	2F
611	11	50	F	50	11L
612	12	26	40SL	40	F
613	13	50	F	7J	F
614	14	40	F	50	F
615	15	7J	F	40	F
616	16	50	F	7J	F
617	17	40	F	50	F

Abs. Addr.	Rel. Addr.	Order Pairs				Comments
618	18	7J	F	40	F	
619	19	50	1S4	7J	9S4	
620	20	66	F	85	F	
621	21	40	1F	50	F	
622	22	7J	9S4	40	F	
623	23	50	F	7J	1S4	
624	24	40	F	L4	1F	
625	25	10	1F	40	2F	
626	26	L5	1F	L0	F	
627	27	10	F	40	1F	
628	28	L5	2F	66	9S4	
629	29	S5	F	40	2F	
630	30	L5	1F	10	2F	$\frac{1}{10^3} (\cos h  1-n ^{1/2} \alpha +$
631	31	66	3F	S5	F	
632	32	66	9S4	S5	F	
633	33	40	4F	L5	2S4	
634	34	66	9S4	7J	4F	$\frac{\sin h  1-n ^{1/2} \alpha \tan \beta_1}{ 1-n ^{1/2}}$
635	35	66	10S4	S5	F	
636	36	L4	2F	40	300F	
637	37	50	4F	7J	3S3	
638	38	40	301F	L5	1S4	$\frac{\rho \sin h \alpha  1-n ^{1/2}}{10^3  1-n ^{1/2}}$
639	39	L0	2F	40	F	
640	40	50	F	7J	3S3	
641	41	40	F	L5	9S4	
642	42	L0	2S3	40	5F	
643	43	L5	F	66	5F	$\frac{\rho (1 - \cos h \alpha  1-n ^{1/2})}{10^3  1-n }$
644	44	S5	F	66	10S4	
645	45	S5	F	40	302F	
646	46	50	4F	7J	1S4	
647	47	66	3S3	S5	F	
648	48	40	F	L7	5F	
649	49	40	6F	50	F	
650	50	7J	6F	66	9S4	
651	51	S5	F	40	6F	
652	52	50	4F	7J	4S4	$\frac{1}{10^3} ( 1-n ^{1/2} \sin h \alpha  1-n ^{1/2}$
653	53	66	3S3	S5	F	
654	54	40	7F	50	2F	
655	55	7J	2S4	66	3S3	
656	56	S5	F	40	8F	$+ \frac{\sin h \alpha  1-n ^{1/2} \tan \beta_1}{ 1-n ^{1/2}}$
657	57	50	2F	7J	3S4	
658	58	66	3S3	S5	F	
659	59	L4	6F	L4	7F	$\frac{\tan \beta_2}{2} + \cos h \alpha  1-n ^{1/2}$
660	60	L4	8F	40	303F	
661	61	50	4F	7J	3S4	$\tan \beta_1 + \cos h \alpha  1-n ^{1/2}$
662	62	66	1S4	S5	F	$\tan \beta_2)$

Abs. Addr.	Rel. Addr.	Order Pairs				Comments
663	53	L4	2F	40	304F	$\frac{1}{10^3} (\cos h \alpha  1-n ^{1/2} + \sin h \alpha  1-n ^{1/2} \tan \beta_2)$
664	64	50	302F	7J	3S4	
665	65	66	3S3	S5	F	
666	66	L4	4F	40	305F	
667	67	L5	8S4	40	306F	
668	68	40	307F	L5	1S4	
669	69	40	308F	26	SN	$\frac{1}{10^3} \left[ \frac{\sin h \alpha  1-n ^{1/2}}{ 1-n ^{1/2}} + \left( \frac{1 - \cos h \alpha  1-n ^{1/2}}{ 1-n } \right) \tan \beta_2 \right]$

SS Radial Bend. Mag. Matrix for  $0 < n < 1$ 

		00	670K			
670	0	L5	9S4	L0	2S3	
671	1	10	8F	66	9S4	
672	2	S5	F	N0	F	
673	3	50	F	50	3L	
674	4	26	30SL	40	5F	
675	5	50	5F	7J	4S3	
676	6	66	S4	S5	F	
677	7	00	4F	40	F	
678	8	50	F	50	8L	
679	9	26	SL	40	9F	
680	10	LJ	F	50	10L	
681	11	26	SL	40	F	
682	12	50	F	7J	1S4	
683	13	00	1F	40	2F	
684	14	50	9F	7J	2S4	$\frac{1}{10^3} (\cos (1-n)^{1/2} \alpha + \sin (1-n)^{1/2} \alpha \tan \beta_1)$
685	15	10	3F	66	5F	
686	16	S5	F	L4	2F	
687	17	40	300F	50	9F	
688	18	7J	3S3	10	3F	
689	19	66	5F	S5	F	
690	20	40	301F	L5	9S4	$\frac{\rho}{10^3} \frac{\sin \alpha (1-n)^{1/2}}{(1-n)^{1/2}}$
691	21	L0	2S3	40	3F	
692	22	50	3S3	7J	9S4	
693	23	66	3F	S5	F	
694	24	40	4F	L5	2F	
695	25	66	3F	7J	3S3	
696	26	66	10S4	S5	F	



Abs. Addr.	Rel. Addr.	Order Pairs				Comments
697	27	40	6F	L5	4F	$\frac{\rho}{10^3 (1-n)} (1 - \cos \alpha (1-n)^{1/2})$
698	28	L0	6F	40	302F	
699	29	50	5F	7J	9F	
700	30	40	7F	50	7F	
701	31	7J	1S4	00	5F	
702	32	40	7F	50	7F	
703	33	7J	1S4	66	3S3	
704	34	S5	F	40	7F	
705	35	50	7F	7J	4S4	
706	36	66	3F	S5	F	
707	37	66	10S4	S5	F	$\frac{1}{10^3 \rho} \left[ - (1-n)^{1/2} \sin (1-n)^{1/2} \alpha + \sin (1-n)^{1/2} \alpha \tan \beta_1 \right]$
708	38	40	8F	50	2F	
709	39	7J	2S4	66	3S3	
710	40	S5	F	40	10F	
711	41	50	2F	7J	3S4	
712	42	66	3S3	S5	F	
713	43	L4	10F	L4	8F	
714	44	L0	7F	40	303F	
715	45	50	9F	7J	3S4	
716	46	66	5F	S5	F	
717	47	10	3F	40	8F	
718	48	L4	2F	40	304F	$\frac{1}{10^3} \left[ \frac{\sin \alpha (1-n)^{1/2} \tan \beta_2}{(1-n)^{1/2}} + \cos (1-n)^{1/2} \alpha \right]$
719	49	L5	1S4	L0	2F	
720	50	66	3F	7J	3S4	
721	51	66	10S4	S5	F	
722	52	40	7F	50	301F	
723	53	7J	1S4	66	3S3	
724	54	S5	F	L4	7F	
725	55	40	305F	L5	8S4	
726	56	40	306F	40	307F	
727	57	L5	1S4	40	308F	
728	58	N0	F	26	SN	

SN Axial Bend. Mag. Matrix for  $0 < n$

		00	730K			
730	0	L5	2S3	10	8F	
731	1	66	9S4	S5	F	
732	2	50	F	50	2L	
733	3	26	30SL	40	5F	
734	4	50	5F	7J	4S3	
735	5	66	S4	S5	F	

Abs. Addr.	Rel. Addr.	Order Pairs				Comments
736	6	00	4F	40	F	
737	7	50	F	50	7L	
738	8	26	SL	40	9F	
739	9	LJ	F	50	9L	
740	10	26	SL	40	F	
741	11	50	F	7J	1S4	
742	12	00	1F	40	2F	
743	13	50	9F	7J	1S4	
744	14	10	3F	66	5F	
745	15	S5	F	40	3F	$\frac{1}{10^3} \left[ \cos n^{1/2} \alpha - \right.$
746	16	50	3F	7J	2S4	
747	17	66	1S4	S5	F	
748	18	40	4F	L5	2F	
749	19	L0	4F	40	309F	
750	20	50	3F	7J	3S3	
751	21	66	1S4	S5	F	$\frac{\rho \sin n^{1/2} \alpha}{10^3 n^{1/2}}$
752	22	40	310F	L5	8S4	
753	23	40	311F	50	9F	
754	24	7J	5F	40	4F	
755	25	50	4F	7J	1S4	
756	26	00	5F	40	4F	
757	27	50	4F	7J	1S4	
758	28	66	3S3	S5	F	
759	29	40	4F	50	9F	
760	30	7J	4S4	40	5F	
761	31	50	5F	7J	1S4	
762	32	66	3S3	S5	F	
763	33	00	1F	40	5F	$\frac{1}{10^3 \rho} \left[ - n^{1/2} \sin \alpha n^{1/2} + \right.$
764	34	50	2F	7J	2S4	$\left. \sin \alpha n^{1/2} \tan \beta_1 \tan \beta_2 \right]$
765	35	66	3S3	S5	F	
766	36	40	6F	50	2F	
767	37	7J	3S4	66	3S3	
768	38	S5	F	40	7F	
769	39	L5	5F	L0	4F	$- \cos \alpha n^{1/2} (\tan \beta_1 +$
770	40	L0	6F	L0	7F	$\left. \tan \beta_2) \right]$
771	41	40	312F	50	3F	
772	42	7J	3S4	66	1S4	$\frac{1}{10^3} \left( \cos \alpha n^{1/2} - \right.$
773	43	S5	F	40	4F	$\left. \sin \alpha n^{1/2} \tan \beta_2 \right)$
774	44	L5	2F	L0	4F	
775	45	40	313F	L5	8S4	
776	46	40	314F	40	315F	
777	47	40	316F	L5	1S4	$\frac{1}{n^{1/2}}$
778	48	40	317F	26	SJ	

## SJ Print Headings and Bend. Mag. Matrices

Abs. Addr.	Rel. Addr.	Order Pairs				Comments
		00	780K			
780	0	92	131F	92	7F	
781	1	92	259F	92	643F	
782	2	92	387F	92	579F	MAG
783	3	92	707F	92	139F	
784	4	92	7F	92	963F	
785	5	92	259F	92	387F	
786	6	92	962F	92	2F	
787	7	92	771F	92	387F	ALPHA
788	8	92	707F	92	835F	
789	9	92	963F	L5	4S3	
790	10	50	10F	50	10L	Print $\alpha/10$
791	11	26	75SL	92	131F	
792	12	92	7F	92	971F	
793	13	92	259F	92	258F	
794	14	92	771F	92	578F	RHO
795	15	92	707F	92	835F	
796	16	92	963F	L5	3S3	
797	17	50	10F	50	17L	Print $\rho/10^3$
798	18	26	75SL	92	131F	
799	19	92	7F	92	979F	
800	20	92	259F	92	770F	N
801	21	92	707F	92	835F	
802	22	92	963F	L5	2S3	
803	23	50	10F	50	23L	Print $n/10$
804	24	26	75SL	92	131F	
805	25	92	7F	92	259F	
806	26	92	195F	92	194F	BETA, 1
807	27	92	322F	92	387F	
808	28	92	707F	92	323F	
809	29	92	66F	92	835F	
810	30	92	963F	L5	S3	
811	31	50	10F	50	31L	Print $\beta_1/10$
812	32	26	75SL	92	131F	
813	33	92	7F	92	259F	
814	34	92	195F	92	194F	
815	35	92	322F	92	387F	BETA, 2
816	36	92	707F	92	323F	
817	37	92	130F	92	835F	
818	38	92	963F	L5	1S3	
819	39	50	10F	50	39L	Print $\beta_2/10$

Abs. Addr.	Rel. Addr.	Order Pairs				Comments
820	40	26	75SL	92	139F	
821	41	92	7F	92	259F	
822	42	92	643F	92	451F	MX
823	43	92	707F	92	135F	
824	44	92	7F	L5	16S4	
825	45	42	48L	L5	13S4	
826	46	40	4F	L5	14S4	
827	47	40	5F	40	6F	
828	48	NO	F	L5	300F	
829	49	50	10F	50	49L	Print bending magnet
830	50	26	75SL	F5	48L	matrices
831	51	42	48L	L5	5F	
832	52	L0	12S4	40	5F	
833	53	32	48L	92	131F	
834	54	92	7F	L5	14S4	
835	55	40	5F	L5	6F	
836	56	L0	12S4	40	6F	
837	57	32	48L	L5	4F	
838	58	L0	12S4	40	4F	
839	50	36	60L	22	63L	
840	60	92	135F	92	259F	MY
841	61	92	643F	92	386F	
842	62	92	135F	92	707F	
843	63	22	46L	L5	16S4	
844	64	42	71L	L4	11S4	
845	65	42	93L	L5	24S4	
846	66	42	72L	42	78L	
847	67	L4	11S4	L4	11S4	
848	68	42	88L	42	94L	
849	69	L5	14S4	40	4F	
850	70	L5	14S4	40	2F	
851	71	40	3F	L5	300F	
852	72	NO	F	40	340F	Restore matrices
853	73	F5	71L	42	71L	
854	74	F5	72L	42	72L	
855	75	F5	78L	42	78L	
856	76	L5	2F	L0	12S4	
857	77	40	2F	32	71L	
858	78	L5	8S4	40	340F	
859	79	F5	72L	42	72L	
860	80	F5	78L	42	78L	
861	81	L5	3F	L0	12S4	
862	82	40	3F	36	78L	

Abs. Addr.	Rel. Addr.	Order Pairs				Comments
863	83	L5	4F	L0	12S4	
864	84	40	4F	36	70L	
865	85	L5	14S4	40	4F	
866	86	L5	14S4	40	2F	
867	87	40	3F	N0	F	
868	88	L5	8S4	40	358F	
869	89	F5	88L	42	88L	
870	90	F5	94L	42	94L	
871	91	L5	2F	L0	12S4	
872	92	40	2F	36	88L	
873	93	41	F	L5	309F	
874	94	N0	F	40	358F	
875	95	F5	88L	40	88L	
876	96	F5	94L	42	94L	
877	97	F5	93L	42	93L	
878	98	L5	3F	L0	12S4	
879	99	40	3F	36	93L	
880	100	L5	4F	L0	12S4	
881	101	40	4F	36	86L	
882	102	N0	F	26	23SF	

Relative Orientation and Separation Matrices, R, and D.

		00	885K			
885	0	L5	8S3	10	5F	
886	1	66	S4	S5	F	
887	2	66	9S4	S5	F	
888	3	00	5F	40	5F	
889	4	50	F	50	4L	
890	5	26	SL	40	6F	
891	6	LJ	5F	50	6L	
892	7	26	SL	40	7F	
893	8	L5	25S4	42	10L	
894	9	L5	15S4	40	2F	
895	10	L5	8S4	40	412F	
896	11	F5	10L	42	10L	
897	12	L5	2F	L0	12S4	
898	13	40	2F	36	10L	
899	14	L5	7F	40	412F	
900	15	40	419F	40	433F	
901	16	40	440F	40	448F	
902	17	40	455F	40	469F	

Abs. Addr.	Rel. Addr.	Order Pairs				Comments
903	18	40	476F	L5	6F	
904	19	40	415F	40	422F	Form $\frac{R}{2}$ and store
905	20	40	466F	40	473F	
906	21	L1	6F	40	430F	
907	22	40	437F	40	451F	
908	23	40	458F	49	F	
909	24	40	426F	40	447F	
910	25	40	462F	40	483F	
911	26	L5	26S4	42	28L	
912	27	L5	32S4	40	F	
913	28	L5	8S4	40	484F	
914	29	F5	28L	40	28L	
915	30	L5	F	L0	12S4	
916	31	40	F	36	28L	
917	32	<b>L5</b>	9S3	40	485F	
918	33	40	506F	50	1S4	Form $\frac{D}{10^4}$ and store
919	34	7J	9S4	40	484F	
920	35	40	491F	40	498F	
921	36	40	505F	40	512F	
922	37	40	519F	L5	22S4	
923	38	40	25F	40	26F	
924	39	92	139F	92	259F	
925	40	92	67F	92	707F	D
926	41	92	835F	92	963F	
927	42	L5	9S3	N0	F	
928	43	50	10F	50	43L	Print $d/10^4$
929	44	26	75SL	92	963F	
930	45	92	259F	92	322F	
931	46	92	771F	92	194F	
932	47	92	322F	92	387F	THETA
933	48	92	707F	92	835F	
934	49	92	963F	L5	8S3	
935	50	50	10F	50	50L	Print $\theta/10^2$
936	51	26	75SL	92	131F	
937	52	92	7F	22	18SF	

## SF Combined Matrix

		00	940K		
940	0	L5	28S4	42	2L
941	1	L5	32S4	40	F
942	2	L5	8S4	40	520F

Abs. Addr.	Rel. Addr.	Order Pairs				Comments	
943	3	F5	2L	40	2L		
944	4	L5	F	L0	12S4	Form a unit matrix and store in place of "previous" matrix.	
945	5	40	F	36	2L		
946	6	50	1S4	7J	9S4		
947	7	40	520F	40	527F		
948	8	40	534F	40	541F		
949	9	40	548F	40	555F		
950	10	50	F	50	10L		
951	11	N6	F	26	3860F		Enter special input routine
952	12	L5	33S4	L0	28S4		
953	13	L0	28S4	42	20L		
954	14	L0	12S4	42	18L		
955	15	L5	18L	L4	10S3		
956	16	42	18L	L5	20L		
957	17	L4	10S3	42	20L		
958	18	26	885F	26	18L		
959	19	NO	F	26	S5		
960	20	26	1270F	26	20L	Test for parameter, b. If b = 1 → S5 If b = 2 → 1270	
961	21	NO	F	26	37L		
962	22	NO	F	26	58L		
963	23	L5	25S4	40	3901F		
964	24	L5	26S4	40	3902F		
965	25	L5	31S4	40	3903F		
966	26	L5	23S4	40	3904F		
967	27	50	F	50	27L		
968	28	26	3900F	L5	32S4		
969	29	40	F	L5	31S4		Enter matrix multi. routine. Form $\frac{RD}{2 \times 10^4}$
970	30	42	31L	42	32L		
971	31	NO	F	L5	556F		
972	32	00	2F	40	556F		
973	33	F5	31L	42	31L		
974	34	42	32L	L5	F		
975	35	L0	12S4	40	F		
976	36	32	31L	22	20L		
977	37	L5	24S4	40	3901F		
978	38	L5	31S4	40	3902F		
979	39	L5	34S4	40	3903F	Form $\frac{2MRD}{10^4}$	
980	40	L5	23S4	40	3904F		
981	41	50	F	50	41L		
982	42	26	3900F	L5	32S4		
983	43	40	F	L5	34S4		
984	44	42	45L	42	47L		
985	45	NO	F	L5	2036F		
986	46	66	1S4	S5	F		

Abs. Addr.	Rel. Addr.	Order Pairs				Comments
987	47	NO	F	40	2036F	
988	48	F5	45L	42	45L	
989	49	42	47L	L5	F	
990	50	L0	12S4	40	F	
991	51	36	45L	L5	29S4	
992	52	40	3901F	L5	34S4	Form $\tilde{RMRD}$
993	53	40	3902F	L5	31S4	$10^4$
994	54	40	3903F	L5	23S4	
995	55	40	3904F	NO	F	
996	56	50	F	50	56L	
997	57	26	3900F	22	79L	
998	58	L5	27S4	40	3901F	
999	59	L5	31S4	40	3902F	
1000	60	L5	34S4	40	3903F	Form $2QRD$
1001	61	L5	23S4	40	3904F	$10^8$
1002	62	50	F	50	62L	
1003	63	26	3900F	L5	32S4	
1004	64	40	F	L5	34S4	
1005	65	42	66L	42	69L	
1006	66	NO	F	L5	2036F	
1007	67	66	1S4	S5	F	
1008	68	66	9S4	S5	F	
1009	69	NO	F	40	2036F	
1010	70	F5	66L	42	66L	
1011	71	42	69L	L5	F	
1012	72	L0	12S4	40	F	
1013	73	36	66L	L5	29S4	Form $\tilde{RQRD}$
1014	74	40	3901F	L5	34S4	$10^4$
1015	75	40	3902F	L5	31S4	
1016	76	40	3903F	L5	23S4	
1017	77	40	3904F	NO	F	
1018	78	50	F	50	78L	
1019	79	26	3900F	L5	31S4	
1020	80	40	3901F	L5	28S4	
1021	81	40	3902F	L5	34S4	Form the product
1022	82	40	3903F	L5	23S4	of $\tilde{R} (M \text{ or } Q) RD$ times
1023	83	40	3904F	NO	F	$10^4$
1024	84	50	F	50	84L	
1025	85	26	3900F	L5	32S4	the "previous" matrix
1026	86	40	F	L5	34S4	and store as "previous"
1027	87	42	88L	42	91L	matrix.
1028	88	NO	F	L5	2036F	
1029	89	66	1S4	S5	F	



Abs. Addr.	Rel. Addr.	Order Pairs				Comments
1030	90	66	9S4	S5	F	
1031	91	N0	F	40	2036F	
1032	92	F5	88L	42	88L	
1033	93	42	91L	L5	F	
1034	94	L0	12S4	40	F	
1035	95	36	88L	L5	32S4	
1036	96	40	F	L5	34S4	
1037	97	42	98L	L5	28S4	
1038	98	42	99L	L5	2036F	
1039	99	N0	F	40	520F	
1040	100	F5	98L	42	98L	
1041	101	F5	99L	42	99L	
1042	102	L5	F	L0	12S4	
1043	103	40	F	32	98L	
1044	104	L5	26S4	L4	31S4	
1045	105	L4	23S4	L4	13S4	
1046	106	42	108L	L5	108L	
1047	107	L4	11S3	42	108L	
1048	108	N0	F	26	109L	Test for parameter, C.
1049	109	N0	F	26	10L	If c = 0, go back to 10L
1050	110	L5	34S4	42	115L	If c = 1, proceed with print out
1051	111	92	135F	92	7F	
1052	112	92	259F	92	643F	
1053	113	92	135F	92	707F	M
1054	114	L5	22S4	40	5F	
1055	115	40	6F	L5	2036F	
1056	116	50	9F	50	116L	Print final matrix
1057	117	26	75SL	F5	115L	
1058	118	42	115L	L5	5F	
1059	119	L0	12S4	40	5F	
1060	120	32	115L	92	131F	
1061	121	92	7F	L5	22S4	
1062	122	40	5F	L5	6F	
1063	123	L0	12S4	40	6F	
1064	124	32	115L	26	1070F	

Calculation of the Properties of the System and Their Print Out

		00	1070K			
1070	0	N0	F	92	131F	
1071	1	92	7F	92	979F	
1072	2	92	259F	92	898F	FX AX BX
1073	3	92	451F	92	1003F	

Abs. Addr.	Rel. Addr.	Order Pairs				Comments
1074	4	92	387F	92	451F	
1075	5	92	1003F	92	195F	
1076	7	92	707F	92	7F	
1078	8	N0	F	L5	2042F	
1079	9	66	9S4	S5	F	
1080	10	40	10F	50	1S4	Calculate $f_x$
1081	11	75	1S4	40	F	
1082	12	50	F	75	10S4	
1083	13	40	4F	L7	4F	
1084	14	L2	10F	36	153L	
1085	15	L1	4F	66	10F	
1086	16	S5	F	40	10F	
1087	17	50	10F	50	17L	Print $f_x/10^5$
1088	18	26	75SL	L5	2043F	
1089	19	66	9S4	S5	F	
1090	20	40	11F	50	11F	Calculate $a_x$
1091	21	75	10F	66	1S4	
1092	22	S5	F	40	11F	
1093	23	50	10F	50	23L	
1094	24	26	75SL	L5	2036F	Print $a_x/10^5$
1095	25	66	9S4	S5	F	
1096	26	40	12F	50	12F	
1097	27	75	10F	66	1S4	Calculate $b_x$
1098	28	S5	F	40	12F	
1099	29	50	10F	50	29L	Print $b_x/10^5$
1100	30	26	75SL	92	131F	
1101	31	92	7F	92	979F	
1102	32	92	259F	92	898F	
1103	33	92	386F	92	1003F	FY AY BY
1104	34	92	387F	92	386F	
1105	35	92	1003F	92	195F	
1106	36	92	386F	92	131F	
1107	37	92	707F	92	7F	
1108	38	N0	F	L5	2063F	
1109	39	66	9S4	S5	F	Calculate $f_y$
1110	40	40	15F	50	1S4	
1111	41	75	1S4	40	F	
1112	42	50	F	75	10S4	
1113	43	40	4F	L7	4F	
1114	44	L2	15F	32	155L	
1115	45	L1	4F	66	15F	
1116	46	S5	F	40	15F	
1117	47	50	10F	50	47L	Print $f_y/10^5$
1118	48	26	75SL	L5	2064F	

Abs. Addr.	Rel. Addr.	Order Pairs				Comments
1119	49	66	9S4	S5	F	
1120	50	40	16F	50	16F	Calculate $a_y$
1121	51	75	15F	66	1S4	
1122	52	S5	F	40	16F	
1123	53	50	10F	50	53L	Print $a_y/10^5$
1124	54	26	75SL	L5	2057F	
1125	55	66	9S4	S5	F	
1126	56	40	17F	50	17F	
1127	57	75	15F	66	1S4	Calculate $b_y$
1128	58	S5	F	40	17F	
1129	59	50	10F	50	59L	Print $b_y/10^5$
1130	60	26	75SL	92	135F	
1131	61	92	7F	92	967F	
1132	62	92	259F	92	67F	
1133	63	92	578F	92	451F	
1134	64	92	983F	92	643F	
1135	65	92	451F	92	991F	
1136	66	92	67F	92	514F	
1137	67	92	451F	92	975F	DOX MX DIX
1138	68	92	258F	92	194F	
1139	69	92	706F	92	707F	RES. RAD. DOY
1140	70	92	643F	92	963F	
1141	71	92	259F	92	258F	MY DIY RES. AX.
1142	72	92	387F	92	67F	
1143	73	92	707F	92	643F	
1144	74	92	259F	92	967F	
1145	75	92	67F	92	578F	
1146	76	92	386F	92	983F	
1147	77	92	643F	92	386F	
1148	78	92	991F	92	67F	
1149	79	92	514F	92	386F	
1150	80	92	975F	92	258F	
1151	81	92	194F	92	706F	
1152	82	92	707F	92	643F	
1153	83	92	963F	92	259F	
1154	84	92	387F	92	451F	
1155	85	92	707F	92	643F	
1156	86	92	131F	92	7F	
1157	87	L5	90SL	L0	165L	
1158	88	40	90SL	L5	13S3	
1159	89	J0	7F	50	89L	Print $d_{ox}/10^5$
1160	90	26	75SL	26	158L	

Abs. Addr.	Rel. Addr.	Order Pairs				Comments
1161	91	NO	F	L5	13S3	
1162	92	L0	11F	40	13F	
1163	93	50	10F	75	1S4	
1164	94	40	5F	L7	5F	Calc. $M_x$
1165	95	L2	13F	36	160L	
1166	96	L5	5F	66	13F	
1167	97	75	10S4	40	13F	
1168	98	50	8F	50	98L	Print $M_x/10^5$
1169	99	26	75SL	50	10F	
1170	100	75	13F	66	1S4	
1171	101	S5	F	66	10S4	
1172	102	S5	F	L4	12F	Calc. $d_{ix}$
1173	103	40	14F	NO	F	
1174	104	50	8F	50	104L	Print $d_{ix}/10^5$
1175	105	26	75SL	NO	F	
1176	106	50	2044F	75	14F	
1177	107	66	1S4	S5	F	
1178	108	66	9S4	S5	F	
1179	109	40	F	50	2038F	
1180	110	75	9S4	L4	F	
1181	111	40	20F	50	13F	Calc. radial resolution/ $10^5$
1182	112	75	10S4	40	6F	
1183	113	L7	6F	L2	20F	
1184	114	NO	F	36	161L	
1185	115	L5	6F	66	20F	
1186	116	S5	F	40	6F	
1187	117	L7	6F	NO	F	
1188	118	J0	8F	50	118L	Print radial resolution
1189	119	26	75SL	L5	14S3	
1190	120	J0	7F	50	120L	
1191	121	26	75SL	26	162L	Print $d_{oy}/10^5$
1192	122	NO	F	L5	14S3	
1193	123	L0	16F	40	18F	
1194	124	50	15F	75	1S4	
1195	125	40	5F	L7	5F	
1196	126	L2	18F	36	152L	Calc. $M_y$
1197	127	L5	5F	66	18F	
1198	128	75	10S4	40	18F	
1199	129	50	8F	50	129L	Print $M_y/10^5$
1200	130	26	75SL	50	15F	
1201	131	75	18F	66	1S4	
1202	132	S5	F	66	10S4	
1203	133	S5	F	L4	17F	Calc. $d_{iy}$
1204	134	40	19F	NO	F	
1205	135	50	8F	50	135L	

Abs. Addr.	Rel. Addr.	Order Pairs				Comments	
1206	136	26	75SL	50	19F	Print $d_{iy}/10^5$	
1207	137	75	2062F	66	9S4		
1208	138	S5	F	66	1S4		
1209	139	S5	F	40	F		
1210	140	50	2056F	75	9S4		
1211	141	L4	F	40	21F		
1212	142	50	18F	75	10S4		
1213	143	40	7F	L7	7F		
1214	144	L2	21F	36	152L		Calc. axial resolution
1215	145	L5	7F	66	21F		
1216	146	S5	F	40	7F	Print axial resolution/ $10^5$	
1217	147	L7	7F	NO	F		
1218	148	J0	8F	50	148L		
1219	149	26	75SL	NO	F		
1220	150	L5	90SL	L4	165L		
1221	151	40	90SL	26	167L		
1222	152	92	651F	26	150L		
1223	153	F5	158L	42	158L		
1224	154	F5	173L	42	173L		
1225	155	22	30L	F5	163L		
1226	156	42	163L	F5	178L		
1227	157	42	178L	22	60L		
1228	158	NO	F	26	159L		
1229	159	26	91L	NO	F		
1230	160	92	999F	92	999F		
1231	161	92	995F	22	119L		
1232	162	NO	F	26	163L		
1233	163	26	122L	NO	F		
1234	164	26	152L	NO	F		
1235	165	00	4F	00	F		
1236	166	00	F	00	1F	Constants	
1237	167	L5	13S3	L4	15S3		
1238	168	40	13S3	L5	14S3	Increment $d_{ox}$ and $d_{oy}$	
1239	169	L4	16S3	40	14S3		
1240	170	92	131F	92	7F		
1241	171	L5	12S3	L0	166L		
1242	172	40	12S3	36	87L		
1243	173	NO	F	26	174L		
1244	174	22	178L	NO	F		
1245	175	L5	158L	L0	166L		
1246	176	42	158L	L5	173L		
1247	177	L0	166L	42	173L		
1248	178	NO	F	26	179L		
1249	179	26	183L	NO	F		

Abs. Addr.	Rel. Addr.	Order Pairs				Comments
1250	180	L5	163L	L0	166L	
1251	181	42	163L	L5	178L	
1252	182	L0	166L	42	178L	
1253	183	24	SF	26	4071F	Black sw., white sw. stop.

## Divergence Quadrupole Sub-matrix

		00	1270K			
1270	0	L5	32S4	40	F	
1271	1	L5	8S4	40	376F	
1272	2	F5	1L	42	1L	
1273	3	L5	F	L0	12S4	
1274	4	40	F	36	1L	
1275	5	50	5S3	7J	6S3	
1276	6	10	4F	66	1S4	
1277	7	S5	F	40	F	
1278	8	L1	F	N0	F	
1279	9	50	F	50	9L	
1280	10	26	40SL	40	F	
1281	11	50	F	7J	F	
1282	12	40	F	50	F	
1283	13	7J	F	40	F	
1284	14	50	F	7J	F	
1285	15	40	F	50	F	
1286	16	7J	F	40	F	
1287	17	50	1S4	7J	9S4	
1288	18	66	F	S5	F	
1289	19	40	1F	50	F	
1290	20	7J	9S4	40	F	
1291	21	50	F	7J	1S4	
1292	22	40	F	L4	1F	$\frac{\cos h KL}{10^4}$
1293	23	10	1F	40	6F	
1294	24	L5	1F	L0	F	
1295	25	10	1F	40	3F	$\frac{\sin h KL}{10^4}$
1296	26	L5	3F	66	5S3	
1297	27	7J	9S4	40	7F	$\frac{1}{10^4}$
1298	28	50	3F	7J	5S3	
1299	29	66	9S4	S5	F	$\frac{1}{K} \frac{\sin h KL}{10^4}$
1300	30	40	8F	L5	27S4	
1301	31	42	1L	26	1330F	

## Convergence Quadrupole Sub-matrix

Abs. Addr.	Rel. Addr.	Order Pairs				Comments
		00	1305K			
1305	0	50	5S3	7J	6S3	
1306	1	10	4F	66	S4	
1307	2	S5	F	66	10S4	
1308	3	S5	F	00	4F	
1309	4	40	4F	NO	F	
1310	5	50	F	50	5L	
1311	6	26	SL	40	5F	
1312	7	50	5F	7J	1S4	
1313	8	00	1F	40	5F	
1314	9	LJ	4F	50	9L	
1315	10	26	SL	40	6F	
1316	11	50	6F	7J	1S4	
1317	12	00	1F	40	F	$\cos KL$
1318	13	50	F	7J	9S4	$10^4$
1319	14	40	6F	50	5F	
1320	15	7J	10S4	66	5S3	$\frac{1}{K} \sin KL$
1321	16	S5	F	40	7F	$10^4$
1322	17	50	5F	79	5S3	
1323	18	40	8F	26	1339F	$-K \sin KL$ $10^4$

## S6 Quadrupole Matrix

Abs. Addr.	Rel. Addr.	Order Pairs				Comments
		00	1330K			
1330	0	L5	28S4	L4	26S4	
1331	1	L4	24S4	L0	13S4	
1332	2	42	8L	42	9L	
1333	3	L4	12S4	42	10L	
1334	4	42	11L	L5	8L	
1335	5	L4	7S3	42	8L	
1336	6	42	9L	L5	10L	
1337	7	L4	7S3	42	10L	
1338	8	42	11L	26	11L	
1339	9	NO	F	22	11L	
1340	10	NO	F	26	13L	
1341	11	NO	F	22	13L	
1342	12	26	16L	26	22L	
1343	13	26	22L	26	16L	
1344	14	26	1305F	26	26L	
1345	15	26	26L	26	1305F	
1346	16	50	1S4	7J	9S4	Test for parameter, a and transfer to appropriate locations.

Abs. Addr.	Rel. Addr.	Order Pairs		Comments
1347	17	40	390F 40	411F
1348	18	L5	6F 40	376F
1349	19	40	383F L5	7F
1350	20	40	377F L5	8F
1351	21	40	382F 26	10L
1352	22	L5	6F 40	397F
1353	23	40	404F L5	7F
1354	24	40	398F L5	8F
1355	25	40	403F 26	11L
1356	26	92	135F 92	7F
1357	27	92	259F 92	642F
1358	28	92	707F 92	835F
1359	29	92	967F L5	5S3
1360	30	50	10F 50	30L
1361	31	26	75SL 92	975F
1362	32	92	259F 92	962F
1363	33	92	707F 92	835F
1364	34	92	967F L5	6S3
1365	35	50	10F 50	35L
1366	36	26	75SL 92	971F
1367	37	92	259F 92	387F
1368	38	92	707F 92	579F
1369	39	L5	28S4 L4	28S4
1370	40	L4	24S4 L0	14S4
1371	41	L0	12S4 42	43L
1372	42	L5	43L L4	7S3
1373	43	42	43L 26	43L
1374	44	92	66F 22	45L
1375	45	92	130F 92	131F
1376	46	92	7F 26	23SF

## Special Input Sub-routine

		00	3860K		
3860	0	K5	F	L4	32L
3861	1	42	29L	46	24L
3862	2	10	2F	46	29L
3863	3	10	2F	46	25L
3864	4	41	36L	41	33L
3865	5	50	33L	F5	33L
3866	6	40	34L	81	4F
3867	7	L0	30L	36	27L



Abs. Addr.	Sub-routines
3960	T5 Sine, <del>Cos</del> ine Sub-routine.
3990	R1 Square root sub-routine.
4000	64 - S2 Exponent Sub-routine.
4035	P2 Print out Sub-routine.

## REFERENCES

1. Judd, David L., "Focusing Properties of a Generalized Magnetic Spectrometer," Review of Scientific Instruments, 21, 213 (1950).
2. Kerst, D. W., and Serber, R., "Electronic Orbits in the Induction Accelerator," Physical Review, 60, 53 (1941).
3. Enge, H. A., "Ion Focusing Properties of a Quadrupole Lens Pair," Review of Scientific Instruments, 30, 248 (1959).
4. Penner, S., "Calculations of Properties of Magnetic Deflection Systems," Review of Scientific Instruments, 32, 150 (1961).
5. Livingood, J. J. Principles of Cyclic Particle Accelerators, Princeton, D. Van Nostrand, 1961.

7

63

0

3

7

9

4